Design of Neuro-Computing Paradigms for Nonlinear Nanofluidic Systems of MHD Jeffery-Hamel Flow

Ammara.Mehmood[1], Nouman-ul-Haq[2], Aneela Zameer[3], Sai Ho Ling[4], Muhammad Asif Zahoor Raja[5, #]

[1]Department of Electrical Engineering, Pakistan Institute of Engineering and Applied Sciences, Islamabad, Pakistan
ms_mehmud16@pieas.edu.pk, zad_mehmud@yahoo.com

[2]Department of Physics, Riphah International University, Islamabad, Pakistan
noumanattari32@yahoo.com

[3] Department of Computer and Information Sciences, Pakistan Institute of Engineering and Applied Sciences (PIEAS), Nilore, Islamabad, 45650, Pakistan
aneelaz@pieas.edu.pk

[4.]School of Biomedical Engineering, Centre for Health Technologies, Department of Engineering and IT, University of Technology, Sydney, NSW, Australia
Steve.Ling@uts.edu.au

[5.]Department of Electrical Engineering, COMSATS Institute of Information Technology, Attock, 43600, Pakistan
rasifzahoor@yahoo.com, Muhammad.asif@ciit-attock.edu.pk
[#]Corresponding author

Abstract: *In this paper, a neuro-heuristic technique by incorporating artificial neural network models (NNMs) optimized with sequential quadratic technique (SQP) is proposed to solve a dynamics of nanofluidics system based on magneto-hydrodynamic (MHD) Jeffery–Hamel (JHF) problem involving nano-meterials. Original partial differential equations (PDEs) associated with MHD-JHF are transformed into third order ordinary differential equations (ODEs) based model. Furthermore, the transformed system implemented by the differential equation NNMs (DE-NNMs) which are constructed by a defined error function using log-sigmoid, radial basis and tan-sigmoid windowing kernels. The parameters of DE-NNM of nanofluidics system is optimized with SQP algorithm. To illustrate the performance of the proposed system, MHD-JHF systems with base-fluid water mixed with alumina, silver and copper nanoparticles for different Hartman numbers, Reynolds numbers, angles of the channel and volume fractions with three*

different proposed DE-NNMs are designed to evaluate. For comparison purpose, the proposed results with reference numerical results of Adams solver illustrates their worth. Statistical inferences through different performance indices are given to demostarte the accuracy, stability and robustness of the stochastic solver.

Keywords: Magneto-hydrodynamic; Jeffery–Hamel flow; Artificial neural networks; Nanofluids; Neurocomputing; Sequential quadratic programming

1. Introduction

The nanofluidic problems of flow and heat transfer characteristics have been extensively studied in various applied science and engineering applications such as mechanics, thermal-power generating systems, civil, chemical and biomedical engineering [1-20]. During recent years, nanofluidic domain have gained practical importance in computational fluid dynamics systems and researchers have shown paramount interest for solving magneto-hydrodynamic nonlinear Jeffery-Hamel Flow (MHD-JHF) problems [21-23]. Numerous numerical, as well as, analytical methods have been introduced in the literature to solve these stiff computational fluid dynamic problems [24-34]. All these existing deterministic techniques have their own benefits, applications and limitations while the stochastic numerical solvers look promising to solve fluid mechanics problems based on nonlinear Jeffery-Hamel Flow in the presence of high magnetic field involving nano-materials. Also these nonlinear MHD-JHF problems merely admit analytical solution, so for these systems, stochastic techniques based on artificial intelligence procedure is a good alternate, accurate and robust computing paradigm.

The stochastic computing paradigms exploit the biological inspired heuristics and are exhaustively utilized by the research community for finding the solution of nonlinear stiff systems [35-39]. Renewed applications of paramount significance include optimization in

electrical machine models [40-41], electromagnetics [42-43], electrical conducting solids [44-45], nonlinear electric circuits [46], parameter estimation of control autoregressive systems [47-48], nonlinear system identification [49-50], optimization in power systems [51-52], atomic physics model [53-54], prediction problems [55], estimation problems [56], fuel ignition models [57-58], nonlinear functional order systems [59-60], nanofluidic systems [61-62], nonlinear JHF problems [63-64], nonlinear Falknar-Skan systems [65], nonlinear model in astronomy [66-67], nonlinear models in plasma physics [68-69], bioinformatics [70-71] and fractional order system model through Riccati and Bagley-Torvik equations [72-75]. These facts inspire authors to explore and exploit intelligent computing paradigms based on artificial neural networks to get an accurate, reliable and stable solution of nonlinear JHF problems in the presence of strong magnetic field and contaminated with different nanoparticles.

In the present research work, a stochastic solver is developed to analyze the dynamics of nonlinear MHD-JHF involving the contamination of Alumina, silver and coper nano-materials in base-fluid of water by the legacy of artificial neural network models (NNMs) optimized with local search efficacy of sequential quadratic programming (SQP). Original partial differential equations (PDEs), representing the dynamics of JHF problem are transformed into third order ordinary differential equation (ODE) with the competency of suitable similarity transformations. The differential equation neural networks models (DE-NNMs) are constructed by using log-sigmoid, radial basis and tan-sigmoid transfer functions and these networks are arbitrary combined to define an energy function for nonlinear MHD-JHF problems in mean squared error sense. Optimization of energy function for all three DE-NNMs are performed through SQP based local search procedure. Salient features of the designed schemes are listed as follows:

- A novel neuro-heuristic technique is exploited for the analysis of velocity profile of the dynamics of nanofluidics system based on MHD-JHF employing rich heritage of neural networks modeling optimized with viable local search procedure of SQP.

- Three different DE-NNMs are designed by exploitation of windowing kernels based on log-sigmoid, radial basis and tan-sigmoid to represent the nonlinear MHD-JHF systems with base-fluid water mixed with alumina, silver and copper nanoparticles and studied the dynamics with variation in Hartman numbers, Reynolds numbers, angles of the channel and volume fractions.

- Accuracy of the designed schemes are established by attaining a good concurrence with numerical results of state of the art Adams method for each case of the nanofluidic MHD-JHF system.

- Validation of invariable accuracy and convergence is established through exhaustive simulations and their statistics in terms of mean absolute error (MAE), root mean squared error (RMSE), Variance Account For (VAF), Nash Sutcliffe Efficiency(NSE), and Theil Inequality Efficiency (TIC) performance indices.

Organization of rest of the paper is as follows: Sect 2 presents overview of the system model based on nonlinear MHD-JHF, the description of the DE-NNMs along with energy function is given in Sect 3 along with performance measuring indicators, in Sect 4, the results of simulation studies are given for four scenarios of nonlinear MHD-JHF problems for convergent and divergent flow cases. Comparative studies on the basis of statistics are narrated in Sect 5, while conclusions along with future recommended studies are narrated in Sect 6.

2. System Model: MHD-JHF Problem

The flow of fluid through non-parallel walls is referred to be a Jeffery-Hamel flow [6]. The geometry of such fluid flow is shown in Figure 1. The laminar Newtonian fluid flow with constant density mixed with nanoparticles is consider with the channel angle between the plates is 2α. If channel angle α is less than zero than flow will be convergent and if α is greater than zero than flow will be divergent [21].

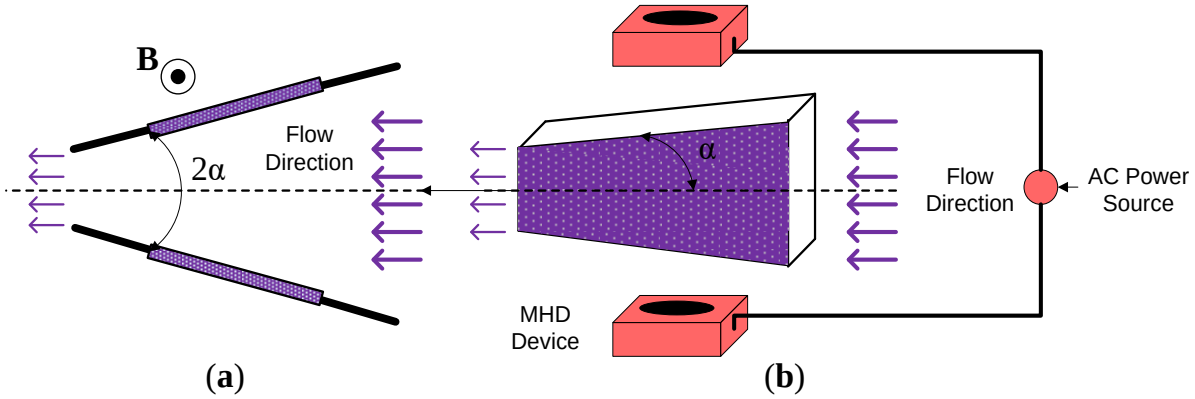

Figure 1: (a) 2-D view of Geometry for MHD-JHF system in a convergent cannel and (b) schematic setup of the problem.

The governing expression for partial differential equations (PDEs) of MHD-JHF problem by considering a cylindrical coordinate system having three components (r,θ,z) are given as [21]:

$$\frac{\rho_{nf}}{r}\frac{\partial}{\partial r}\left[ru(r,\theta)\right]=0, \tag{1}$$

$$u(r,\theta)\frac{\partial}{\partial r}\left[u(r,\theta)\right]=-\frac{1}{\rho_{nf}}\frac{\partial P}{\partial r}+\mu_{nf}\left(\begin{array}{c}\frac{\partial^2 u(r,\theta)}{\partial r^2}+\frac{1}{r}\frac{\partial u(r,\theta)}{\partial r}+\\ \frac{1}{r^2}\frac{\partial^2 u(r,\theta)}{\partial \theta^2}-\frac{u(r,\theta)}{r^2}\end{array}\right)-\frac{\sigma B^2}{\rho_{nf}r^2}u(r,\theta), \tag{2}$$

$$\frac{1}{\rho_{nf}r}\frac{\partial p}{\partial \theta}-\frac{2\mu_{nf}}{r^2}\frac{\partial u(r,\theta)}{\partial \theta}=0, \tag{3}$$

here the magnetic field is represented with B, the component of velocity along radial direction is $u(r)$, P is the pressure exerted by the fluid, μ_{nf} is the kinematic viscosity coefficient, the fluid density is ρ_{nf} and the electrical conductivity of the fluid is represented with σ [21].

$$\rho_{nf} = (1-\varphi)\rho_f + \varphi\rho_s,\ \mu_{nf} = \frac{\mu_f}{(1-\varphi)^{2.5}},\ \mu_{nf} = \frac{\mu_f}{\rho_{nf}}. \quad \textbf{(4)}$$

The solid volume of nanoparticles in the above equations is represented with φ. The velocity profile of the fluid dynamics is $f(\theta) = ru(r)$. If $\eta = \theta/\alpha$ then the velocity profile of fluid dynamics is given by $f(\eta) = f(\theta)/f_{\max}$.

By applying many similarity transforms the final ordinary differential equation (ODE) for the MHD-JHF system is given by [21]

$$f'''(\eta) + 2\alpha \,\mathrm{Re}\left[(1-\varphi)^{2.5}\left(1-\varphi+\varphi\frac{\rho_s}{\rho_f}\right)\right] f(\eta) f'(\eta) + (4-((1-\varphi)^{1.25} H))\alpha^2 f'(\eta) = 0, \quad \textbf{(5)}$$

with boundary conditions

$$f(0) = 1,\ f'(0) = 0,\ f(1) = 0. \quad \textbf{(6)}$$

In equation (6), Reynolds number *Re* and Hartmann number *H* are given respectively as:

$$\mathrm{Re} = \frac{f_{\max}\alpha}{\mu_f} = \frac{U_{\max} r\alpha}{\mu_f}\begin{pmatrix} \textit{divergent channel}: & \alpha > 0,\ U_{\max} > 0 \\ \textit{convergent channel}: & \alpha < 0,\ U_{\max} < 0 \end{pmatrix},$$
$$H = \sqrt{\frac{\sigma B^2}{\rho_f \mu_f}}. \quad \textbf{(7)}$$

3. Methodology

The proposed design methodology to study the dynamics of nonlinear MHD-JHF involving nanoparticles is a two phase procedure. Initial phase is the construction of NNMs, while in the second phase description is provided for the optimization of weights NNMs by using efficiency of SQP method. The overall workflow diagram of the scheme is shown schematically in Fig. 2.

3.1 Mathematical Modeling

Mathematical modeling for the differential equations NNM (DE-NNMs) for the solutions $f(n)$ and its n^{th} order derivative $\left(f^{(n)}(\eta)\right)$ of the ODEs in terms of input, single hidden, and output layers is given as:

$$\hat{f}(\eta) = \sum_{i=1}^{m} \delta_i g(w_i \eta + \beta_i), \tag{8}$$

$$\hat{f}^{(n)}(\eta) = \sum_{i=1}^{m} \delta_i g^{(n)}(w_i \eta + \beta_i),, \tag{9}$$

where m stands for number of neurons, g is representing the type of activation function, $\boldsymbol{\delta}$, $\boldsymbol{w}$ and $\boldsymbol{\beta}$ are real-valued bounded vectors that formulate the weight vector $\boldsymbol{W}$ as:

$$\boldsymbol{W} = [\boldsymbol{\delta}, \boldsymbol{w}, \boldsymbol{\beta}] = [\delta_1, \delta_2, ..., \delta_m, w_1, w_2, ..., w_m, \beta_1, \beta_2, ..., \beta_m]. \tag{10}$$

Three different activation functions are used to construct three DE-NNMs, i.e., for log-sigmoid g_{LS}, radial basis g_{RB} and tan-sigmoid g_{TS}. The expression for g_{LS}, g_{RB} and g_{TS} activation functions are given as follows:

$$g_{LS}(t) = \frac{1}{1+e^{-t}}, \tag{11}$$

$$g_{RB}(t) = e^{-t^2}, \tag{12}$$

$$g_{TS}(t) = \frac{2}{1+e^{-2t}} - 1. \tag{13}$$

The NNMs based on g_{LS} (NNM-LS), g_{RB} (NNM-RB) and g_{TS} (NNM-TS) functions have been developed to find the solutions of nonlinear MHD-JHF along with its higher order derivatives. In case of differential equation NNM-LS (DE-NNM-LS), the solution $f(\eta)$ along with derivatives, i.e., $f'(\eta)$ and $f'''(\eta))$, are approximated by the following networks:

$$\hat{f}_{LS}(\eta) = \sum_{i=1}^{m} \delta_i \frac{1}{1+e^{-(w_i\eta+\beta_i)}}, \tag{14}$$

$$\hat{f}'_{LS}(\eta) = \sum_{i=1}^{m} \delta_i w_i \frac{e^{-(w_i\eta+\beta_i)}}{\left(1+e^{-(w_i\eta+\beta_i)}\right)^2}, \tag{15}$$

$$f'''_{LS}(\eta) = \sum_{i=1}^{m} \delta_i w_i^3 \left(\frac{6e^{-3(w_i\eta+\beta_i)}}{\left(1+e^{-(w_i\eta+\beta_i)}\right)^4} - \frac{6e^{-2(w_i\eta+\beta_i)}}{\left(1+e^{-(w_i\eta+\beta_i)}\right)^3} + \frac{e^{-(w_i\eta+\beta_i)}}{\left(1+e^{-(w_i\eta+\beta_i)}\right)^2} \right). \tag{16}$$

In case of differential equation NNM-RB (DE-NMM-RB), networks for the solution $f(\eta)$ and few of its derivatives can be given as:

$$\hat{f}_{RB}(\eta) = \sum_{i=1}^{m} \delta_i e^{-(w_i\eta+\beta_i)^2}, \tag{17}$$

$$\hat{f}'_{RB}(\eta) = \sum_{i=1}^{m} -2\delta_i w_i \left(w_i\eta+\beta_i\right) e^{-(w_i\eta+\beta_i)^2}, \tag{18}$$

$$\hat{f}'''_{RB}(\eta) = \sum_{i=1}^{m} \delta_i w_i^3 \left(12\left(w_i\eta+\beta_i\right)e^{-(w_i\eta+\beta_i)^2} - 8\left(w_i\eta+\beta_i\right)^3 e^{-(w_i\eta+\beta_i)^2}\right). \tag{19}$$

Accordingly, for differential equation NNM-TS (DE-NNM-TS), the networks for the solution and its derivatives are written as follows:

$$\hat{f}_{TS}(\eta)=\sum_{i=1}^{m}\delta_i\left(\frac{2}{1+e^{-2(w_i\eta+\beta_i)}}-1\right), \tag{20}$$

$$\hat{f}'_{TS}(\eta)=\sum_{i=1}^{m}4\delta_i w_i\left(\frac{e^{-2(w_i\eta+\beta_i)}}{\left(1+e^{-2(w_i\eta+\beta_i)}\right)^2}\right), \tag{21}$$

$$\hat{f}'''_{TS}(\eta)=\sum_{i=1}^{m}2\delta_i w_i^3\left(\frac{48e^{-6(w_i\eta+\beta_i)}}{\left(1+e^{-2(w_i\eta+\beta_i)}\right)^4}-\frac{48e^{-4(w_i\eta+\beta_i)}}{\left(1+e^{-2(w_i\eta+\beta_i)}\right)^3}+\frac{8e^{-2(w_i\eta+\beta_i)}}{\left(1+e^{-2(w_i\eta+\beta_i)}\right)^2}\right). \tag{22}$$

The networks DE-NNM-LS, DE-NNM-LS, DE-NNM-RB, and DE-NNM-TS presented in equations (14-16), (17-19) and (20-22) are used to model nonlinear MHD-JHF system in (5-6), respectively.

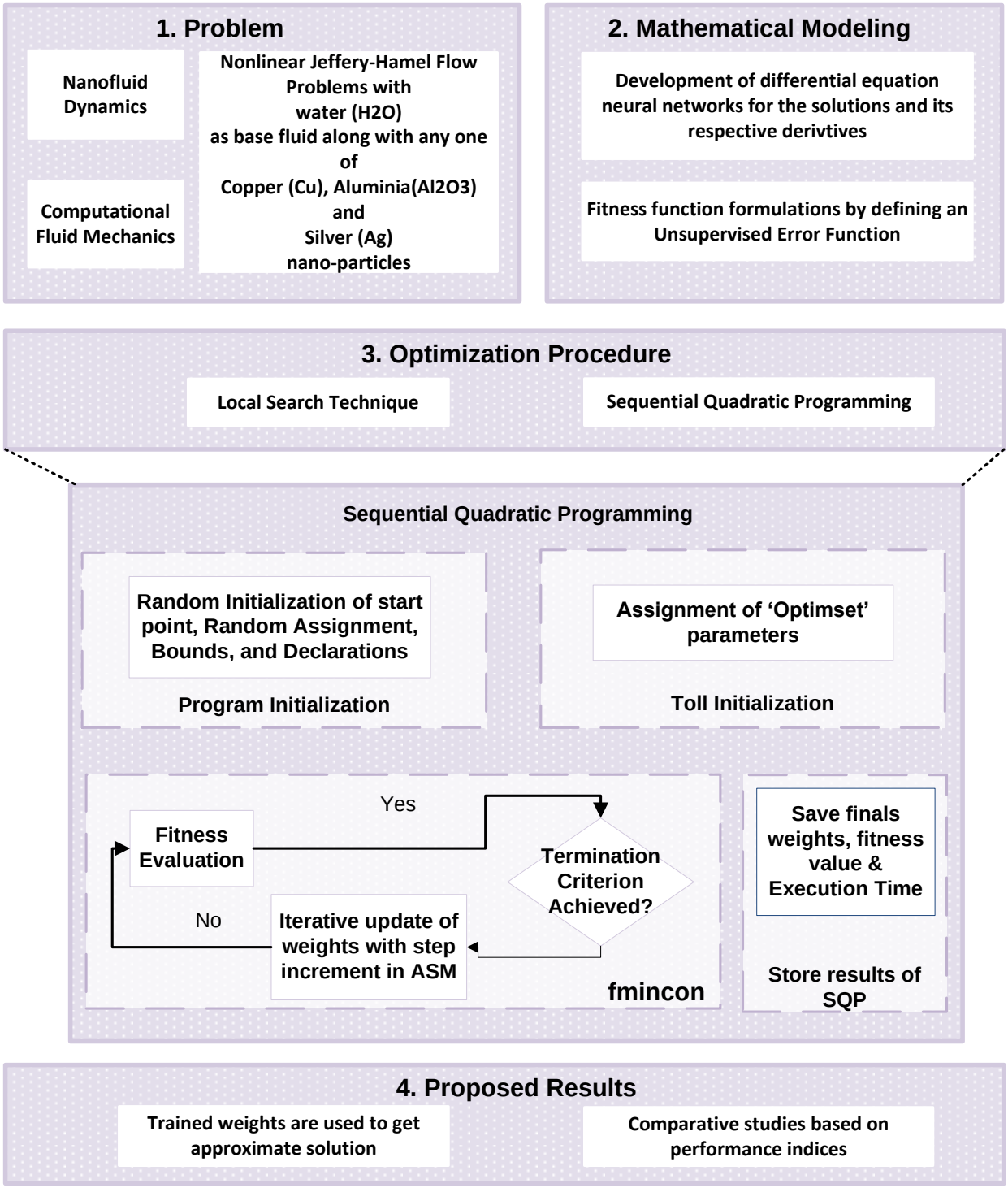

Figure 2: Workflow diagram of proposed methodology to solve nonlinear MHD-JHF system involving nanoparticles.

Design parameters of all three DE-NNM-LS, DE-NNM-RB, and DE-NNM-TS are determined by development of the fitness function based on sum of two mean square error functions as:

$$\varepsilon = \varepsilon_1 + \varepsilon_2, \tag{23}$$

where ε_1 and ε_2 are the error functions for the main body of the equation () and its associated conditions, respectively. The mathematical expressions for ε_1 and ε_2 are respectively given as:

$$\varepsilon_1 = \frac{1}{N}\sum_{m=1}^{N}\left(\begin{array}{l}\hat{f}_m''' + 2\alpha\,\mathrm{Re}\left[(1-\varphi)^{2.5}\left(1-\varphi+\varphi\frac{\rho_s}{\rho_f}\right)\right]\hat{f}_m\hat{f}_m' \\ +(4-(1-\varphi)^{1.25}H)\alpha^2\hat{f}_m'\end{array}\right)^2. \tag{24}$$

for,

$$\eta \in (0,1),\ N = \frac{1}{h},\ \hat{f}_m = \hat{f}(\eta_m),\ \eta_m = mh.$$

and

$$\varepsilon_2 = \frac{1}{3}\left(\left(\hat{f}_0 - 1\right)^2 + \left(\hat{f}_0'\right)^2 + \left(\hat{f}_N\right)^2\right). \tag{25}$$

The generic model of MHD-JHF using any of DE-NNM is given in Figure 3.

3.2 Learning procedure with SQP algorithm

In order to study the dynamics of the system, optimization problem based on the fitness function ε given in equation (23) is conducted using SQP for all three DE-NNMs for finding the solution of nonlinear MHD-JHF problems. SQP algorithm is one of the prominent local search procedure for finding the solution of nonlinear constrained optimization problems [76-78]. Like other optimization techniques, SQP is not just a single procedure, but a significant concrete routine from which various explicit algorithms have been developed. Few potential applications of SQP include multi-material topology optimization [79], profile error evaluation of free-form surface [80], optimal energy management systems [81] and fractal image compression [82]. The built-in

software package 'fimincon' with algorithms SQP available in Matlab optimization toolbox is used for finding the weights of ANN models. Fixed setting of the SQP algorithm is taken for all three DE-NNMs of nonlinear MHD-FHF problem and its pseudocode is given in Table 1.

Table 1: Pseudocode for SQP for optimization of DE-NNMs of nonlinear MHD-FHF problem

Start: SQP method through 'fmincon' function of Matlab optimization toolbox

Inputs:

Unknown weight vector $\boldsymbol{W}$ of system is represented with individual S as:

$$S = [\delta_1, \delta_2, ..., \delta_m, w_1, w_2, ..., w_m, \beta_1, \beta_2, ..., \beta_m],$$

Set of S creates population P as:

$$I = [\boldsymbol{S}_1, \boldsymbol{S}_2, ..., \boldsymbol{S}_k]^t = \begin{bmatrix} (\delta_1, \delta_2, ..., \delta_m, w_1, w_2, ..., w_m, \beta_1, \beta_2, ..., \beta_m)_1 \\ (\delta_1, \delta_2, ..., \delta_m, w_1, w_2, ..., w_m, \beta_1, \beta_2, ..., \beta_m)_2 \\ \vdots \\ (\delta_1, \delta_2, ..., \delta_m, w_1, w_2, ..., w_m, \beta_1, \beta_2, ..., \beta_m)_k \end{bmatrix},$$

for k no of individuals in S and t is used for transpose.

Output: The best individual by SQP, *i.e.*, $\boldsymbol{S}_b$

Begin:

```
//Initialization step
   Randomly generate individuals as a start point.
//Termination step
   Set stopping criteria parameters as:
         The value of maximum iterations (MaxIter), i.e., MaxIter
         → 1000,
         TolFun → 10^-20,
         TolCon → 10^-20, and
         Tolerance in the variables (TolX) values, i.e., TolX →
         10^-15,
// the settings of SQP parameters are given in 'optimset' routine.
While {fulfillment of any of stopping criteria} do %
   //Fitness step
         Calculate fitness ε values using equation (23) and its
         parts given in equations (24) and (25).
   // Stopping criteria step
         If any of termination criteria attained, exit while loop
         else continues.
   //Refinement step
         Refine the random values of the weight vector at each
         step increment in SQP procedure.
   Repeat the procedure from fitness step with updated weight
   vector
  End
//Storage step
      Save the final weight vector and its fitness value, time,
      cycles consumed and function evaluated for the current run of
      the SQP method.
```

End

Statistics: Repeat the procedure for finding the appropriate parameter of ODEs using hybrid optimization procedure SQP for multiple independent runs to generate a sufficient large dataset for effective analysis of performance.

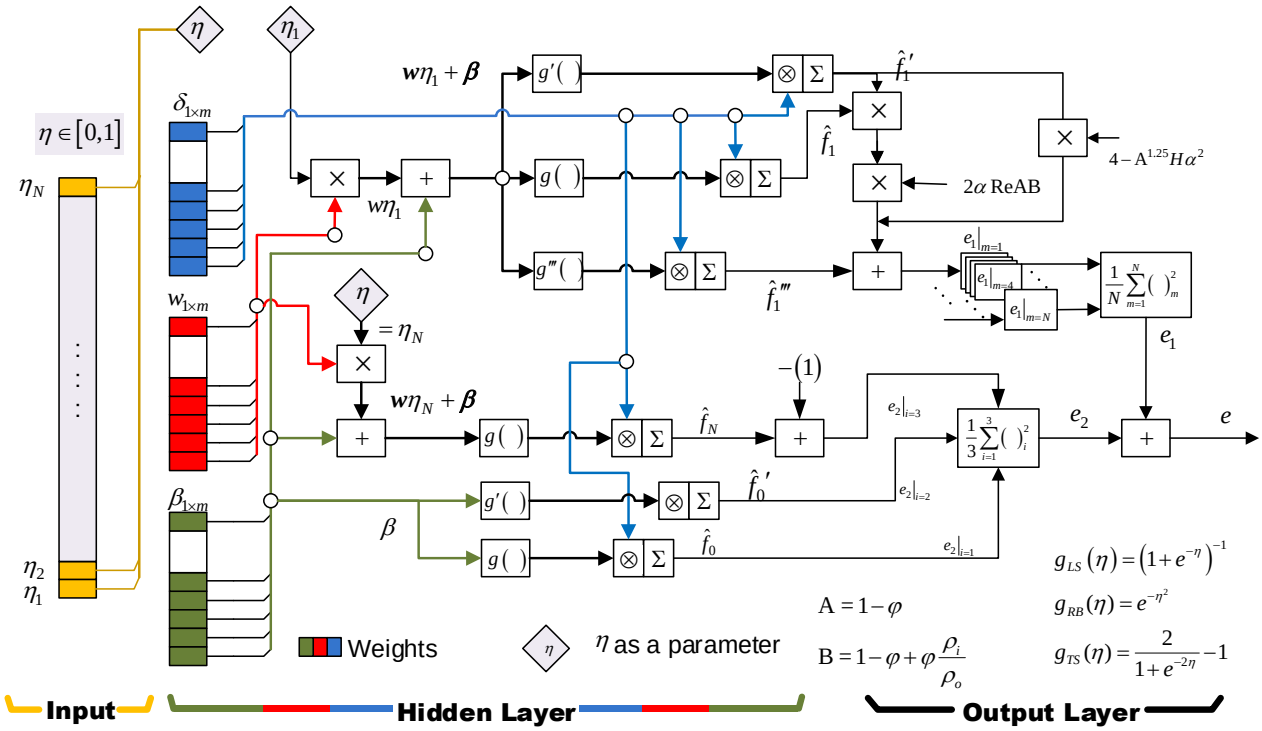

Figure 3: Neural network architecture for nonlinear MHD-JHF problem

3.3 Performance Measures

For the validation of the performance of the proposed scheme, five performance operator on the basis of the MAE, RMSE, NSE, EVAF and TIC are computed. Mathematical formulations for these performance indices for MHD-JHF are written as:

$$\begin{bmatrix} MAE_f & RMSE_f \\ NSE_f & TIC_f \\ VAF_f & \varepsilon \end{bmatrix} = \begin{bmatrix} \frac{1}{m}\sum_{i=1}^{m}\left| f_i - \hat{f} \right| & \sqrt{\frac{1}{m}\sum_{i=1}^{m}\left(f_i - \hat{f}_i \right)^2} \\ 1 - \frac{\sum_{i=1}^{m}(f_i - \hat{f}_i)^2}{\sum_{i=1}^{m}(f_i - \bar{f})^2} & \frac{\sqrt{\frac{1}{m}\sum_{i=1}^{m}\left(f_i - \hat{f}_i \right)^2}}{\sqrt{\frac{1}{m}\sum_{i=1}^{m} f_i^2} + \sqrt{\frac{1}{m}\sum_{i=1}^{m} \hat{f}_i^2}} \\ 1 - \frac{\mathrm{var}(f - \hat{f})}{\mathrm{var}(f)} & \varepsilon_1 + \varepsilon_2 \end{bmatrix} \quad \textbf{(26)}$$

$$\begin{bmatrix} ENSE_f & EVAF_f \end{bmatrix} = \begin{bmatrix} \left|1 - NSE_f\right| & 100 - VAF_f \end{bmatrix}. \quad \textbf{(27)}$$

Here, m stands for the number of input grid points, the reference Adam's numerical method results f, and their mean values, $\bar{f}$, and computed solutions $\hat{f}$, respectively. For an ideal system, the required magnitudes of performance indicators based on MAE, RMSE, ENSE, EVAF, and TIC are zero.

4. Numerical Simulations and Results

In this section, the proposed methodology is applied to three nonlinear MHD-JHF problems with four scenarios by variation in the channel angles α, Reynolds number *Re*, concentration of nanoparticles φ and Hartman number *H*. The details for the cases and scenarios are given in Table 2. The dynamics of nonlinear MHD-JHF is analyzed for both convergent and divergent channels for different base fluids and nanoparticles.

Table 2: A set of parameter α, *Re*, φ and *H* for each variation in nonlinear MHD-JHF systems

Cases	**Scenario 1**				**Scenario 2**				**Scenario 3**				**Scenario 4**			
	α	***Re***	φ	***H***	α	***Re***	φ	***H***	α	***Re***	φ	***H***	α	***Re***	φ	***H***
c-1	2	100	0.1	250	6	50	0.1	250	6	50	0.1	250	6	50	0.1	250
c-2	5	100	0.1	250	6	100	0.1	250	5	50	0.1	500	5	50	0.3	250
c-3	8	100	0.1	250	5	150	0.1	250	5	50	0.1	1000	5	50	0.5	250
d-1	-2	100	0.1	250	-6	50	0.1	250	-6	50	0.1	250	-6	50	0.1	250
d-2	-5	100	0.1	250	-6	100	0.1	250	-5	50	0.1	500	-5	50	0.3	250
d-3	-8	100	0.1	250	-5	150	0.1	250	-5	50	0.1	1000	-5	50	0.5	250

Problem 4.1: *Study the dynamics of nonlinear MHD-JHF with base fluid water mixed with alumina nanoparticles*: In this problem, the dynamics of nonlinear MHD-JHF with base fluid water and alumina nanoparticles is analyzed in case of four scenarios as listed in Table 2 for convergent and divergent cases. The governing mathematical relation derived from equations (5-6) using $\rho_s = 3970$, $\rho_f = 997$ for the problem is written as:

$$f'''(\eta) + 2\alpha \,\mathrm{Re}(1-\varphi)^{2.5}(1-\varphi+3.918\varphi)\, f(\eta)\, f'(\eta) + \left(4-(1-\varphi)^{1.25} H\right)\alpha^2 f'(\eta) = 0 \quad \textbf{(28)}$$

with boundary conditions:

$$f(0)=1,\ f'(0)=0,\ f(1)=0. \quad \textbf{(29)}$$

The exact solution for equations (28-29) is difficult to obtained, therefore, the reference numerical solution is obtained with the help of Adams method (AM) and these results are used for comparison throughout in the study.

The proposed stochastic numerical methodology is also applied to solve the equations (28-29) as per procedure given in the last section, while the fitness function for this problem is given in case of inputs $\eta \in [0,1]$ with step size $h = 0.1$ as:

$$\begin{aligned}\varepsilon = \frac{1}{11}\sum_{m=0}^{10}\left(\hat{f}_m''' + 2\alpha\,\mathrm{Re}(1-\varphi)^{2.5}(1-\varphi+3.9819\varphi)\,\hat{f}_m\,\hat{f}_m' + (4-H(1-\varphi)^{1.25})\alpha^2\,\hat{f}_m'\right)^2 \\ + \frac{1}{3}\left(\left(\hat{f}_0-1\right)^2 + \left(\hat{f}_0'\right)^2 + \left(\hat{f}_{10}\right)^2\right).\end{aligned} \quad \textbf{(30)}$$

Optimization of fitness function ε as given in (30) is carried out by SQP algorithms as per settings and procedure described in the last section. The proposed three DE-NNM-LS, DE-NNM-RB and DE-NNM-LS are executed with SQP for 100 independent runs to get the appropriate weight vectors *W* and these weights are used in equations (14), (17) and (20) to find

the respective approximate solution of the problem. The proposed results are compared with reference numerical solutions of AM on the basis of MAE, RMSE, EVAF, ENSE and TIC as defined in equations (27-28). The best run of the model is defined on the basis of minimum values of these five measures and results in term of best runs out of 100 independent executions for each case of problem 1 for all three models are given in Table 3.

A set of weight trained through best runs of SQP for NNM-LS (NNM-LS-SQP), NNM-RB(NNM-RB-SQP) and NNM-TS (NNM-TS-SQP) for both convergent and divergent cases of scenario 1 are given graphically in Fig. 4 (a), (b) and (c), respectively. These weights are used in equations (14), (17) and (20) to derive the approximate solutions $\hat{f}_{LS}$, $\hat{f}_{RB}$ and $\hat{f}_{TS}$ of the problem (28). In first case of convergent flow, c-1, the derived solutions for NNM-LS-SQP, NNM-RB-SQP and NNM-TS-SQP are given as:

$$\begin{aligned}\hat{f}_{LS}(\eta) = {} & \frac{-2.166}{1+e^{-(-1.800\eta-1.235)}} + \frac{3.456}{1+e^{-(-3.498\eta+7.950)}} + \frac{-2.231}{1+e^{-(-2.167\eta-0.429)}} + \frac{3.676}{1+e^{-(-2.208\eta+0.869)}} + \\ & \frac{-1.589}{1+e^{-(1.461\eta-1.196)}} + \frac{-1.949}{1+e^{-(2.506\eta-0.317)}} + \frac{-2.102}{1+e^{-(0.599\eta-1.354)}} + \frac{-0.091}{1+e^{-(-1.619\eta-0.108)}} + \\ & \frac{-0.841}{1+e^{-(-1.660\eta+0.675)}} + \frac{-2.575}{1+e^{-(-2.086\eta-0.262)}}\end{aligned}, \quad \textbf{(31)}$$

$$\begin{aligned}\hat{f}_{RB}(\eta) = {} & -5.173e^{-(0.028\eta-0.180)^2} - 2.796e^{-(1.061\eta-0.162)^2} - 0.582e^{-(-1.555\eta+1.944)^2} \\ & -4.829e^{-(-0.027\eta-0.111)^2} + 13.090e^{-(0.820\eta-1.396)^2} - 2.189e^{-(-0.841\eta+3.252)^2} \\ & -5.349e^{-(0.619\eta-0.931)^2} + 9.532e^{-(-0.382\eta-0.321)^2} - 1.287e^{-(0.906\eta-1.483)^2} \\ & -1.269e^{-(-1.505\eta+2.617)^2}\end{aligned}, \quad \textbf{(32)}$$

$$\hat{f}_{TS}(\eta) = -7.311 + \frac{-0.696}{1+e^{-2(-1.728\eta-0.780)}} + \frac{0.058}{1+e^{-2(3.567\eta+1.568)}} + \frac{0.633}{1+e^{-2(1.579\eta+0.267)}} + \frac{1.718}{1+e^{-2(-0.471\eta-1.518)}} + \frac{0.305}{1+e^{-2(1.511\eta-1.046)}} + \frac{-2.770}{1+e^{-2(-0.911\eta+3.162)}} + \frac{-0.965}{1+e^{-2(1.297\eta-0.817)}} + \frac{2.547}{1+e^{-2(-0.558\eta-0.466)}} + \frac{2.263}{1+e^{-2(-1.423\eta+3.243)}} + \frac{-3.134}{1+e^{-2(-1.532\eta-2.444)}} \quad \textbf{(33)}$$

While for first case of divergent flow d-1, the derived solutions are given as:

$$\hat{f}_{LS}(\eta) = \frac{-9.268}{1+e^{-(-2.413\eta-3.708)}} + \frac{1.039}{1+e^{-(0.268\eta+0.739)}} + \frac{8.323}{1+e^{-(3.905\eta-7.277)}} + \frac{8.750}{1+e^{-(-1.064\eta-2.174)}} + \frac{1.148}{1+e^{-(-1.351\eta-0.229)}} + \frac{9.712}{1+e^{-(0.978\eta-4.457)}} + \frac{-14.430}{1+e^{-(-1.505\eta-1.588)}} + \frac{10.958}{1+e^{-(-1.719\eta-1.813)}} + \frac{7.868}{1+e^{-(2.902\eta-7.543)}} + \frac{-15.295}{1+e^{-(2.922\eta-5.072)}}, \quad \textbf{(34)}$$

$$\hat{f}_{RB}(\eta) = 7.999e^{-(0.555\eta+0.043)^2} - 3.513e^{-(0.435\eta+0.549)^2} + 10.529e^{-(0.761\eta-2.744)^2} + 18.450e^{-(0.747\eta-2.437)^2} + 3.537e^{-(-0.088\eta-0.885)^2} - 3.992e^{-(1.001\eta-1.691)^2} - 9.754e^{-(-1.332\eta+2.944)^2} + 0.190e^{-(-1.519\eta+1.567)^2} - 5.902e^{-(0.772\eta+2.096)^2} - 5.779e^{-(-0.674\eta+0.043)^2}, \quad \textbf{(35)}$$

$$\hat{f}_{TS}(\eta) = -7.311 + \frac{2.376}{1+e^{-2(0.885\eta+0.764)}} + \frac{-3.047}{1+e^{-2(1.166\eta-1.607)}} + \frac{0.655}{1+e^{-2(-1.417\eta-0.663)}} + \frac{-1.212}{1+e^{-2(0.913\eta-0.082)}} + \frac{1.067}{1+e^{-2(0.278\eta+0.231)}} + \frac{-1.142}{1+e^{-2(-0.209\eta+0.869)}} + \frac{2.809}{1+e^{-2(0.420\eta-1.017)}} + \frac{0.110}{1+e^{-2(0.995\eta-1.053)}} + \frac{2.356}{1+e^{-2(-0.595\eta-2.112)}} + \frac{-2.050}{1+e^{-2(1.819\eta-2.706)}} \quad \textbf{(36)}$$

Similarly the solutions are determined for each case of all four scenarios of the problems and respective results are given graphically in Figs. 5(a), 5(c), 5(e) and 5(g) for NNM-LS-SQP by taking the inputs $\eta \in [0, 1]$ with step size h = 0.05 along with the result of AM. It is seen that proposed solutions are consistently overlapping the reference solution for each case of all four scenarios. In order to analyze the accuracy of the proposed method. the values of Absolute Error (AE) are also calculated for $\eta \in [0,1]$ with step size h = 0.05 and results are plotting in Figs. 5(b),

5(d), 5(f) and 5(i) for scenarios 1, 2, 3, and 4, respectively, of the problem. Accordingly, the AE calculated by the algorithms NNM-RB-SQP and NNM-TS-SQP. Results of NNM-RB-SQP algorithm are shown graphically in Figs. 6(a), (c), (e) and (g) for scenarios 1, 2, 3 and 4, respectively, while the respective results of NNM-TS-SQP approach is presented in Figs. 6(b), 6(d), 6(f) and 6(i). It is seen that the values of velocity profile of the fluid for the convergent channel decrease with increase in the values of angle of the channel $\alpha = 2$ to 8 while in case of divergence channel for $\alpha = -2$ to -8 decreased in the rate velocity profile of the fluid is observed. Accordingly, for scenario 2 with the increase in Reynolds number the velocity of fluid decreases and with the decrease in Reynolds number the velocity of the fluid increases, In case of scenario 3 with the increase in magnetic effect the velocity profile increases and in case of scenario 4 the decrease in concentration of nanoparticles the velocity of fluid decreases. Additionally with the change in angle of channel, concentration of nanoparticles, Reynolds and Hartman numbers the behavior of both results for proposed models is on a similar pattern as reference numerical method. Comparison of the accuracy of all three models based on values of AEs shows that results for convergent channel for each scenarios is relatively better from divergent channels.

Table 3: List of best independent runs of the algorithms on different performance indices

Problem	Scenario	Case	ANN-LS-SQP					ANN-RB-SQP					ANN-TS-SQP				
			MAE	RMSE	EVAF	ENSE	TIC	MAE	RMSE	EVAF	ENSE	TIC	MAE	RMSE	EVAF	ENSE	TIC
4.1	1	c-1	15	15	16	15	15	47	47	29	47	47	7	7	88	7	7
		c-2	2	43	43	43	43	71	71	36	71	71	71	71	49	71	71
		c-3	16	16	16	16	16	66	66	66	66	66	40	7	49	7	7
		d-1	37	37	15	37	37	15	15	6	15	15	66	66	90	66	66
		d-2	53	53	65	53	53	15	15	3	15	15	50	50	32	50	50
		d-3	42	24	24	24	24	13	13	13	13	13	95	95	95	95	95
	2	c-2	24	24	75	24	24	6	6	9	6	6	94	94	94	94	94
		c-3	22	22	22	22	22	96	96	96	96	96	27	27	27	27	27
		d-2	12	12	12	12	12	18	18	28	18	18	86	86	86	86	86
		d-3	10	10	45	10	10	100	100	100	100	100	74	74	83	74	74
	3	c-2	83	83	72	83	83	2	2	18	2	2	94	94	92	94	94
		c-3	69	69	59	69	69	3	3	3	3	3	72	72	72	72	72
		d-2	79	79	35	79	79	85	85	85	85	85	70	70	76	70	70
		d-3	84	84	84	84	84	60	60	60	60	60	53	70	40	70	70
	4	c-2	55	55	7	55	55	70	70	70	70	70	76	76	72	72	76
		c-3	27	27	27	27	27	19	32	40	32	32	29	29	29	29	29
		d-2	95	95	95	95	95	3	3	3	3	3	47	47	47	47	47
		d-3	82	82	84	82	82	13	13	13	13	13	50	50	14	50	50
4.2	1	c-1	3	3	3	3	3	7	7	7	7	7	51	51	64	51	51
		c-2	17	17	17	17	17	25	25	25	25	25	57	57	57	57	57
		c-3	36	36	15	36	36	8	8	8	8	8	68	68	68	68	68
		d-1	52	52	15	52	52	44	44	44	44	44	71	71	71	71	71
		d-2	26	26	26	26	26	74	74	74	74	74	88	88	88	88	88
		d-3	67	67	67	67	67	49	49	49	49	49	95	95	68	95	95
	2	c-2	25	25	25	25	25	10	10	3	10	10	93	93	93	93	93
		c-3	70	70	70	70	70	84	84	84	84	84	28	28	28	28	28
		d-2	88	88	23	88	88	4	4	4	4	4	50	50	40	50	50
		d-3	53	53	53	53	53	95	95	95	95	95	29	29	29	29	29
	3	c-2	48	48	76	48	48	86	86	73	86	86	73	73	73	73	73
		c-3	74	74	44	74	74	58	58	58	58	58	80	80	80	80	80
		d-2	26	26	26	26	26	91	91	53	91	91	64	64	64	64	64
		d-3	65	65	65	65	65	94	94	94	94	94	39	39	68	39	39
	4	c-2	37	37	37	37	37	2	2	44	2	2	60	60	15	60	60
		c-3	82	82	61	82	82	74	74	74	74	74	40	40	35	40	40
		d-2	84	84	84	84	84	74	74	74	74	74	74	53	53	53	53
		d-3	97	97	97	97	97	66	66	66	66	66	91	91	91	91	91
4.3	1	c-1	7	7	42	7	7	61	61	61	61	61	58	58	58	58	58
		c-2	39	39	48	39	39	24	41	41	41	41	15	15	15	15	15
		c-3	97	97	58	97	97	99	99	99	99	99	19	19	19	19	19
		d-1	22	22	53	22	22	58	58	69	58	58	53	53	53	53	53
		d-2	40	40	40	40	40	53	53	33	53	53	27	27	27	27	27
		d-3	74	74	74	74	74	78	78	78	78	78	85	85	85	85	85
	2	c-2	87	87	46	87	87	42	42	42	42	42	37	37	37	37	37
		c-3	5	5	5	5	5	42	42	62	42	42	38	38	38	38	38
		d-2	84	84	44	84	84	48	48	48	48	48	10	10	10	10	10
		d-3	34	34	24	34	34	6	6	100	6	6	49	73	73	73	73
	3	c-2	52	52	64	52	52	62	62	14	62	62	16	16	16	16	16
		c-3	81	81	81	81	81	99	96	30	96	96	55	52	52	52	52
		d-2	79	79	79	79	79	98	98	98	98	98	95	95	25	95	95
		d-3	70	70	70	70	70	67	67	67	67	67	93	93	85	93	93
	4	c-2	19	25	25	25	25	47	47	47	47	47	40	40	54	40	40
		c-3	26	26	45	26	26	27	27	9	27	27	20	20	20	20	20
		d-2	56	56	56	56	56	61	61	99	61	61	26	26	26	26	26
		d-3	72	72	72	72	72	21	21	21	21	21	14	14	14	14	14

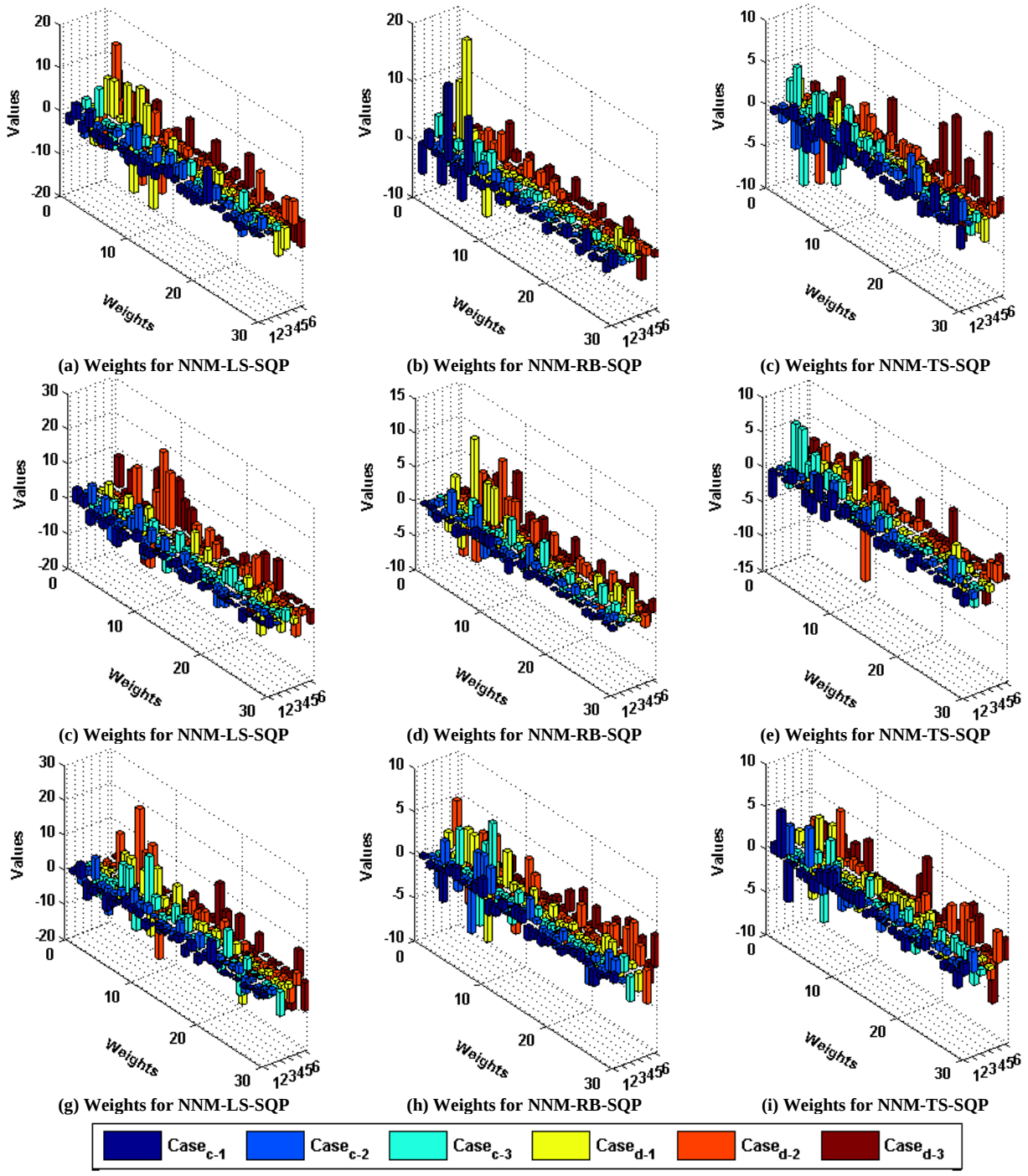

Figure 4: One set of weight vector of DE-NNM-LS, DE-NMM-RB, DE-NMM-TS for scenario 1 for all six cases of nonlinear MHD-JHF problems, Figs. (a-c), Figs. (d-f) and Figs. (g-i) for problem 1, 2 and 3, respectively.

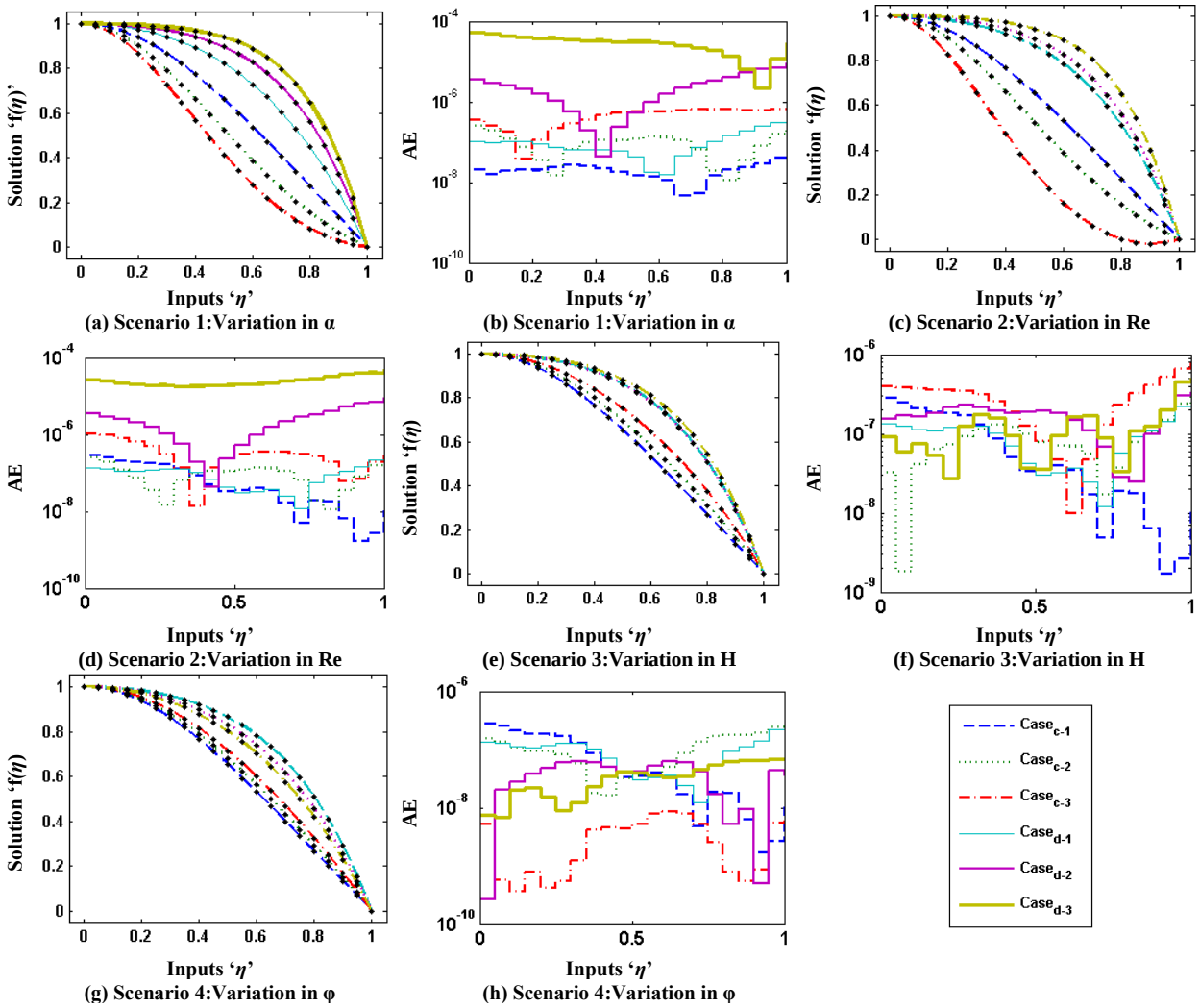

Figure 5: Proposed results of NNM-LS-SQP for nonlinear MHD-JHF problem 4.1**;** Figs. (a, c, e, g) for the approximate solution and Figs. (b, d, f, h) for AEs.

Results of statistical analysis based on 100 independent runs of each model in terms of mean and standard deviation (STD) values are determined in order to analyze the accuracy and convergence. These results are listed in Table 4 for inputs $\eta \in [0.1, 0.9]$ with step size h = 0.2 for all three NNM-LS-SQP, NNM-LS-SQP and NNM-LS-SQP approaches for each case of all four scenarios of problem 1. It seems that the values of mean are generally lies between 10^{-03} to 10^{-06} for all three algorithms, but the values of these statistical measures are relatively better for NNM-LS-SQP and NNM-TS-SQP from NNM-RB-SQP, while comparing the performance of NNM-

LS-SQP and NNM-TS-SQP algorithm, the results of NNM-TS-SQP are slightly superior. Additionally, it is observed that in case of convergent channel results are obtained with better precision than that of divergent channel. The small values STD further validate the consistency of the all three algorithms for finding the solution of nonlinear MHD-JHF model as given in equations (28-29).

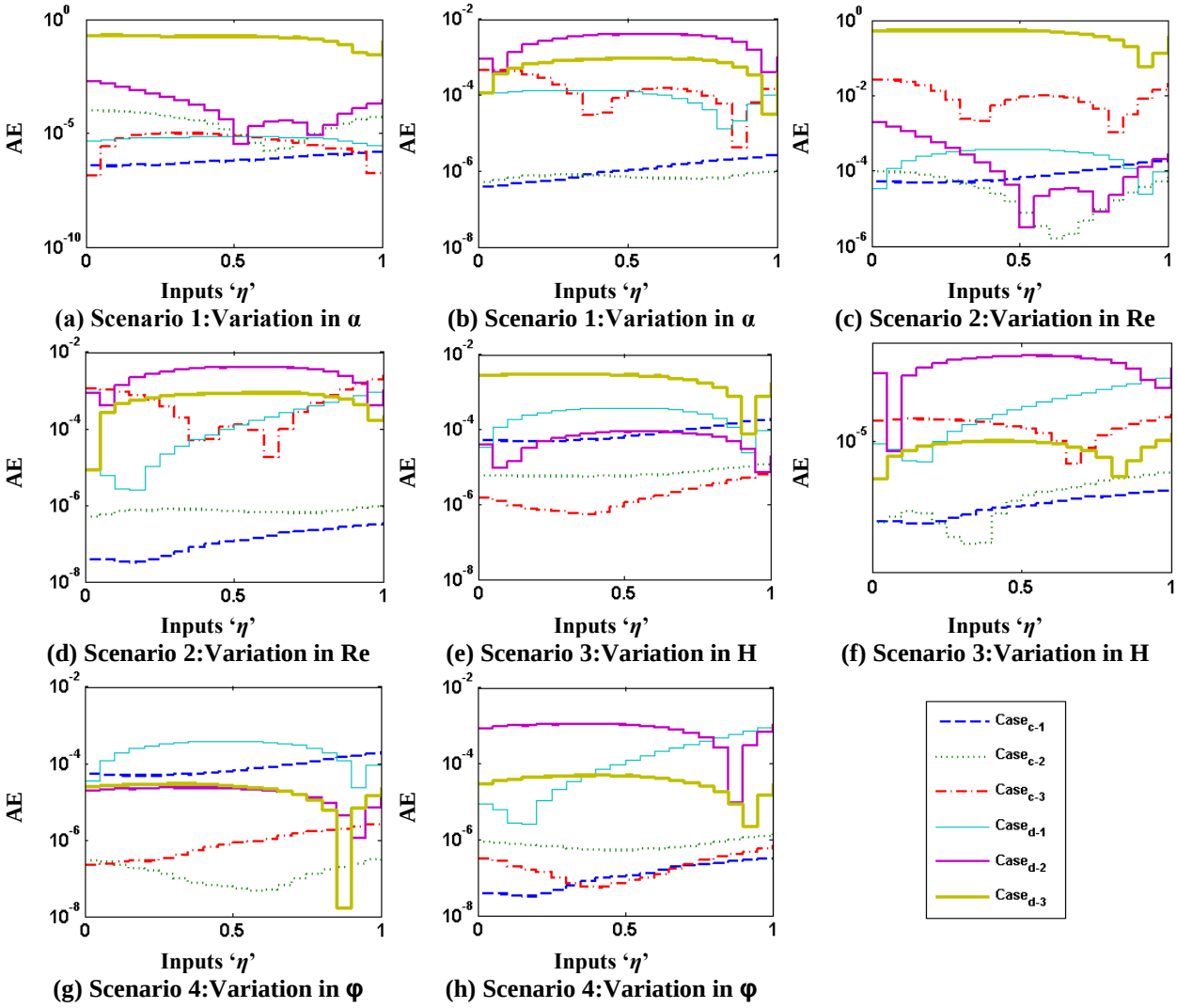

Figure 6: Plots of AEs of for nonlinear MHD-JHF in problem 4.1; Figs. (a, c, e, g) for NNM-RB-SQP and Figs. (b, d, f, h) for NNM-TS-SQP.

Table 4: Comparison of the statistical results through mean and STD for Problem 4.1

NNM	Scenario	Case	Mean of AEs for inputs η					STD of AEs for inputs η				
			$\eta = 0.1$	$\eta = 0.3$	$\eta = 0.5$	$\eta = 0.7$	$\eta = 0.9$	$\eta = 0.1$	$\eta = 0.3$	$\eta = 0.5$	$\eta = 0.7$	$\eta = 0.9$
LS	1	c-1	1.94E-06	1.57E-06	1.38E-06	2.30E-06	3.70E-06	3.12E-06	2.54E-06	2.00E-06	3.06E-06	5.39E-06
		c-2	3.00E-05	2.18E-05	1.40E-05	1.41E-05	2.28E-05	5.70E-05	4.31E-05	3.02E-05	3.07E-05	4.87E-05
		c-3	3.97E-05	2.24E-05	1.40E-05	2.22E-05	3.74E-05	7.95E-05	4.58E-05	3.18E-05	5.46E-05	9.27E-05
		d-1	1.56E-05	1.65E-05	1.49E-05	9.88E-06	4.37E-06	4.38E-05	4.57E-05	4.04E-05	2.61E-05	6.63E-06
		d-2	1.01E-03	1.69E-03	1.86E-03	1.56E-03	4.46E-04	1.20E-03	2.27E-03	2.58E-03	2.18E-03	5.87E-04
		d-3	6.48E-03	7.44E-03	7.42E-03	6.36E-03	2.86E-03	2.22E-02	2.20E-02	2.09E-02	1.63E-02	8.86E-03
	2	c-2	1.33E-05	1.07E-05	7.14E-06	7.44E-06	1.36E-05	4.17E-05	3.22E-05	1.88E-05	1.55E-05	2.84E-05
		c-3	1.46E-04	6.28E-05	1.40E-05	2.25E-05	7.07E-05	8.73E-04	3.75E-04	3.64E-05	6.12E-05	3.35E-04
		d-2	2.90E-04	3.92E-04	3.97E-04	2.94E-04	9.12E-05	1.20E-03	1.85E-03	1.97E-03	1.54E-03	3.50E-04
		d-3	1.13E-02	1.21E-02	1.16E-02	8.94E-03	2.46E-03	6.35E-02	6.29E-02	5.85E-02	4.30E-02	8.16E-03
	3	c-2	6.71E-06	5.31E-06	3.66E-06	4.77E-06	1.02E-05	1.37E-05	1.06E-05	6.65E-06	1.31E-05	2.68E-05
		c-3	6.88E-05	6.23E-05	4.35E-05	1.75E-05	3.70E-05	1.06E-04	9.19E-05	6.18E-05	2.98E-05	6.15E-05
		d-2	1.76E-04	1.90E-04	1.75E-04	1.18E-04	3.47E-05	7.68E-04	7.90E-04	7.04E-04	4.53E-04	1.29E-04
		d-3	6.66E-04	1.02E-03	1.07E-03	8.42E-04	2.02E-04	1.56E-03	2.63E-03	2.86E-03	2.30E-03	4.96E-04
	4	c-2	8.45E-06	7.01E-06	4.76E-06	5.23E-06	1.00E-05	2.01E-05	1.72E-05	1.15E-05	9.94E-06	1.86E-05
		c-3	2.43E-06	2.00E-06	1.57E-06	1.30E-06	2.15E-06	5.39E-06	4.64E-06	3.33E-06	2.59E-06	4.33E-06
		d-2	2.50E-05	2.60E-05	2.33E-05	1.54E-05	7.68E-06	7.42E-05	7.73E-05	6.85E-05	4.42E-05	1.71E-05
		d-3	5.28E-06	5.00E-06	4.08E-06	2.51E-06	3.38E-06	1.34E-05	1.24E-05	9.23E-06	4.93E-06	9.42E-06
RB	1	c-1	2.23E-05	2.19E-05	2.48E-05	4.62E-05	7.72E-05	8.78E-05	9.96E-05	1.72E-04	2.99E-04	4.79E-04
		c-2	1.84E-05	1.33E-05	8.42E-06	8.11E-06	1.28E-05	3.05E-05	2.24E-05	1.31E-05	1.16E-05	1.83E-05
		c-3	9.50E-04	5.56E-04	3.03E-04	4.62E-04	9.13E-04	4.40E-03	2.86E-03	1.73E-03	2.34E-03	5.27E-03
		d-1	1.23E-04	1.32E-04	1.24E-04	9.40E-05	3.06E-05	2.85E-04	3.05E-04	2.83E-04	2.08E-04	5.43E-05
		d-2	3.55E-03	3.68E-03	3.31E-03	2.01E-03	1.79E-03	2.66E-02	2.57E-02	2.16E-02	1.07E-02	1.51E-02
		d-3	2.46E-02	2.52E-02	2.41E-02	1.88E-02	5.14E-03	7.06E-02	7.11E-02	6.66E-02	4.97E-02	1.69E-02
	2	c-2	7.72E-05	4.69E-05	5.43E-05	1.20E-04	2.15E-04	2.74E-04	1.15E-04	2.59E-04	6.85E-04	1.21E-03
		c-3	1.09E-03	3.87E-04	3.58E-04	6.77E-04	9.31E-04	5.20E-03	1.66E-03	2.04E-03	3.98E-03	4.60E-03
		d-2	3.81E-04	4.55E-04	4.46E-04	3.26E-04	5.18E-05	1.29E-03	1.41E-03	1.34E-03	9.80E-04	1.07E-04
		d-3	3.39E-02	3.40E-02	3.24E-02	2.56E-02	5.87E-03	9.38E-02	9.35E-02	8.84E-02	6.89E-02	1.76E-02
	3	c-2	3.81E-05	2.93E-05	1.77E-05	2.62E-05	6.00E-05	3.71E-05	3.12E-05	2.09E-05	2.99E-05	5.27E-05
		c-3	6.42E-05	5.68E-05	3.33E-05	3.40E-05	8.02E-05	7.96E-05	6.46E-05	3.62E-05	6.02E-05	1.57E-04
		d-2	3.99E-04	4.50E-04	4.27E-04	3.02E-04	4.54E-05	1.75E-03	1.93E-03	1.80E-03	1.24E-03	1.41E-04
		d-3	6.79E-04	7.66E-04	7.35E-04	5.43E-04	1.02E-04	2.46E-03	2.04E-03	1.80E-03	1.31E-03	2.22E-04
	4	c-2	1.21E-05	9.50E-06	7.10E-06	8.44E-06	1.64E-05	1.49E-05	1.27E-05	1.26E-05	2.19E-05	3.64E-05
		c-3	2.58E-05	2.14E-05	1.22E-05	1.37E-05	3.32E-05	1.20E-04	9.77E-05	4.90E-05	4.88E-05	1.35E-04
		d-2	1.15E-04	1.24E-04	1.14E-04	8.08E-05	2.13E-05	3.33E-04	3.47E-04	3.11E-04	2.11E-04	5.96E-05
		d-3	3.16E-05	3.26E-05	2.90E-05	1.99E-05	9.43E-06	6.59E-05	6.75E-05	5.82E-05	3.70E-05	1.95E-05
TS	1	c-1	1.93E-06	1.65E-06	1.33E-06	1.52E-06	2.61E-06	4.49E-06	3.86E-06	3.02E-06	3.32E-06	5.19E-06
		c-2	1.55E-05	1.17E-05	8.17E-06	8.07E-06	1.27E-05	5.69E-05	4.22E-05	2.84E-05	2.74E-05	4.43E-05
		c-3	1.90E-05	1.19E-05	9.19E-06	1.36E-05	2.54E-05	2.98E-05	1.88E-05	1.84E-05	3.00E-05	5.36E-05
		d-1	6.25E-06	6.44E-06	5.79E-06	3.69E-06	1.81E-06	1.28E-05	1.34E-05	1.21E-05	8.05E-06	3.09E-06
		d-2	3.90E-04	7.51E-04	8.50E-04	7.18E-04	2.13E-04	8.63E-04	1.92E-03	2.23E-03	1.91E-03	5.14E-04
		d-3	8.63E-04	1.76E-03	2.02E-03	1.89E-03	8.73E-04	5.92E-04	1.16E-03	1.34E-03	1.26E-03	6.14E-04
	2	c-2	4.16E-06	3.52E-06	2.97E-06	4.17E-06	7.40E-06	8.62E-06	6.82E-06	4.68E-06	7.38E-06	1.34E-05
		c-3	8.53E-05	3.88E-05	1.00E-05	1.81E-05	4.63E-05	2.60E-04	1.18E-04	1.77E-05	4.44E-05	1.55E-04
		d-2	2.89E-05	3.37E-05	3.30E-05	2.51E-05	1.16E-05	7.12E-05	8.93E-05	9.06E-05	7.06E-05	2.62E-05
		d-3	9.75E-04	1.82E-03	2.06E-03	1.92E-03	8.61E-04	2.04E-03	2.45E-03	2.55E-03	2.29E-03	8.85E-04
	3	c-2	5.55E-06	4.81E-06	3.69E-06	3.52E-06	6.91E-06	1.11E-05	9.52E-06	6.77E-06	7.35E-06	1.35E-05
		c-3	9.44E-06	8.46E-06	6.17E-06	2.92E-06	5.44E-06	1.37E-05	1.19E-05	8.35E-06	3.82E-06	8.43E-06
		d-2	2.29E-05	2.62E-05	2.52E-05	1.79E-05	6.54E-06	5.53E-05	6.12E-05	5.85E-05	4.33E-05	1.50E-05
		d-3	4.14E-04	6.22E-04	6.55E-04	5.17E-04	1.11E-04	1.46E-03	2.25E-03	2.39E-03	1.90E-03	4.18E-04
	4	c-2	3.88E-06	3.22E-06	1.93E-06	1.67E-06	3.40E-06	1.22E-05	1.01E-05	6.31E-06	3.48E-06	7.69E-06
		c-3	1.78E-06	1.62E-06	1.40E-06	1.10E-06	1.53E-06	2.35E-06	2.42E-06	2.30E-06	2.15E-06	2.31E-06
		d-2	1.21E-05	1.21E-05	1.04E-05	5.66E-06	6.66E-06	7.19E-05	6.72E-05	5.26E-05	2.35E-05	3.94E-05
		d-3	6.58E-07	6.53E-07	5.93E-07	4.70E-07	5.18E-07	7.83E-07	8.05E-07	7.52E-07	7.31E-07	1.09E-06

Problem 4.2: *Study the dynamics of nonlinear MHD-JHF with base fluid water mixed with silver nanoparticle*: In this problem, the dynamics of nonlinear MHD-JHF with base fluid water and silver nanoparticles is analyzed for the four scenarios with parameter as listed in Table 2. The governing mathematical relations derived from equations (5-6) using ρs = 10500 and ρf = 997 for the problem is written as:

$$\begin{aligned} &f'''(\eta)+2\alpha\,\mathrm{Re}(1-\varphi)^{2.5}(1-\varphi+10.531\varphi)\,f(\eta)\,f'(\eta)+\left(4-(1-\varphi)^{1.25}H\right)\alpha^2 f'(\eta)=0,\\ &f'(0)=0,\ f(1)=0,\ f(0)=1 \end{aligned} \tag{37}$$

The proposed stochastic numerical methodologies have also been applied to solve the equation (47) with fitness function formulation as:

$$\begin{aligned} \varepsilon=\frac{1}{11}\sum_{m=0}^{10}&\left(\begin{array}{l}\hat{f}_m'''+2\alpha\,\mathrm{Re}(1-\varphi)^{2.5}(1-\varphi+10.531\varphi)\,\hat{f}_m\hat{f}_m'+\\ (4-(1-\varphi)^{1.25}H)\alpha^2\hat{f}_m'\end{array}\right)^2\\ &+\frac{1}{3}\left(\left(\hat{f}_0-1\right)^2+\left(\hat{f}_0'\right)^2+\left(\hat{f}_{10}\right)^2\right). \end{aligned} \tag{38}$$

Optimization of the fitness function (38) is carried out with NNM-LS-SQP, NNM-RB-SQP and NNM-TS-TS methodologies for 100 independent executions. The runs of the algorithms with minimum values of five performance measures, i.e., MAE, RMSE, EVAF, ENSE and TIC, for each case of all four scenarios of problem 2 are listed in Table 3. A set of weight trained for all three models for both convergent and divergent cases of scenario 1 are given graphically in Figs 4(d), 4(e) and 4(f). The derived solution for the first case of convergent flow c-1 for ANN-LS-SQP, ANN-RB-SQP and ANN-TS-SQP are given as:

$$\hat{f}_{LS}(\eta)=\frac{3.976}{1+e^{-(-2.420\eta+0.570)}}+\frac{3.079}{1+e^{-(-2.191\eta+0.104)}}+\frac{-3.829}{1+e^{-(0.342\eta-0.481)}}+\frac{-0.825}{1+e^{-(0.865\eta-0.496)}}+\frac{-2.456}{1+e^{-(-1.073\eta-0.050)}}+\frac{1.685}{1+e^{-(1.977\eta-3.254)}}+\frac{-4.966}{1+e^{-(-2.433\eta-0.434)}}+\frac{-2.126}{1+e^{-(-2.043\eta-0.424)}}+\frac{-0.141}{1+e^{-(3.287\eta-0.458)}}+\frac{2.743}{1+e^{-(-1.482\eta+2.858)}} \quad \textbf{(39)}$$

$$\hat{f}_{RB}(\eta)=0.236e^{-(1.620\eta-0.078)^2}+0.362e^{-(-0.822\eta-0.382)^2}-1.201e^{-(-0.090\eta+0.358)^2}+0.054e^{-(-1.918\eta-0.141)^2}-0.084e^{-(-0.025\eta+0.138)^2}-1.564e^{-(0.936\eta-0.756)^2}-0.590e^{-(-0.938\eta-0.655)^2}+0.406e^{-(0.721\eta+0.346)^2}+1.385e^{-(0.589\eta-0.242)^2}+1.418e^{-(0.768\eta-0.468)^2} \quad \textbf{(40)}$$

$$\hat{f}_{TS}(\eta)=-7.311+\frac{-3.726}{1+e^{-2(-0.418\eta+0.408)}}+\frac{-0.034}{1+e^{-2(1.602\eta-1.535)}}+\frac{-0.375}{1+e^{-2(0.038\eta+1.665)}}+\frac{1.793}{1+e^{-2(0.228\eta+0.384)}}+\frac{0.134}{1+e^{-2(0.711\eta-0.014)}}+\frac{-2.011}{1+e^{-2(0.391\eta-0.688)}}+\frac{-2.403}{1+e^{-2(-1.294\eta-0.261)}}+\frac{3.479}{1+e^{-2(-1.129\eta+0.203)}}+\frac{-2.274}{1+e^{-2(0.490\eta-1.080)}}+\frac{2.408}{1+e^{-2(0.049\eta-1.588)}} \quad \textbf{(41)}$$

While for divergent flow case, d-1, the derived solutions are given as:

$$\hat{f}_{LS}(\eta)=\frac{0.991}{1+e^{-(0.004\eta+0.526)}}+\frac{3.882}{1+e^{-(0.173\eta-3.132)}}+\frac{0.814}{1+e^{-(-2.047\eta+3.022)}}+\frac{-6.350}{1+e^{-(-3.455\eta-5.040)}}+\frac{3.895}{1+e^{-(6.139\eta-11.030)}}+\frac{0.160}{1+e^{-(-1.732\eta+2.985)}}+\frac{-6.055}{1+e^{-(3.597\eta-5.263)}}+\frac{4.421}{1+e^{-(0.628\eta-6.415)}}+\frac{-0.661}{1+e^{-(-3.007\eta+1.631)}}+\frac{-0.594}{1+e^{-(3.041\eta-1.634)}} \quad \textbf{(42)}$$

$$\hat{f}_{RB}(\eta)=-5.146e^{-(0.706\eta-0.287)^2}+3.441e^{-(0.697\eta-1.036)^2}-6.397e^{-(0.442\eta+0.136)^2}-2.546e^{-(-1.486\eta+2.459)^2}+10.800e^{-(0.626\eta+0.328)^2}-3.694e^{-(0.411\eta+1.015)^2}+5.505e^{-(-0.886\eta+2.975)^2}+5.425e^{-(0.340\eta+2.975)^2}-2.788e^{-(-1.874\eta+3.481)^2}+2.337e^{-(1.038\eta-0.460)^2} \quad \textbf{(43)}$$

$$\hat{f}_{TS}(\eta) = -7.311 + \frac{-1.446}{1+e^{-2(-1.281\eta+0.245)}} + \frac{2.640}{1+e^{-2(-0.935\eta-0.054)}} + \frac{-4.075}{1+e^{-2(1.346\eta-0.725)}} + \frac{-3.863}{1+e^{-2(-1.402\eta+0.799)}} + \frac{2.211}{1+e^{-2(-2.047\eta+2.810)}} + \frac{0.692}{1+e^{-2(0.697\eta-3.325)}} + \frac{2.933}{1+e^{-2(-0.917\eta+0.870)}} + \frac{-0.141}{1+e^{-2(0.001\eta+0.073)}} + \frac{-3.440}{1+e^{-2(-0.659\eta-0.772)}} + \frac{5.677}{1+e^{-2(0.473\eta-0.971)}} \quad \textbf{(44)}$$

Similarly the solutions are determined for each case of all four scenarios of the problems and respective results are given graphically in Figs 7(a), 7(c), 7(e) and 7(g) for NNM-LS-SQP method by taking the inputs $\eta \in [0,1]$ with step size h = 0.05 along with the numerical results of AM. The values of AE are the plotted for NNM-LS-SQP in Figs. 7(b), 7(d), 7(f) and 7(h) for scenarios 1, 2, 3 and 4, respectively, of the problem. Accordingly, the AE calculated by the algorithms NNM-RB-SQP and NNM-TS-SQP are shown graphically in Fig. 8. It is seen that the values of velocity profile of the fluid for the convergent channel decrease with increase in the values of angle of the channel α while in case of divergence channel for α = -2 to -8 decreased in the rate velocity profile of the fluid is observed. Accordingly, for scenario 2 with the increase in *Re* the velocity of fluid decreases and vice versa, In case of scenario 3 with the increase in *H* the velocity profile also increases and in case of scenario 4 the decrease in concentration of nanoparticles the velocity of fluid decreases.

Statistics in terms of mean and STD values based on 100 independent runs of SQP for finding the weight of DE-NNM-LS, DE-NMM-RB and DE-NNM-TS are determined and results are listed in Table 5 for each case of all four scenarios of problem 2. It is seen that the mean values of absolute error are generally lies between 10^{-02} to 10^{-06} for all three algorithms, but the values of these statistical measures are relatively better for NNM-LS-SQP and NNM-TS-SQP approaches from NNM-RB-SQP method while comparing the performance of NNM-LS-SQP

and NNM-TS-SQP algorithm, the results of NNM-TS-SQP are better. In this case also results of convergent channels have better precision than that of divergent channels.

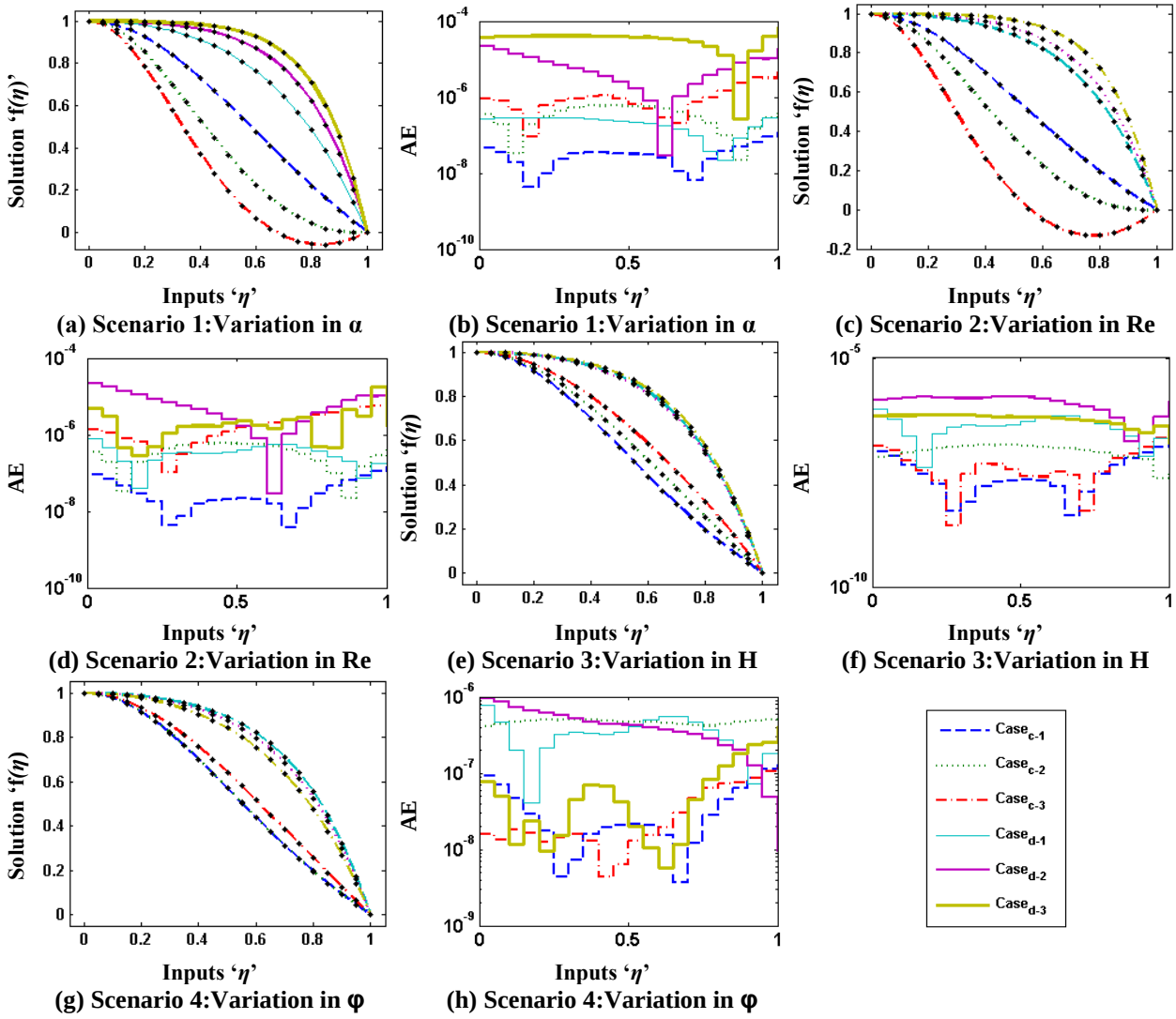

Figure 7*:* Proposed results of NNM-LS-SQP for nonlinear MHD-JHF problem 4.2; Figs. (a, c, e, g) for the approximate solution and Figs. (b, d, f, h) for AEs.

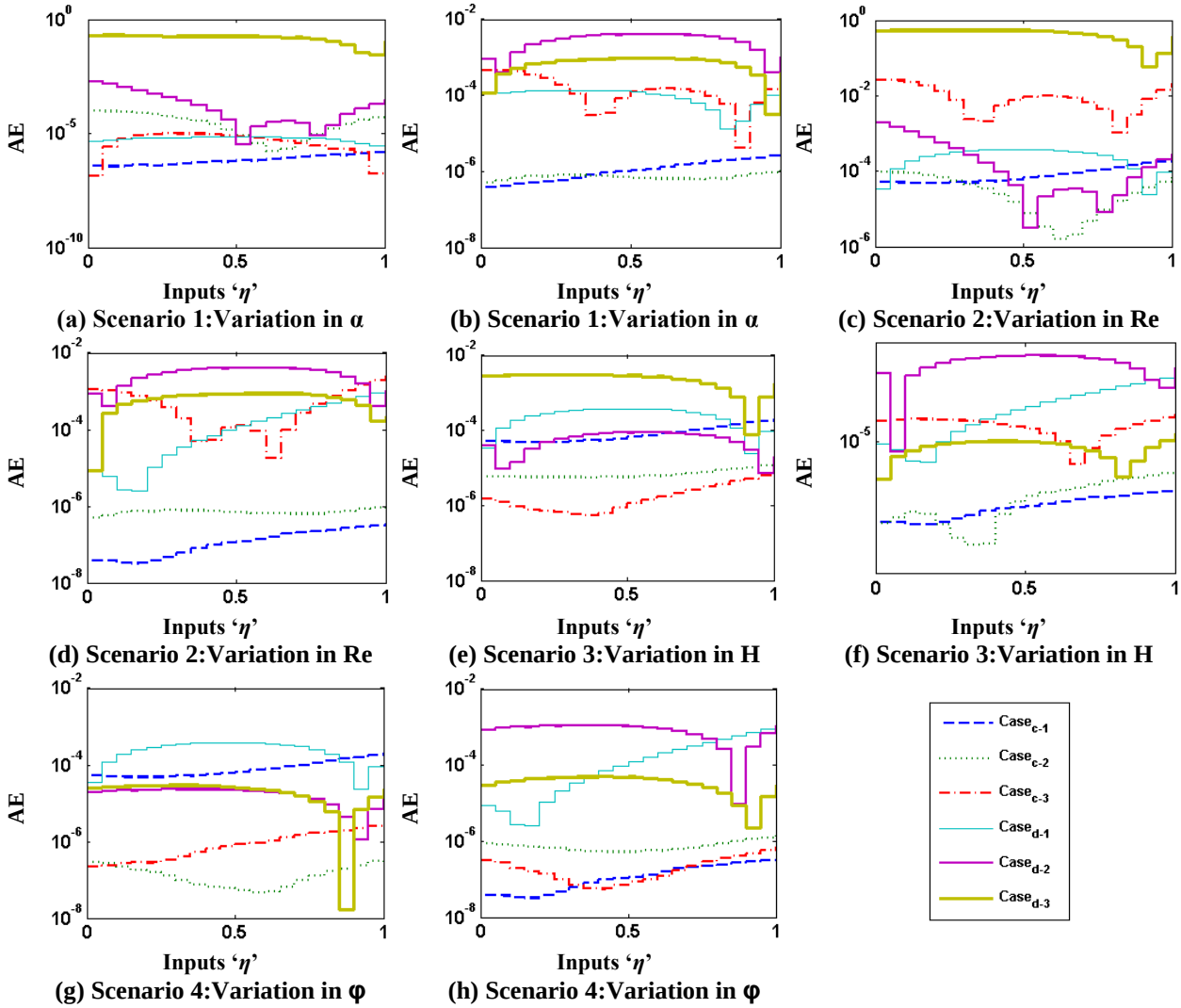

Figure 8*:* Plots of AEs of for nonlinear MHD-JHF in problem 4.2; Figs. (a, c, e, g) for NNM-RB-SQP and Figs. (b, d, f, h) for NNM-TS-SQP.

Table 5: Comparison of the statistical results through mean and STD for Problem 4.2

NNM	Scenario	Case	Mean of AEs for Input η					STD of AEs for Input η				
			$\eta = 0.1$	$\eta = 0.3$	$\eta = 0.5$	$\eta = 0.7$	$\eta = 0.9$	$\eta = 0.1$	$\eta = 0.3$	$\eta = 0.5$	$\eta = 0.7$	$\eta = 0.9$
LS	1	c-1	2.3E-05	2.3E-05	2.8E-05	3.9E-05	5.7E-05	5.2E-05	5.2E-05	6.2E-05	8.4E-05	1.2E-04
		c-2	1.2E-04	6.3E-05	2.5E-05	3.6E-05	8.0E-05	2.9E-04	1.5E-04	5.7E-05	1.1E-04	2.0E-04
		c-3	7.0E-04	1.9E-04	1.7E-04	1.3E-04	3.6E-04	3.6E-03	9.5E-04	8.2E-04	6.1E-04	1.9E-03
		d-1	1.2E-04	1.4E-04	1.4E-04	1.0E-04	3.4E-05	6.0E-04	7.2E-04	7.2E-04	5.6E-04	1.6E-04
		d-2	1.6E-03	3.0E-03	3.4E-03	3.1E-03	1.1E-03	2.4E-03	2.7E-03	2.8E-03	2.3E-03	7.8E-04
		d-3	1.6E-01	1.6E-01	1.5E-01	1.2E-01	2.3E-02	2.2E-01	2.2E-01	2.1E-01	1.6E-01	3.6E-02
	2	c-2	3.2E-05	2.7E-05	2.5E-05	3.5E-05	5.4E-05	6.5E-05	5.0E-05	4.5E-05	6.3E-05	9.9E-05
		c-3	1.6E-03	2.4E-04	5.5E-04	5.4E-04	1.2E-03	6.3E-03	1.1E-03	2.2E-03	2.1E-03	6.4E-03
		d-2	1.4E-03	2.3E-03	2.5E-03	2.0E-03	4.4E-04	1.9E-03	3.4E-03	3.8E-03	3.1E-03	6.9E-04
		d-3	1.5E-01	1.5E-01	1.5E-01	1.2E-01	2.3E-02	2.1E-01	2.1E-01	2.0E-01	1.6E-01	3.0E-02
	3	c-2	8.9E-06	7.2E-06	5.7E-06	7.3E-06	1.2E-05	1.8E-05	1.4E-05	9.4E-06	1.3E-05	2.1E-05
		c-3	1.6E-05	1.3E-05	7.7E-06	7.4E-06	1.5E-05	3.3E-05	2.7E-05	1.8E-05	1.4E-05	2.7E-05
		d-2	1.2E-03	1.7E-03	1.8E-03	1.4E-03	3.6E-04	2.3E-03	3.2E-03	3.4E-03	2.7E-03	7.2E-04
		d-3	1.6E-03	2.7E-03	3.0E-03	2.5E-03	6.9E-04	1.8E-03	3.3E-03	3.7E-03	3.1E-03	9.2E-04
	4	c-2	7.4E-05	6.7E-05	6.7E-05	8.3E-05	1.2E-04	1.2E-04	1.1E-04	1.1E-04	1.4E-04	2.0E-04
		c-3	3.7E-06	3.8E-06	4.6E-06	7.3E-06	1.1E-05	1.2E-05	1.2E-05	1.4E-05	1.9E-05	2.8E-05
		d-2	5.7E-04	8.6E-04	9.1E-04	7.0E-04	9.9E-05	1.5E-03	2.4E-03	2.6E-03	2.0E-03	2.4E-04
		d-3	9.2E-05	1.0E-04	9.3E-05	6.1E-05	2.8E-05	2.7E-04	2.9E-04	2.6E-04	1.6E-04	9.5E-05
RB	1	c-1	5.7E-06	6.0E-06	7.2E-06	1.0E-05	1.5E-05	6.6E-06	6.4E-06	7.4E-06	1.0E-05	1.5E-05
		c-2	6.6E-04	7.8E-05	6.8E-04	1.3E-03	1.9E-03	3.9E-03	2.2E-04	4.5E-03	8.4E-03	1.2E-02
		c-3	5.8E-03	1.2E-03	2.2E-03	2.8E-03	2.8E-03	1.7E-02	3.8E-03	7.7E-03	1.1E-02	1.0E-02
		d-1	3.8E-04	4.4E-04	4.3E-04	3.2E-04	6.3E-05	1.2E-03	1.5E-03	1.5E-03	1.1E-03	2.1E-04
		d-2	8.3E-03	8.6E-03	8.2E-03	6.2E-03	3.0E-03	3.7E-02	3.7E-02	3.4E-02	2.3E-02	1.3E-02
		d-3	1.6E-01	1.6E-01	1.5E-01	1.2E-01	2.4E-02	1.8E-01	1.8E-01	1.7E-01	1.4E-01	3.9E-02
	2	c-2	5.5E-05	5.3E-05	6.5E-05	9.5E-05	1.5E-04	9.9E-05	8.5E-05	7.9E-05	1.0E-04	1.6E-04
		c-3	1.3E-02	1.5E-03	5.6E-03	5.6E-03	5.5E-03	2.6E-02	3.9E-03	1.2E-02	1.6E-02	1.3E-02
		d-2	7.1E-04	9.0E-04	9.1E-04	7.3E-04	2.1E-04	1.0E-03	1.4E-03	1.5E-03	1.2E-03	7.1E-04
		d-3	1.5E-01	1.5E-01	1.5E-01	1.2E-01	2.7E-02	1.8E-01	1.8E-01	1.7E-01	1.4E-01	3.2E-02
	3	c-2	8.9E-05	6.8E-05	5.4E-05	9.2E-05	1.7E-04	1.2E-04	9.7E-05	6.6E-05	1.0E-04	1.7E-04
		c-3	1.6E-04	1.3E-04	9.4E-05	1.1E-04	2.3E-04	2.4E-04	1.9E-04	1.4E-04	2.1E-04	3.4E-04
		d-2	8.8E-04	1.1E-03	1.1E-03	8.4E-04	1.4E-04	1.8E-03	2.5E-03	2.6E-03	2.0E-03	3.2E-04
		d-3	1.2E-03	1.4E-03	1.4E-03	1.1E-03	3.2E-04	1.6E-03	1.9E-03	1.9E-03	1.5E-03	4.8E-04
	4	c-2	8.8E-06	8.3E-06	9.2E-06	1.3E-05	1.9E-05	1.4E-05	1.3E-05	1.5E-05	2.0E-05	3.1E-05
		c-3	1.6E-05	1.4E-05	1.3E-05	1.6E-05	2.9E-05	7.3E-05	6.5E-05	4.3E-05	3.8E-05	6.8E-05
		d-2	5.5E-04	6.8E-04	6.9E-04	5.4E-04	1.3E-04	1.2E-03	1.5E-03	1.5E-03	1.3E-03	4.7E-04
		d-3	1.5E-04	1.6E-04	1.5E-04	1.1E-04	2.3E-05	4.8E-04	5.2E-04	4.9E-04	3.6E-04	8.3E-05
TS	1	c-1	5.5E-06	5.5E-06	6.3E-06	8.7E-06	1.3E-05	9.5E-06	9.5E-06	1.1E-05	1.5E-05	2.1E-05
		c-2	1.0E-04	5.4E-05	2.4E-05	2.9E-05	7.2E-05	4.4E-04	2.5E-04	1.1E-04	1.5E-04	3.7E-04
		c-3	1.3E-04	3.6E-05	4.0E-05	3.7E-05	7.0E-05	3.4E-04	8.9E-05	9.4E-05	1.0E-04	1.4E-04
		d-1	1.9E-05	1.9E-05	1.8E-05	1.2E-05	7.5E-06	6.1E-05	5.7E-05	5.2E-05	4.0E-05	2.3E-05
		d-2	7.6E-04	1.6E-03	1.9E-03	1.8E-03	7.0E-04	7.1E-04	1.6E-03	1.9E-03	1.7E-03	7.1E-04
		d-3	2.1E-02	2.1E-02	2.0E-02	1.5E-02	2.4E-03	9.9E-02	9.8E-02	9.2E-02	7.0E-02	8.5E-03
	2	c-2	3.6E-05	3.5E-05	4.0E-05	5.6E-05	8.6E-05	1.5E-04	1.4E-04	1.5E-04	2.1E-04	3.2E-04
		c-3	3.2E-03	5.0E-04	1.1E-03	7.3E-04	2.2E-03	1.2E-02	1.9E-03	4.3E-03	3.3E-03	8.2E-03
		d-2	3.0E-04	5.1E-04	5.6E-04	4.6E-04	1.3E-04	8.9E-04	1.7E-03	2.0E-03	1.7E-03	3.9E-04
		d-3	2.5E-02	2.5E-02	2.5E-02	2.0E-02	3.7E-03	1.0E-01	1.0E-01	9.7E-02	7.6E-02	1.1E-02
	3	c-2	2.1E-05	1.8E-05	1.3E-05	1.2E-05	1.7E-05	1.1E-04	9.4E-05	7.2E-05	6.0E-05	7.0E-05
		c-3	9.1E-06	7.8E-06	5.1E-06	4.1E-06	9.1E-06	2.7E-05	2.2E-05	1.1E-05	6.7E-06	2.2E-05
		d-2	3.6E-04	5.8E-04	6.2E-04	4.9E-04	8.7E-05	1.2E-03	2.0E-03	2.2E-03	1.8E-03	2.7E-04
		d-3	7.1E-04	1.2E-03	1.3E-03	1.1E-03	3.4E-04	1.3E-03	2.3E-03	2.6E-03	2.2E-03	6.7E-04
	4	c-2	2.9E-05	2.6E-05	2.6E-05	3.3E-05	4.9E-05	4.8E-05	4.3E-05	4.4E-05	5.5E-05	8.2E-05
		c-3	2.2E-06	1.9E-06	2.3E-06	4.1E-06	6.7E-06	5.0E-06	4.3E-06	7.8E-06	1.7E-05	2.8E-05
		d-2	1.7E-04	2.7E-04	2.9E-04	2.2E-04	6.5E-05	6.0E-04	1.4E-03	1.6E-03	1.3E-03	2.4E-04
		d-3	1.7E-05	1.8E-05	1.7E-05	1.1E-05	5.9E-06	5.5E-05	6.0E-05	5.6E-05	3.7E-05	1.3E-05

Problem 4.3: *Study the dynamics of nonlinear MHD-JHF with base fluid water mixed with copper nanoparticle***:** In this problem, the dynamics of nonlinear MHD-JHF with base fluid water and silver nanoparticles is analyzed for four scenarios with parameter as listed in Table 2. The governing mathematical relation derived from equations (5-6) using ρ_s =8833, ρ_f = 997 for the problem is written as:

$$f'''(\eta)+2\alpha\,\mathrm{Re}(1-\varphi)^{2.5}(1-\varphi+8.859\varphi)\,f(\eta)\,f'(\eta)=-\left(4-(1-\varphi)^{1.25}H\right)\alpha^2 f'(\eta),$$
$$f'(0)=0\;\; f(1)=0\;\; f(0)=1. \qquad \textbf{(45)}$$

The proposed stochastic solvers have also been applied to solve the equation (45) by construction of the fitness function as:

$$\varepsilon=\frac{1}{11}\sum_{m=0}^{10}\left(\hat{f}_m'''+2\alpha\,\mathrm{Re}(1-\varphi)^{2.5}(1-\varphi+8.859\varphi)\,\hat{f}_m\hat{f}_m'+(4-(1-\varphi)^{1.25}H)\alpha^2\hat{f}_m'\right)^2$$
$$+\frac{1}{3}\left(\left(\hat{f}_0-1\right)^2+\left(\hat{f}_0'\right)^2+\left(\hat{f}_{10}\right)^2\right) \qquad \textbf{(46)}$$

Optimization of fitness function (46) is carried out by proposed three procedure based on NNM-LS-SQP, NNM-RB-SQP and NNM-TS-SQP for 100 independent trails to get the appropriate weights. The best run of the model is defined on the basis of minimum values of these five measures based on MAE, RMSE, EVAF, ENSE and TIC and results in term of best runs out of 100 independent executions for each case of problem 3 are given in Table 3. A set of weight trained by NNM-LS-SQP, NNM-RB-SQP and NNM-TS-SQP for both convergent and divergent cases of scenario 1 are given graphically in Figs 4(g), 4(h) and 4(i), respectively. The derived approximate solutions $\hat{f}_{LS}$, $\hat{f}_{RB}$ and $\hat{f}_{TS}$ of the convergent flow c-1 for NNM-LS-SQP, NNM-RB-SQP and NNM-TS-SQP are given as:

$$\hat{f}_{LS}(\eta)=\frac{1.249}{1+e^{-(1.563\eta+1.297)}}+\frac{4.221}{1+e^{-(-2.441\eta+6.595)}}+\frac{-4.979}{1+e^{-(0.008\eta+0.940)}}+\frac{-2.276}{1+e^{-(1.195\eta-0.789)}}+\frac{-0.239}{1+e^{-(0.553\eta+0.130)}}+\frac{-4.438}{1+e^{-(-0.640\eta+0.272)}}+\frac{-1.873}{1+e^{-(2.030\eta-0.739)}}+\frac{0.438}{1+e^{-(-2.843\eta+0.458)}}+\frac{2.883}{1+e^{-(2.626\eta+0.675)}}+\frac{1.715}{1+e^{-(-2.553\eta+0.758)}} \quad \textbf{(47)}$$

$$\hat{f}_{RB}(\eta)=0.405e^{-(-1.542\eta-0.072)^2}-0.638e^{-(-1.171\eta-0.763)^2}-0.314e^{-(0.946\eta+0.423)^2}-3.459e^{-(-0.124\eta+0.649)^2}+0.953e^{-(1.267\eta+1.166)^2}+1.510e^{-(1.169\eta+0.489)^2}+0.254e^{-(-1.514\eta-1.826)^2}+0.089e^{-(-0.864\eta-0.450)^2}+1.225e^{-(-1.127\eta+0.315)^2}+2.153e^{-(-0.612\eta+0.958)^2} \quad \textbf{(48)}$$

$$\hat{f}_{TS}(\eta)=-7.311+\frac{1.132}{1+e^{-2(1.039\eta-1.599)}}+\frac{5.454}{1+e^{-2(1.0710\eta+0.118)}}+\frac{-4.678}{1+e^{-2(1.144\eta-0.180)}}+\frac{0.086}{1+e^{-2(1.721\eta+1.373)}}+\frac{-0.892}{1+e^{-2(-0.586\eta+0.020)}}+\frac{-0.932}{1+e^{-2(0.671\eta+0.109)}}+\frac{-1.653}{1+e^{-2(0.199\eta-0.851)}}+\frac{1.351}{1+e^{-2(-0.099\eta-0.630)}}+\frac{1.753}{1+e^{-2(-0.595\eta-1.947)}}+\frac{2.146}{1+e^{-2(-0.751\eta+1.401)}} \quad \textbf{(49)}$$

While for divergent flow case d-1, the derived solutions, $\hat{f}_{LS}$, $\hat{f}_{RB}$ and $\hat{f}_{TS}$, are given as:

$$\hat{f}_{LS}(\eta)=\frac{-1.682}{1+e^{-(2.660\eta-2.066)}}+\frac{-7.246}{1+e^{-(-0.845\eta+3.058)}}+\frac{0.608}{1+e^{-(8.587\eta-13.128)}}+\frac{-7.142}{1+e^{-(-0.141\eta+1.681)}}+\frac{8.121}{1+e^{-(-2.008\eta+0.554)}}+\frac{8.004}{1+e^{-(1.697\eta-0.738)}}+\frac{-2.810}{1+e^{-(2.489\eta+1.234)}}+\frac{6.965}{1+e^{-(1.021\eta-2.217)}}+\frac{-10.729}{1+e^{-(2.996\eta-4.505)}}+\frac{9.968}{1+e^{-(1.134\eta+1.399)}} \quad \textbf{(50)}$$

$$\hat{f}_{RB}(\eta)=1.985e^{-(0.940\eta-0.717)^2}-1.479e^{-(1.061\eta-0.392)^2}-1.355e^{-(-0.816\eta-1.011)^2}+3.796e^{-(1.754\eta-2.573)^2}+3.606e^{-(-1.594\eta+1.796)^2}-3.565e^{-(-1.319\eta+1.647)^2}-7.702e^{-(1.360\eta-2.12532690088603)^2}+1.888e^{-(-0.899\eta-0.544)^2}+0.440e^{-(-1.352\eta+0.659)^2}+4.147e^{-(0.746\eta-2.090)^2} \quad \textbf{(51)}$$

$$\hat{f}_{TS}(\eta) = -7.311 + \frac{1.570}{1+e^{-2(1.418\eta+1.766)}} + \frac{0.546}{1+e^{-2(1.661\eta-1.271)}} + \frac{-5.474}{1+e^{-2(1.841\eta-2.676)}} + \frac{4.570}{1+e^{-2(0.409\eta-0.863)}} + \frac{-2.207}{1+e^{-2(1.120\eta-0.964)}} + \frac{4.671}{1+e^{-2(1.513\eta-2.366)}} + \frac{1.104}{1+e^{-2(1.573\eta-0.250)}} + \frac{-1.135}{1+e^{-2(1.602\eta-0.287)}} + \frac{-2.080}{1+e^{-2(-1.258\eta+0.480)}} + \frac{-3.514}{1+e^{-2(0.878\eta-0.484)}} \quad \textbf{(52)}$$

Similarly, the solutions are determined for each case of all four scenarios of the problem and respective results of all four scenarios are given graphically in Figs. 9(a), 9(c), 9(e) and 9(g) for NNM-LS-SQP scheme, while results of AEs are presented in Figs. 9(b), 9(d), 9(f) and 9(h) for scenarios 1, 2, 3 and 4, respectively. It is seen that proposed solutions are consistently overlapping the reference AM solutions for each case of all four scenarios. Accordingly, the AEs calculated by the algorithms, NNM-RB-SQP and NNM-TS-SQP, are shown graphically in Fig. 10 for each variation. It is seen that the values of velocity profile of the fluid with the change in angle of channel, concentration of nanoparticles, Reynolds and Hartman numbers the behavior of results obtained by the proposed models are similar with reference AM. Comparison of the accuracy in case of all three models based on AEs show that results for convergent channels for each scenarios are relatively superior than that of divergent channels.

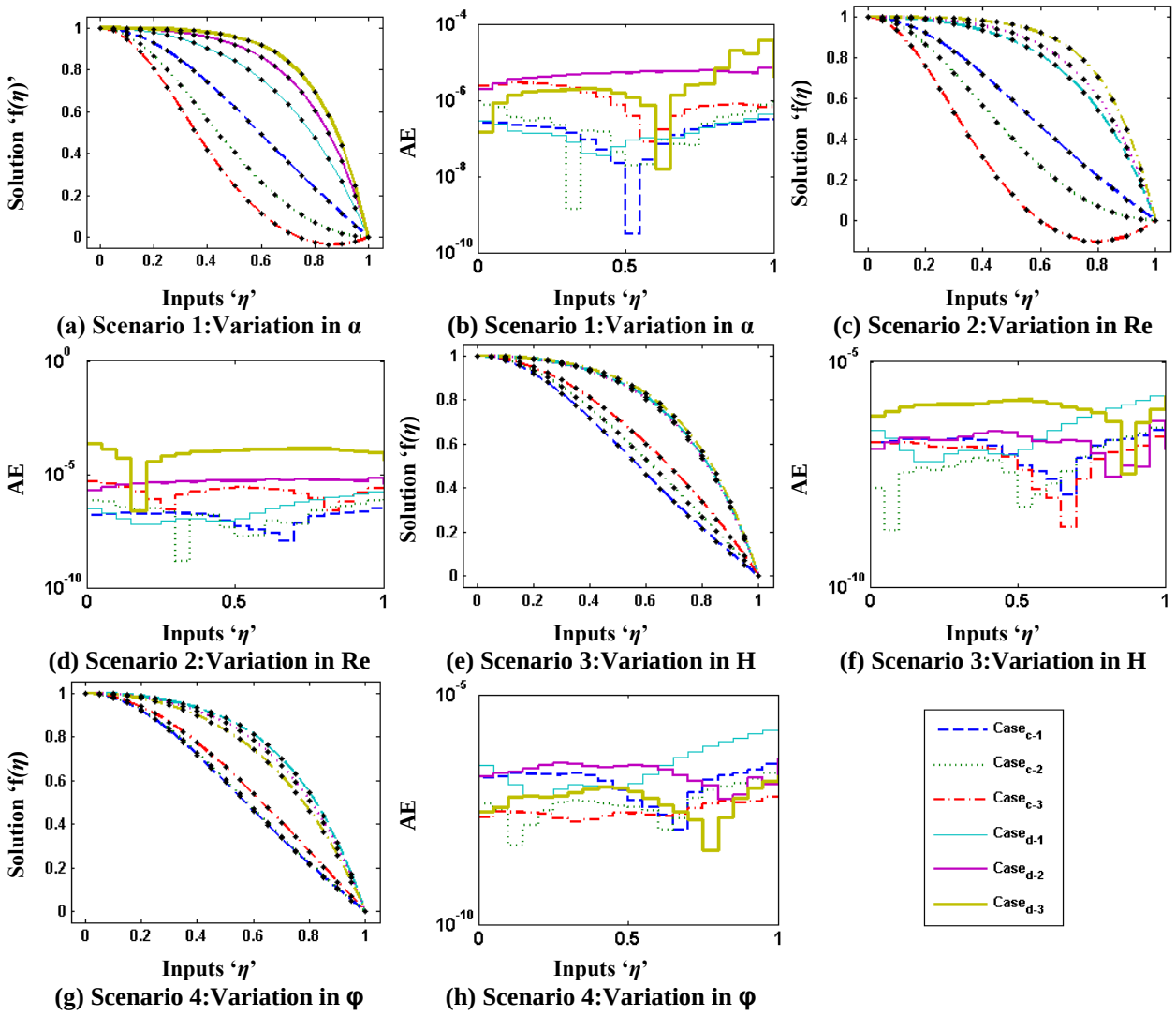

Figure 9: Proposed results of NNM-LS-SQP for nonlinear MHD-JHF problem 4.3; Figs. (a, c, e, g) for the approximate solution and Figs. (b, d, f, h) for AEs.

Results of statistical analysis for 100 independent runs of NNM-LS-SQP, NNM-LS-SQP and NNM-LS-SQP procedures in terms of mean and STD values are calculated and results are listed in Table 6 for each case of all four scenarios of problem 3. It is observed that the magnitude of mean are generally lies between 10^{-02} to 10^{-06} for all three algorithms, however level attained by statistical measures are better for NNM-TS-SQP than that of both NNM-LS-SQP and NNM-RB-

SQP schemes. Additionally, in case of convergent channel, results are better in precision than that of divergent channels. The consistent small STDs further validate the operation of all three algorithms for finding the solution of nonlinear MHD-JHF problem as given in equations (45).

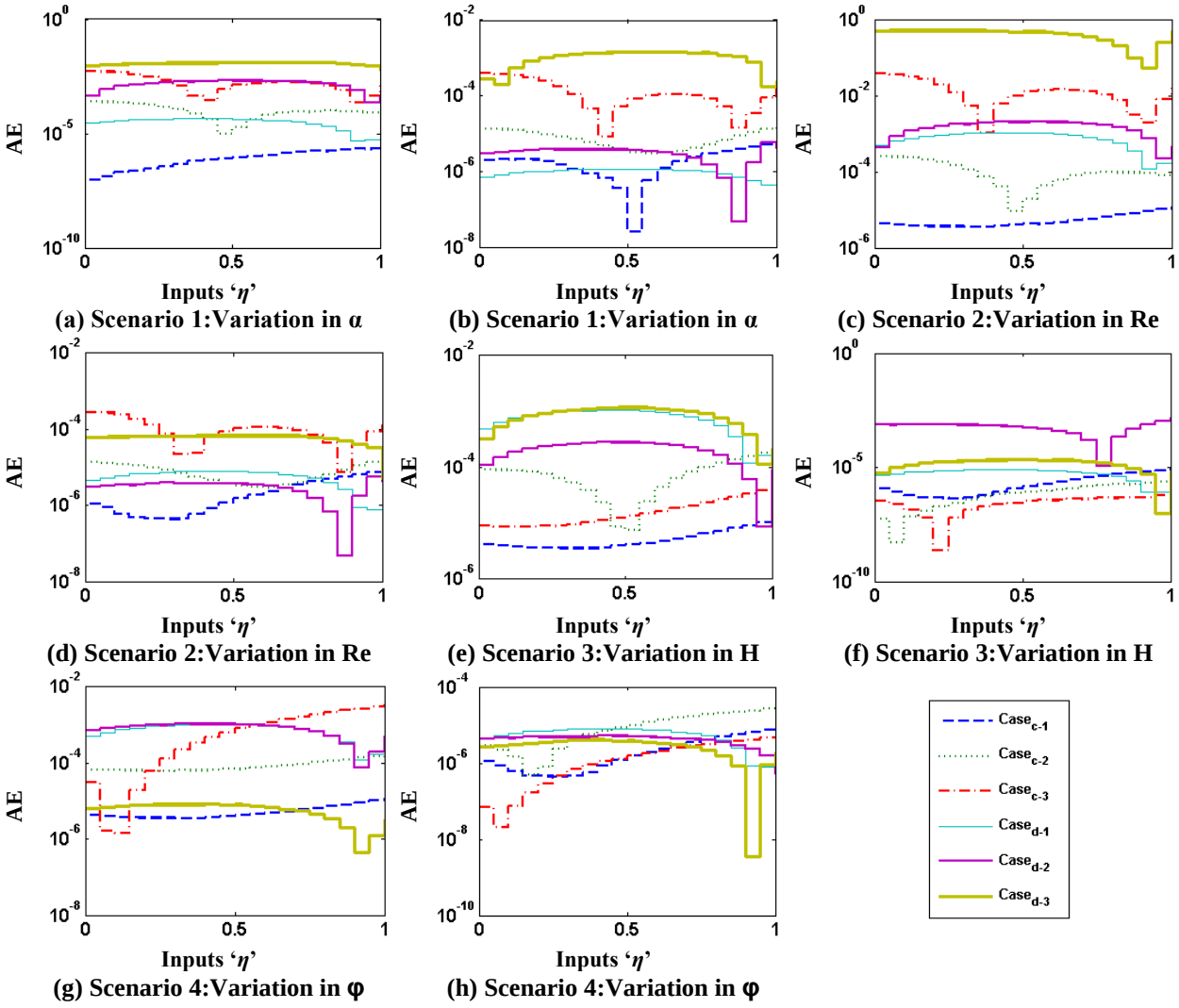

Figure 10: Plots of AEs of for nonlinear MHD-JHF in problem 4.3; Figs. (a, c, e, g) for NNM-RB-SQP and Figs. (b, d, f, h) for NNM-TS-SQP.

.

Table 6: Comparison of the statistical results through mean and STD for Problem 4.3

NNM	Scenario	Case	Mean					STD				
			$\eta_1 = 0.1$	$\eta_2 = 0.3$	$\eta_3 = 0.5$	$\eta_4 = 0.7$	$\eta_5 = 0.9$	$\eta_1 = 0.1$	$\eta_2 = 0.3$	$\eta_3 = 0.5$	$\eta_4 = 0.7$	$\eta_5 = 0.9$
LS	1	c-1	3.8E-06	4.2E-06	5.7E-06	8.6E-06	1.3E-05	6.0E-06	7.0E-06	9.9E-06	1.6E-05	2.4E-05
		c-2	7.3E-05	4.7E-05	2.4E-05	2.8E-05	6.1E-05	1.7E-04	1.1E-04	7.3E-05	1.0E-04	2.0E-04
		c-3	3.0E-04	9.6E-05	6.9E-05	8.0E-05	1.5E-04	8.5E-04	2.7E-04	1.8E-04	1.9E-04	3.7E-04
		d-1	3.8E-05	4.0E-05	3.7E-05	2.4E-05	1.0E-05	9.7E-05	1.0E-04	9.4E-05	5.9E-05	2.4E-05
		d-2	1.2E-03	2.6E-03	3.0E-03	2.6E-03	9.2E-04	9.5E-04	1.8E-03	2.1E-03	1.9E-03	7.3E-04
		d-3	1.2E-01	1.2E-01	1.1E-01	8.9E-02	2.1E-02	1.9E-01	1.9E-01	1.8E-01	1.4E-01	3.9E-02
	2	c-2	1.5E-05	1.6E-05	1.9E-05	2.9E-05	4.5E-05	4.9E-05	5.4E-05	7.3E-05	1.1E-04	1.7E-04
		c-3	5.7E-04	1.3E-04	1.4E-04	1.1E-04	4.6E-04	1.8E-03	4.3E-04	4.0E-04	2.9E-04	1.6E-03
		d-2	8.7E-04	1.4E-03	1.5E-03	1.2E-03	2.4E-04	1.6E-03	2.8E-03	3.1E-03	2.5E-03	4.6E-04
		d-3	1.1E-01	1.1E-01	1.1E-01	8.4E-02	1.4E-02	1.9E-01	1.9E-01	1.8E-01	1.4E-01	2.0E-02
	2	c-2	2.6E-05	2.0E-05	1.2E-05	1.8E-05	3.5E-05	7.7E-05	5.6E-05	2.2E-05	4.1E-05	9.1E-05
		c-3	1.8E-05	1.5E-05	9.0E-06	6.2E-06	1.4E-05	6.2E-05	5.0E-05	3.1E-05	1.7E-05	3.6E-05
		d-2	9.6E-04	1.3E-03	1.3E-03	1.0E-03	2.0E-04	2.2E-03	3.0E-03	3.1E-03	2.4E-03	4.5E-04
		d-3	1.3E-03	2.1E-03	2.3E-03	1.8E-03	4.9E-04	1.6E-03	2.9E-03	3.2E-03	2.6E-03	7.7E-04
	2	c-2	2.0E-05	2.0E-05	2.3E-05	3.1E-05	4.5E-05	8.6E-05	8.2E-05	8.9E-05	1.1E-04	1.7E-04
		c-3	3.5E-06	2.5E-06	1.7E-06	3.4E-06	5.9E-06	9.1E-06	6.6E-06	3.6E-06	6.4E-06	1.3E-05
		d-2	4.0E-04	5.4E-04	5.5E-04	4.2E-04	1.0E-04	1.5E-03	2.2E-03	2.3E-03	1.8E-03	3.9E-04
		d-3	3.6E-05	3.7E-05	3.3E-05	2.2E-05	6.4E-06	1.2E-04	1.3E-04	1.1E-04	7.5E-05	1.3E-05
RB	1	c-1	7.8E-06	8.1E-06	1.1E-05	1.7E-05	2.6E-05	1.2E-05	1.4E-05	1.8E-05	2.8E-05	4.2E-05
		c-2	9.8E-05	4.6E-05	3.7E-05	7.6E-05	1.1E-04	1.9E-04	8.9E-05	4.2E-05	9.8E-05	1.3E-04
		c-3	2.1E-03	5.9E-04	8.3E-04	1.3E-03	1.8E-03	4.4E-03	1.1E-03	2.1E-03	3.4E-03	4.4E-03
		d-1	2.7E-04	3.1E-04	2.9E-04	2.2E-04	4.6E-05	7.7E-04	8.5E-04	8.2E-04	6.1E-04	1.4E-04
		d-2	4.7E-03	5.1E-03	4.9E-03	3.8E-03	1.2E-03	2.1E-02	2.1E-02	1.9E-02	1.3E-02	4.8E-03
		d-3	9.5E-02	9.4E-02	9.1E-02	7.4E-02	2.3E-02	1.5E-01	1.5E-01	1.4E-01	1.2E-01	3.6E-02
	2	c-2	4.5E-05	3.5E-05	3.5E-05	6.0E-05	9.6E-05	6.5E-05	5.2E-05	5.0E-05	7.3E-05	1.2E-04
		c-3	5.9E-03	1.0E-03	2.2E-03	2.1E-03	1.7E-03	8.5E-03	1.5E-03	3.1E-03	3.0E-03	3.2E-03
		d-2	6.6E-04	8.0E-04	8.0E-04	6.3E-04	1.5E-04	8.0E-04	1.1E-03	1.1E-03	9.1E-04	2.2E-04
		d-3	1.0E-01	1.0E-01	9.8E-02	8.1E-02	1.8E-02	1.5E-01	1.5E-01	1.4E-01	1.1E-01	2.9E-02
	3	c-2	9.6E-05	7.7E-05	6.0E-05	9.0E-05	1.7E-04	1.2E-04	1.1E-04	1.0E-04	1.4E-04	2.2E-04
		c-3	1.5E-03	9.3E-04	2.2E-04	1.2E-03	2.6E-03	9.4E-03	5.9E-03	1.1E-03	7.3E-03	1.6E-02
		d-2	1.0E-03	1.3E-03	1.3E-03	9.3E-04	1.1E-04	3.2E-03	4.0E-03	4.0E-03	2.9E-03	2.1E-04
		d-3	8.7E-04	1.2E-03	1.3E-03	9.9E-04	3.1E-04	1.4E-03	2.3E-03	2.5E-03	2.1E-03	6.6E-04
	4	c-2	2.2E-05	2.0E-05	2.3E-05	3.6E-05	5.4E-05	4.2E-05	4.0E-05	4.7E-05	6.7E-05	1.0E-04
		c-3	1.9E-04	1.6E-04	9.9E-05	1.2E-04	2.2E-04	1.0E-03	8.5E-04	5.8E-04	5.9E-04	1.0E-03
		d-2	4.7E-04	5.3E-04	5.2E-04	3.9E-04	8.1E-05	1.4E-03	1.4E-03	1.4E-03	1.1E-03	2.3E-04
		d-3	1.6E-04	1.8E-04	1.7E-04	1.2E-04	1.8E-05	6.4E-04	7.6E-04	7.3E-04	5.1E-04	4.6E-05
TS	1	c-1	3.1E-06	3.1E-06	3.6E-06	4.9E-06	7.1E-06	5.9E-06	5.9E-06	6.7E-06	8.8E-06	1.3E-05
		c-2	3.4E-05	2.1E-05	1.0E-05	1.1E-05	2.4E-05	1.1E-04	6.3E-05	2.3E-05	2.2E-05	5.8E-05
		c-3	2.6E-04	7.3E-05	8.5E-05	8.2E-05	1.7E-04	1.5E-03	4.7E-04	5.9E-04	6.4E-04	9.8E-04
		d-1	2.2E-05	2.3E-05	2.0E-05	1.2E-05	8.4E-06	1.0E-04	1.0E-04	8.8E-05	5.2E-05	2.7E-05
		d-2	7.1E-04	1.5E-03	1.7E-03	1.6E-03	5.4E-04	7.9E-04	1.8E-03	2.1E-03	1.9E-03	6.8E-04
		d-3	7.0E-03	7.4E-03	7.1E-03	5.5E-03	1.7E-03	5.1E-02	5.0E-02	4.7E-02	3.5E-02	6.6E-03
	2	c-2	1.4E-05	1.0E-05	1.3E-05	2.2E-05	3.6E-05	3.9E-05	2.6E-05	3.7E-05	7.7E-05	1.3E-04
		c-3	2.3E-04	5.4E-05	7.5E-05	4.0E-05	1.8E-04	8.9E-04	1.9E-04	2.1E-04	7.5E-05	7.4E-04
		d-2	2.5E-04	3.1E-04	3.1E-04	2.3E-04	5.3E-05	1.1E-03	1.3E-03	1.2E-03	9.3E-04	1.5E-04
		d-3	6.5E-03	6.7E-03	6.4E-03	5.0E-03	2.4E-03	5.0E-02	4.9E-02	4.6E-02	3.5E-02	8.5E-03
	3	c-2	7.1E-06	6.0E-06	4.7E-06	6.7E-06	1.2E-05	1.5E-05	1.4E-05	1.4E-05	2.0E-05	3.1E-05
		c-3	1.5E-04	1.1E-04	3.3E-05	8.3E-05	2.2E-04	1.4E-03	1.0E-03	2.5E-04	7.5E-04	2.0E-03
		d-2	1.0E-04	1.3E-04	1.3E-04	9.6E-05	3.5E-05	3.8E-04	5.5E-04	5.8E-04	4.5E-04	1.2E-04
		d-3	4.8E-04	8.3E-04	9.2E-04	7.7E-04	2.2E-04	1.2E-03	2.2E-03	2.4E-03	2.0E-03	5.5E-04
	4	c-2	1.0E-05	1.1E-05	1.3E-05	1.9E-05	2.9E-05	2.3E-05	2.3E-05	3.1E-05	4.7E-05	7.2E-05
		c-3	2.1E-06	1.8E-06	1.7E-06	2.2E-06	3.8E-06	4.3E-06	4.1E-06	4.0E-06	6.5E-06	1.1E-05
		d-2	2.5E-05	2.8E-05	2.7E-05	1.9E-05	6.7E-06	4.9E-05	5.4E-05	5.2E-05	3.5E-05	1.3E-05
		d-3	4.6E-06	5.0E-06	4.6E-06	2.8E-06	2.1E-06	8.2E-06	9.3E-06	8.5E-06	5.1E-06	4.7E-06

5. Comparative Analysis through Statistics

Comparative analysis of proposed three DE-NNM-LS, DE-NNM-LS and DE-NNM-LS models optimized with SQP is carried out on the basis of performance monitoring gauges based on MAE, RMSE, EVAF, TIC and ENSEs, also with their global variants for all three problems of nonlinear MHD-JHF systems.

Proposed three schemes, NNM-LS-SQP, NNM-RB-SQP and NNM-TS-SQP, runs 100 times to solve all three nanofluidics problems and values of fitness achieved along with the calculated values of MAE, RMSE, EVAF, TIC and ENSE as defined in (26-27) are plotted in Figs. 10, 11, and 12 for problems 1, 2 and 3, respectively, for both convergent and divergent cases. It is seen that mostly the small values of all six performance measures has been obtained by all three proposed models but results of ANN-RB-SQP procedure are relatively degraded from NNM-LS-SQP and NNM-TS-SQP, while the results obtained by NNM-TS-SQP is a bit better form NNM-LS-SQP model.

In order to compare or evaluate the precision of the methods based on NNM-LS-SQP, NNM-RB-SQP and NNM-TS-SQP further, the convergent rate analysis is performed for each case of all three MHD-JHF problems. Results of percentage convergence based on pre-defined levels of MAE, EVAF and TIC values are given in tables 7, 8 and 9 for NNM-LS-SQP, NNM-RB-SQP, and NNM-TS-SQP, respectively. It is observed that percentage convergence is about 100% for all three models on the basis of the criteria with reasonable accuracy while for tough criteria, *i.e.*, higher accuracy, the rate of percentage convergence decreases for all three models but still the better results are obtained by NNM-TS-SQP algorithm from the rest.

Comparative studies of the models are continued further through global performance indices defines as a mean gauges of fitness, MAE, RMSE, EVAF, ENSE and TIC measures. The values of global performance indicators are given in tables 10, 11 and 12 for NNM-LS-SQP, NNM-RB-SQP and NNM-TS-SQP, respectively. It is seen that smaller (better) the values of fitness attained then corresponding values of all five global performance parameters are also found better and vice versa. Such behavior in the results show the consistency of proposed models accessed through different performance indices. Additionally, it is seen that generally the small values of global performance operators are obtained for all three mathematical models that validate the consistent accuracy of the proposed schemes, but still the supremacy in accuracy and convergent is found with NNM-TS-SQP method over rest of the models.

Computational complexity of proposed three DE-NNM-LS, DE-NNM-LS and DE-NNM-LS models has been measured on operators depends on mean execution time (MT), mean number of generations (MGs) and mean number of function counts (MFCs) required for optimization of design variables to solve nonlinear MHD-JHF type nanofluidics problems. Results of the complexity operator for NNM-LS-SQP, NNM-RB-SQP and NNM-TS-SQP approaches are given in Table 13 for each scenario of all three nonlinear MHD-JHF problems. It is seen that values of complexity operator are relatively on lesser side for the convergent cases than that of divergent runs. The values of complexity operator are found least for NNM-LS-SQP model as compared with rest of the algorithms. All numerical simulations are conducted on Dell workstation model d2000, with 2.7 processer, 8GB RAM running Matlab 2015a in windows 8.1 environment.

Table 7: Convergence analysis on difference performance indices for NNM-LS-SQP algorithm

Problem	Scenario	Case	MAE ≤				EVAF ≤				TIC ≤			
			10^{-03}	10^{-04}	10^{-05}	10^{-06}	10^{-06}	10^{-08}	10^{-10}	10^{-11}	10^{-03}	10^{-04}	10^{-05}	10^{-06}
4.1	1	c-1	100	100	100	90	100	100	90	66	100	100	100	92
		c-2	100	100	89	53	100	92	59	35	100	100	89	56
		c-3	100	100	87	30	100	87	36	14	100	100	87	31
		d-1	100	100	97	56	100	98	66	36	100	100	98	66
		d-2	93	52	19	2	56	22	3	0	100	57	23	3
		d-3	90	10	2	0	13	3	0	0	90	15	3	0
	2	c-2	100	100	95	66	100	96	69	47	100	100	95	71
		c-3	100	99	83	22	99	81	28	8	100	99	80	20
		d-2	98	93	61	25	93	69	30	13	98	93	69	32
		d-3	90	18	2	0	18	5	0	0	94	20	6	0
	3	c-2	100	100	99	69	100	99	70	55	100	100	99	70
		c-3	100	100	72	22	100	79	27	13	100	100	81	26
		d-2	99	93	74	25	96	76	34	15	100	97	76	36
		d-3	94	82	50	14	82	56	17	4	96	83	57	16
	4	c-2	100	100	97	72	100	97	72	47	100	100	98	73
		c-3	100	100	100	93	100	100	93	75	100	100	100	93
		d-2	100	100	91	57	100	95	65	38	100	100	94	63
		d-3	100	100	99	85	100	99	88	73	100	100	100	86
4.2	1	c-1	100	99	82	36	100	88	48	28	100	100	87	41
		c-2	100	96	73	26	97	75	33	12	100	96	73	24
		c-3	98	94	65	13	94	64	17	3	98	94	61	11
		d-1	99	97	76	24	98	81	32	15	100	98	80	32
		d-2	97	20	2	0	21	7	0	0	98	23	6	0
		d-3	42	5	1	0	9	1	0	0	47	14	1	0
	2	c-2	100	100	78	40	100	87	49	26	100	100	80	45
		c-3	98	78	32	4	80	38	6	0	98	73	28	2
		d-2	82	58	25	7	64	32	9	3	98	64	31	10
		d-3	40	5	1	1	6	1	0	0	47	11	1	1
	3	c-2	100	100	97	59	100	97	62	35	100	100	98	64
		c-3	100	100	93	60	100	96	61	36	100	100	96	61
		d-2	91	62	31	7	67	39	10	2	95	69	41	10
		d-3	81	48	19	5	51	21	7	5	100	51	22	7
	4	c-2	100	99	56	9	99	70	22	4	100	99	60	11
		c-3	100	100	98	78	100	99	81	62	100	100	98	80
		d-2	96	81	41	6	86	48	12	2	97	86	48	8
		d-3	100	96	83	35	98	83	38	22	100	98	83	39
4.3	1	c-1	100	100	97	68	100	98	74	44	100	100	97	71
		c-2	100	98	78	36	98	83	37	14	100	98	78	34
		c-3	100	92	68	16	92	68	22	3	100	92	65	15
		d-1	100	99	83	41	100	89	46	24	100	100	89	48
		d-2	99	26	9	2	28	9	3	0	100	28	9	5
		d-3	54	6	1	0	9	1	0	0	59	12	1	0
	2	c-2	100	99	90	50	99	92	61	34	100	99	91	54
		c-3	99	88	54	5	90	56	7	1	98	86	49	5
		d-2	91	68	41	13	73	46	16	5	96	73	46	16
		d-3	58	9	0	0	16	0	0	0	63	22	0	0
	3	c-2	100	100	90	51	100	89	52	25	100	100	90	54
		c-3	100	100	95	70	100	95	70	50	100	100	96	72
		d-2	93	77	42	12	78	44	16	7	96	78	43	18
		d-3	88	49	25	8	52	28	10	4	99	52	29	10
	4	c-2	100	98	91	53	100	93	61	43	100	99	91	54
		c-3	100	100	100	86	100	100	83	58	100	100	100	86
		d-2	97	91	64	24	93	75	29	10	99	93	74	27
		d-3	100	99	91	42	100	94	56	27	100	99	94	53

Table 8: Convergence analysis on difference performance indices for NNM-RB-SQP algorithm

Problem	Scenario	Case	MAE ≤				EVAF ≤				TIC ≤			
			10^{-03}	10^{-04}	10^{-05}	10^{-06}	10^{-06}	10^{-08}	10^{-10}	10^{-11}	10^{-03}	10^{-04}	10^{-05}	10^{-06}
4.1	1	c-1	100	99	94	71	99	95	69	40	100	99	94	72
		c-2	100	100	95	44	100	98	56	18	100	100	95	46
		c-3	98	93	35	15	91	38	15	9	98	92	36	15
		d-1	100	92	76	27	97	80	42	14	100	97	80	41
		d-2	99	49	16	5	62	23	6	2	99	62	23	6
		d-3	67	27	5	0	32	6	0	0	72	34	6	0
	2	c-2	99	98	64	22	98	62	22	8	99	98	69	22
		c-3	98	78	34	10	78	35	9	1	98	77	33	8
		d-2	99	84	35	4	94	43	6	3	99	95	42	6
		d-3	66	20	4	0	25	4	0	0	73	28	4	0
	3	c-2	100	100	77	18	100	77	20	10	100	100	86	19
		c-3	100	99	58	22	99	61	21	8	100	100	64	25
		d-2	99	95	32	6	97	44	6	3	99	97	42	6
		d-3	97	78	22	5	87	31	6	0	99	87	31	7
	4	c-2	100	100	98	32	100	99	31	6	100	100	99	42
		c-3	100	98	93	79	98	94	78	48	100	99	94	79
		d-2	100	95	73	26	98	82	30	15	100	98	81	29
		d-3	100	100	84	63	100	89	63	48	100	100	89	63
4.2	1	c-1	100	100	100	43	100	100	53	20	100	100	100	46
		c-2	98	95	54	12	98	58	19	7	98	95	53	12
		c-3	88	41	18	1	41	20	2	0	84	40	16	1
		d-1	99	92	55	9	93	60	13	4	99	93	60	12
		d-2	84	31	2	0	32	6	0	0	91	34	7	0
		d-3	25	7	2	0	9	2	0	0	29	9	2	1
	2	c-2	100	99	48	12	100	53	17	9	100	100	50	13
		c-3	54	35	9	1	36	9	1	0	50	33	9	1
		d-2	99	63	22	1	74	25	3	1	100	74	29	2
		d-3	23	7	2	0	7	2	0	0	28	9	3	0
	3	c-2	100	100	43	14	100	43	18	7	100	100	43	17
		c-3	100	95	54	10	93	51	11	1	100	95	55	10
		d-2	97	65	18	2	74	25	4	0	98	73	24	3
		d-3	96	45	13	2	56	14	3	0	99	59	17	3
	4	c-2	100	100	91	66	100	100	73	56	100	100	96	69
		c-3	100	100	92	51	100	92	50	24	100	100	93	54
		d-2	99	75	21	2	80	24	3	0	99	79	27	3
		d-3	100	95	71	15	97	77	25	7	100	97	77	24
3	1	c-1	100	100	93	44	100	96	44	12	100	100	94	46
		c-2	100	99	54	24	99	56	30	14	100	98	54	25
		c-3	92	54	22	2	54	24	3	0	91	49	18	2
		d-1	100	90	66	17	92	73	26	8	100	92	73	24
		d-2	88	42	14	3	41	18	4	1	91	47	17	4
		d-3	27	9	1	0	10	1	0	0	30	10	1	0
	2	c-2	100	100	60	22	100	62	25	15	100	100	60	23
		c-3	74	43	20	3	46	20	5	3	70	41	17	3
		d-2	99	62	22	3	70	26	5	2	100	69	26	5
		d-3	31	7	1	0	9	1	0	0	41	11	1	0
	3	c-2	100	98	29	19	98	32	18	8	100	98	33	19
		c-3	98	94	48	11	92	49	18	4	98	95	49	14
		d-2	97	63	20	4	73	21	3	0	97	73	22	4
		d-3	95	59	21	4	70	23	5	0	98	71	25	6
	4	c-2	100	100	84	24	100	90	32	11	100	100	88	27
		c-3	99	96	92	56	96	93	51	8	100	96	93	60
		d-2	98	83	28	2	91	36	5	0	99	90	35	4
		d-3	99	95	77	23	95	84	38	13	100	95	84	36

Table 9: Convergence analysis on difference performance indices for NNM-TS-SQP algorithm

Problem	Scenario	Case	MAE ≤				EVAF ≤				TIC ≤			
			10^{-03}	10^{-04}	10^{-05}	10^{-06}	10^{-06}	10^{-08}	10^{-10}	10^{-11}	10^{-03}	10^{-04}	10^{-05}	10^{-06}
4.1	1	c-1	100	100	100	89	100	100	93	77	100	100	100	93
		c-2	100	100	96	72	100	98	82	58	100	100	96	76
		c-3	100	100	90	51	100	91	57	30	100	100	90	52
		d-1	100	100	99	83	100	100	84	60	100	100	100	84
		d-2	93	85	55	20	86	64	23	12	100	86	64	25
		d-3	100	28	14	2	30	17	5	2	100	30	20	6
	2	c-2	100	100	100	71	100	100	77	54	100	100	100	77
		c-3	100	98	89	48	96	90	51	28	100	96	89	47
		d-2	100	100	83	53	100	93	61	34	100	100	93	62
		d-3	99	28	7	0	31	11	0	0	99	31	11	0
	3	c-2	100	100	100	76	100	100	76	58	100	100	100	78
		c-3	100	100	100	64	100	100	69	44	100	100	100	70
		d-2	100	100	89	57	100	95	59	40	100	100	95	61
		d-3	96	90	79	40	90	82	40	30	98	90	82	42
	4	c-2	100	100	99	88	100	99	92	66	100	100	99	93
		c-3	100	100	100	95	100	100	100	79	100	100	100	98
		d-2	100	99	98	77	100	98	85	59	100	100	98	84
		d-3	100	100	100	100	100	100	99	98	100	100	100	100
4.2	1	c-1	100	100	98	63	100	100	74	54	100	100	98	68
		c-2	100	98	86	50	98	88	56	25	100	97	85	49
		c-3	100	97	73	22	97	76	24	3	100	97	68	18
		d-1	100	100	94	57	100	95	60	41	100	100	95	60
		d-2	100	44	22	5	46	23	6	0	100	47	26	5
		d-3	95	21	6	0	35	6	0	0	96	49	6	0
	2	c-2	100	99	86	53	99	88	60	36	100	99	87	55
		c-3	93	85	46	4	84	49	7	1	93	82	42	3
		d-2	97	88	59	27	91	67	30	15	99	92	69	31
		d-3	85	22	2	0	33	2	0	0	88	57	2	0
	3	c-2	100	99	96	63	100	95	71	45	100	99	96	69
		c-3	100	100	98	70	100	99	75	52	100	100	99	74
		d-2	95	90	74	37	92	79	46	25	99	92	80	45
		d-3	94	69	48	20	74	50	22	12	100	74	52	23
	4	c-2	100	100	82	30	100	93	44	22	100	100	87	35
		c-3	100	100	99	87	100	99	89	69	100	100	99	88
		d-2	99	94	73	36	95	79	44	26	99	95	79	40
		d-3	100	100	92	71	100	95	75	55	100	100	94	76
4.3	1	c-1	100	100	100	77	100	100	82	56	100	100	100	78
		c-2	100	100	90	49	100	93	56	24	100	100	91	49
		c-3	98	98	81	33	98	82	39	14	98	98	79	30
		d-1	100	99	94	68	100	95	75	49	100	100	95	76
		d-2	100	53	30	8	61	30	13	4	100	61	31	12
		d-3	97	22	1	0	26	2	0	0	97	28	4	0
	2	c-2	100	100	91	61	99	93	63	37	100	100	93	61
		c-3	100	96	74	13	96	71	17	5	99	94	68	12
		d-2	98	93	68	30	95	73	34	13	100	95	73	38
		d-3	91	26	4	1	33	7	1	0	96	49	6	3
	3	c-2	100	100	98	70	100	97	69	46	100	100	98	69
		c-3	99	99	94	69	99	93	71	43	99	99	94	73
		d-2	100	96	80	44	96	84	47	22	100	97	86	49
		d-3	96	83	62	25	84	65	29	15	98	84	65	29
	4	c-2	100	100	91	58	100	94	65	39	100	100	91	61
		c-3	100	100	100	89	100	99	93	74	100	100	100	91
		d-2	100	100	86	48	100	91	52	30	100	100	90	57
		d-3	100	100	100	82	100	100	86	66	100	100	100	86

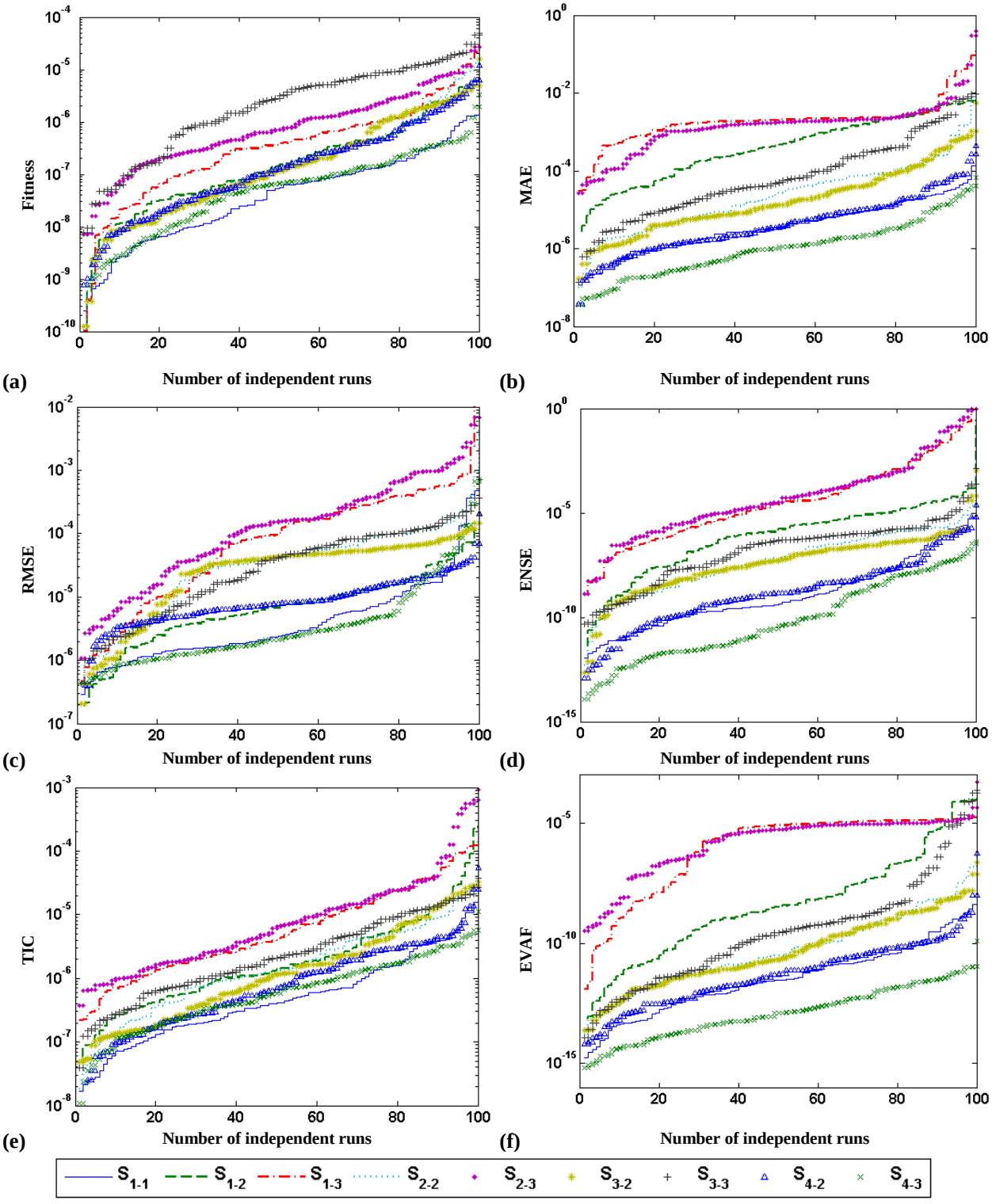

Figure 11: Result of statistical analysis, (a, c, e) for convergent cases, while (b, d, f) for divergent cases for all three NNM-LS-SQP, NNM-RB-SQP, and NNM-TS-SQP, algorithms, respectively, for problem 4.1

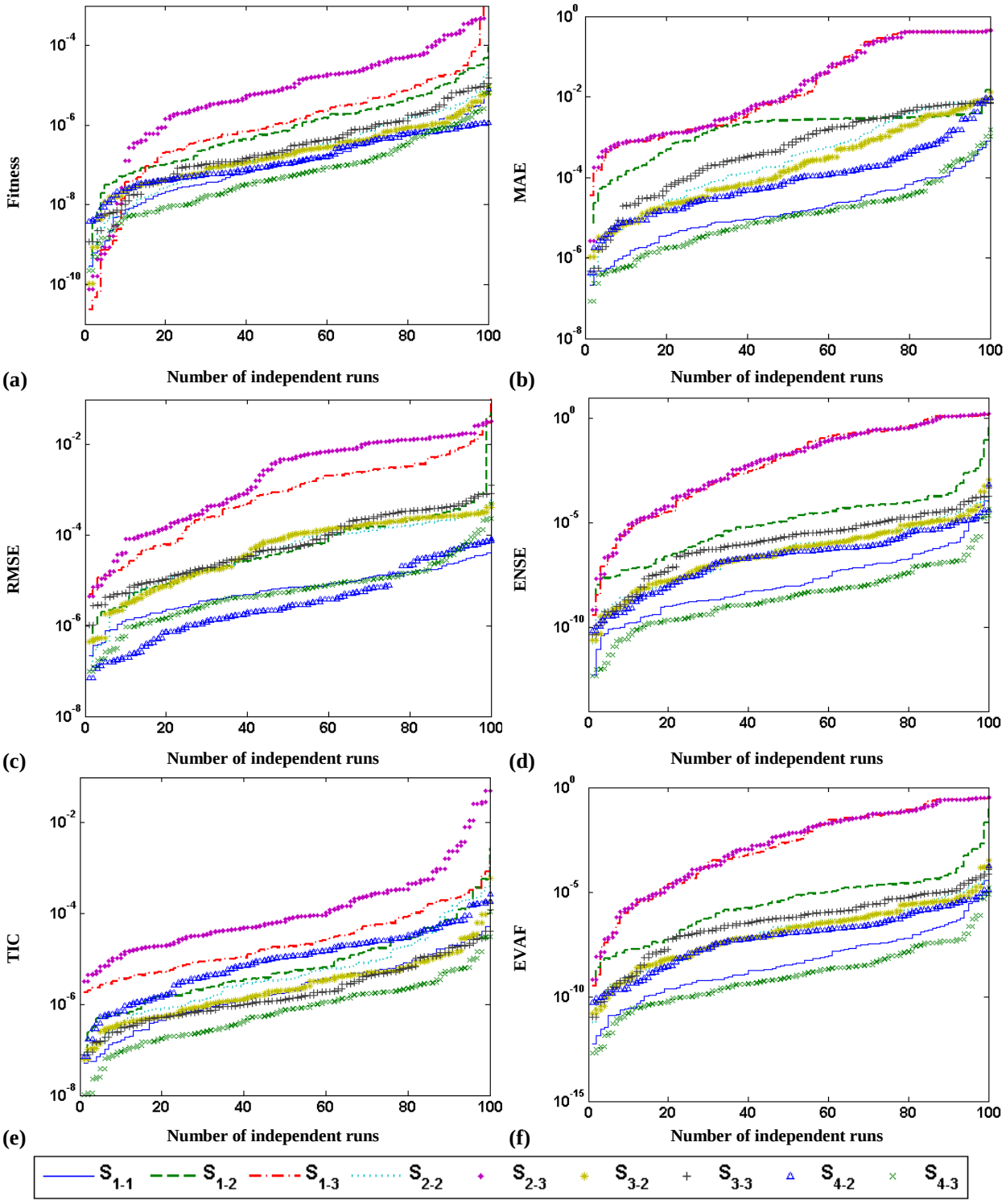

Figure 12: Result of statistical analysis, (a, c, e) for convergent cases, while (b, d, f) for divergent cases for all three NNM-LS-SQP, NNM-RB-SQP, and NNM-TS-SQP, algorithms, respectively, for problem 4.2

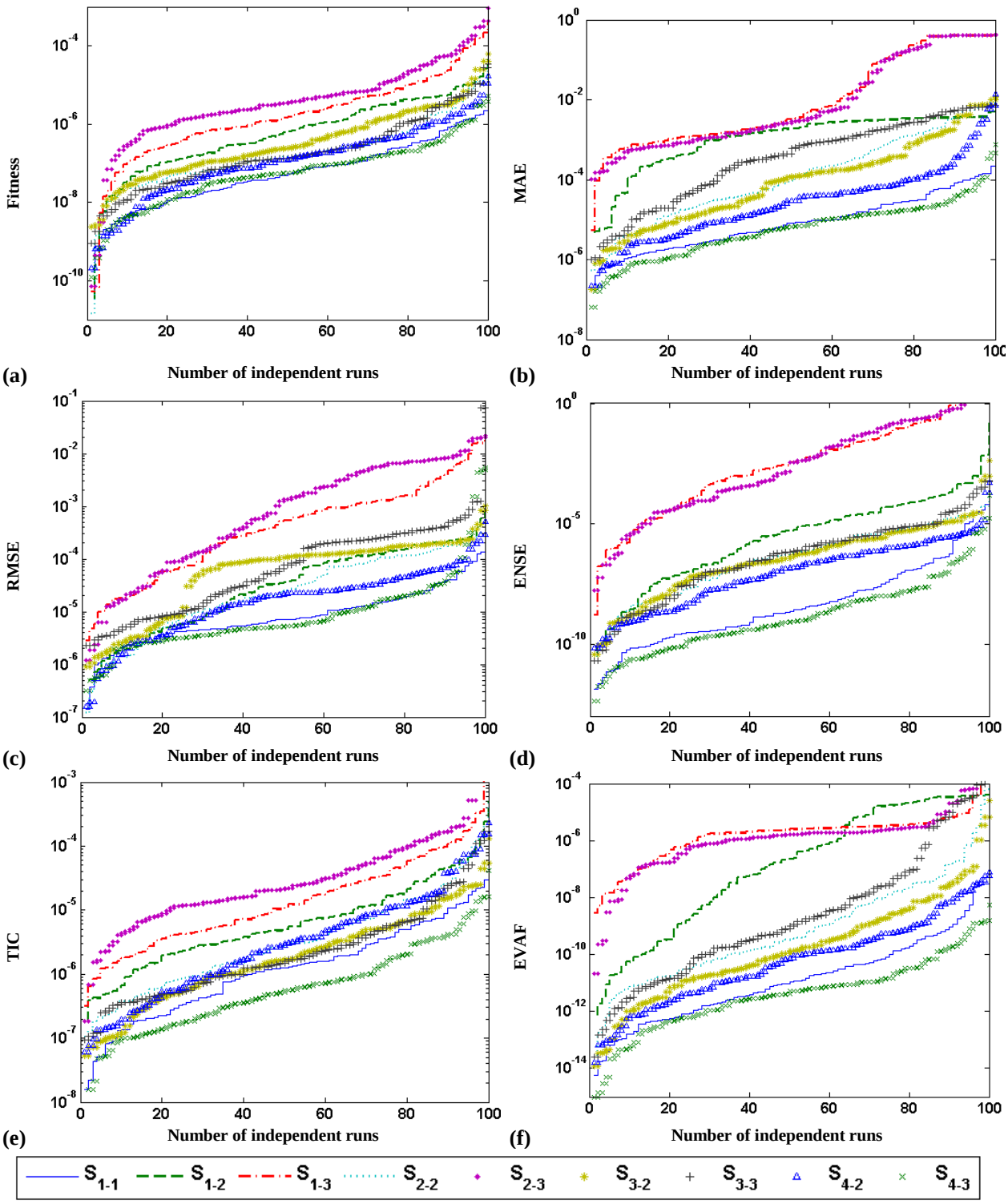

Figure 13: Result of statistical analysis, (a, c, e) for convergent cases, while (b, d, f) for divergent cases for all three NNM-LS-SQP, NNM-RB-SQP, and NNM-TS-SQP, algorithms, respectively, for problem 4.2

Table 10: Comparison of difference global performance indices for NNM-LS-SQP algorithm

Problem	Scenario	Case	Fitness		MAE		RMSE		EVAF		ENSE		TIC	
			Mean	STD	Mean	STD	Mean	STD	Mean	STD	Mean	STD	Mean	STD
4.1	1	c-1	1.6E-07	3.1E-07	2.3E-06	2.8E-06	2.7E-06	3.4E-06	5.7E-11	1.7E-10	7.8E-11	2.0E-10	2.0E-06	2.5E-06
		c-2	7.3E-07	1.4E-06	2.1E-05	4.3E-05	2.3E-05	4.5E-05	2.0E-09	5.9E-09	1.0E-08	3.7E-08	1.8E-05	3.6E-05
		c-3	1.8E-06	4.4E-06	2.9E-05	5.6E-05	3.5E-05	6.6E-05	1.3E-08	4.9E-08	2.2E-08	8.4E-08	3.0E-05	5.7E-05
		d-1	8.7E-07	1.7E-06	1.2E-05	3.3E-05	1.3E-05	3.6E-05	2.3E-09	1.7E-08	6.9E-09	4.9E-08	8.8E-06	2.3E-05
		d-2	1.6E-04	2.8E-04	1.3E-03	1.7E-03	1.4E-03	1.9E-03	1.1E-05	2.4E-05	3.0E-05	6.4E-05	8.7E-04	1.2E-03
		d-3	8.9E-04	3.3E-03	6.3E-03	1.8E-02	6.9E-03	1.9E-02	6.8E-04	3.3E-03	2.6E-03	1.4E-02	4.2E-03	1.2E-02
	2	c-2	1.1E-06	2.5E-06	1.1E-05	2.5E-05	1.3E-05	2.9E-05	2.7E-09	1.5E-08	4.2E-09	2.1E-08	9.3E-06	2.1E-05
		c-3	6.8E-06	4.5E-05	6.8E-05	3.6E-04	8.8E-05	4.9E-04	7.6E-07	7.4E-06	1.0E-06	9.9E-06	8.1E-05	4.5E-04
		d-2	4.3E-05	2.3E-04	2.9E-04	1.4E-03	3.2E-04	1.5E-03	3.9E-06	2.8E-05	1.2E-05	8.5E-05	2.0E-04	9.4E-04
		d-3	2.7E-03	1.8E-02	9.7E-03	5.0E-02	1.0E-02	5.3E-02	4.2E-03	3.0E-02	1.8E-02	1.3E-01	7.2E-03	3.9E-02
	3	c-2	8.2E-07	1.9E-06	6.4E-06	1.3E-05	7.7E-06	1.6E-05	1.1E-09	6.9E-09	1.4E-09	8.4E-09	5.5E-06	1.2E-05
		c-3	6.3E-06	8.8E-06	4.7E-05	6.8E-05	5.3E-05	7.6E-05	1.8E-08	5.2E-08	3.8E-08	1.1E-07	3.6E-05	5.2E-05
		d-2	1.8E-05	9.1E-05	1.4E-04	5.8E-04	1.5E-04	6.3E-04	6.5E-07	5.8E-06	2.1E-06	1.9E-05	9.7E-05	4.0E-04
		d-3	1.1E-04	3.4E-04	7.6E-04	1.9E-03	8.3E-04	2.1E-03	9.9E-06	3.8E-05	2.7E-05	1.0E-04	5.1E-04	1.3E-03
	4	c-2	6.9E-07	1.6E-06	7.4E-06	1.4E-05	8.7E-06	1.6E-05	8.5E-10	2.8E-09	1.4E-09	5.1E-09	6.3E-06	1.2E-05
		c-3	1.7E-07	4.1E-07	1.9E-06	3.7E-06	2.2E-06	4.2E-06	4.6E-11	1.8E-10	9.6E-11	3.7E-10	1.5E-06	2.9E-06
		d-2	2.1E-06	7.4E-06	2.0E-05	5.6E-05	2.1E-05	6.1E-05	6.5E-09	4.0E-08	2.0E-08	1.2E-07	1.4E-05	3.9E-05
		d-3	3.3E-07	9.1E-07	4.2E-06	9.5E-06	4.7E-06	1.1E-05	2.7E-10	1.2E-09	6.2E-10	2.8E-09	3.1E-06	7.0E-06
4.2	1	c-1	5.6E-07	1.2E-06	3.5E-05	7.7E-05	3.8E-05	8.3E-05	1.0E-08	5.1E-08	3.4E-08	1.7E-07	2.9E-05	6.3E-05
		c-2	4.8E-06	1.2E-05	6.9E-05	1.5E-04	8.3E-05	1.9E-04	1.0E-07	5.2E-07	1.7E-07	7.0E-07	7.3E-05	1.6E-04
		c-3	4.2E-05	2.2E-04	3.4E-04	1.7E-03	4.3E-04	2.1E-03	1.3E-05	8.6E-05	2.1E-05	1.4E-04	4.2E-04	2.1E-03
		d-1	9.2E-06	4.6E-05	1.1E-04	5.4E-04	1.2E-04	5.8E-04	5.1E-07	4.8E-06	1.7E-06	1.6E-05	7.4E-05	3.7E-04
		d-2	2.5E-04	2.8E-04	2.4E-03	2.2E-03	2.6E-03	2.3E-03	2.2E-05	4.1E-05	7.2E-05	1.9E-04	1.6E-03	1.4E-03
		d-3	4.6E-02	6.6E-02	1.3E-01	1.7E-01	1.4E-01	1.8E-01	7.5E-02	1.1E-01	3.7E-01	5.5E-01	1.0E-01	1.4E-01
	2	c-2	1.3E-06	3.9E-06	3.6E-05	6.3E-05	3.9E-05	6.9E-05	9.0E-09	3.1E-08	2.5E-08	8.3E-08	3.0E-05	5.4E-05
		c-3	1.5E-04	7.2E-04	9.1E-04	3.7E-03	1.2E-03	4.9E-03	6.5E-05	5.0E-04	1.3E-04	8.9E-04	1.2E-03	5.1E-03
		d-2	2.5E-04	4.4E-04	1.7E-03	2.5E-03	1.9E-03	2.8E-03	2.2E-05	4.3E-05	6.0E-05	1.2E-04	1.2E-03	1.7E-03
		d-3	4.5E-02	6.5E-02	1.3E-01	1.7E-01	1.4E-01	1.8E-01	7.1E-02	1.1E-01	3.5E-01	5.5E-01	9.7E-02	1.3E-01
	3	c-2	6.7E-07	1.4E-06	8.6E-06	1.3E-05	1.0E-05	1.5E-05	8.6E-10	3.4E-09	1.4E-09	4.2E-09	7.4E-06	1.1E-05
		c-3	1.4E-06	2.8E-06	1.2E-05	2.2E-05	1.4E-05	2.5E-05	2.0E-09	8.0E-09	3.5E-09	1.2E-08	1.0E-05	1.8E-05
		d-2	1.7E-04	3.7E-04	1.3E-03	2.4E-03	1.4E-03	2.6E-03	1.5E-05	4.5E-05	4.7E-05	1.4E-04	8.8E-04	1.6E-03
		d-3	2.7E-04	3.7E-04	2.0E-03	2.4E-03	2.2E-03	2.7E-03	2.5E-05	4.4E-05	6.8E-05	1.1E-04	1.4E-03	1.6E-03
	4	c-2	3.6E-07	8.3E-07	8.6E-05	1.4E-04	8.9E-05	1.5E-04	2.1E-08	1.2E-07	1.2E-07	6.6E-07	6.9E-05	1.1E-04
		c-3	4.2E-07	1.2E-06	6.3E-06	1.6E-05	7.4E-06	1.8E-05	7.7E-10	3.9E-09	1.6E-09	7.7E-09	5.4E-06	1.4E-05
		d-2	1.0E-04	3.7E-04	6.5E-04	1.8E-03	7.0E-04	1.9E-03	7.8E-06	3.6E-05	2.2E-05	9.6E-05	4.4E-04	1.2E-03
		d-3	8.6E-06	2.7E-05	7.6E-05	2.1E-04	8.1E-05	2.3E-04	9.2E-08	4.8E-07	2.9E-07	1.5E-06	5.2E-05	1.5E-04
4.3	1	c-1	2.8E-07	6.6E-07	7.1E-06	1.2E-05	8.3E-06	1.5E-05	7.4E-10	2.9E-09	1.2E-09	4.0E-09	6.2E-06	1.1E-05
		c-2	2.8E-06	5.9E-06	4.9E-05	1.3E-04	5.6E-05	1.5E-04	3.8E-08	2.3E-07	1.0E-07	6.5E-07	4.8E-05	1.3E-04
		c-3	1.7E-05	5.5E-05	1.5E-04	3.7E-04	1.9E-04	4.8E-04	7.5E-07	3.9E-06	1.2E-06	6.0E-06	1.8E-04	4.6E-04
		d-1	2.8E-06	8.1E-06	3.0E-05	7.6E-05	3.3E-05	8.2E-05	1.2E-08	8.2E-08	3.8E-08	2.7E-07	2.1E-05	5.2E-05
		d-2	2.2E-04	1.9E-04	2.0E-03	1.4E-03	2.2E-03	1.6E-03	1.6E-05	1.6E-05	4.3E-05	4.6E-05	1.3E-03	9.5E-04
		d-3	3.2E-02	5.7E-02	9.6E-02	1.5E-01	1.0E-01	1.6E-01	5.1E-02	9.6E-02	2.5E-01	4.7E-01	7.3E-02	1.2E-01
	2	c-2	1.3E-06	4.3E-06	2.6E-05	9.4E-05	2.9E-05	1.1E-04	2.5E-08	1.9E-07	4.9E-08	3.8E-07	2.2E-05	8.1E-05
		c-3	3.4E-05	1.1E-04	3.1E-04	9.6E-04	4.1E-04	1.3E-03	4.6E-06	2.9E-05	8.3E-06	5.3E-05	4.1E-04	1.3E-03
		d-2	1.5E-04	3.6E-04	1.1E-03	2.1E-03	1.2E-03	2.3E-03	1.3E-05	3.9E-05	3.5E-05	1.0E-04	7.2E-04	1.4E-03
		d-3	3.2E-02	6.0E-02	9.2E-02	1.5E-01	9.7E-02	1.6E-01	5.0E-02	9.8E-02	2.4E-01	4.8E-01	6.9E-02	1.2E-01
	3	c-2	2.6E-06	8.1E-06	2.3E-05	5.6E-05	2.7E-05	6.5E-05	1.1E-08	5.1E-08	2.0E-08	9.9E-08	2.0E-05	4.8E-05
		c-3	1.6E-06	4.7E-06	1.3E-05	3.8E-05	1.5E-05	4.3E-05	4.6E-09	2.4E-08	8.9E-09	4.5E-08	1.1E-05	3.0E-05
		d-2	1.2E-04	3.4E-04	9.5E-04	2.2E-03	1.0E-03	2.4E-03	1.1E-05	4.2E-05	3.6E-05	1.3E-04	6.4E-04	1.5E-03
		d-3	2.0E-04	3.2E-04	1.6E-03	2.1E-03	1.7E-03	2.3E-03	1.7E-05	3.7E-05	4.7E-05	9.3E-05	1.1E-03	1.4E-03
	4	c-2	7.3E-07	2.1E-06	2.9E-05	1.1E-04	3.1E-05	1.2E-04	1.3E-08	8.7E-08	5.8E-08	4.2E-07	2.3E-05	8.8E-05
		c-3	2.9E-07	7.7E-07	3.6E-06	6.8E-06	4.4E-06	8.4E-06	2.9E-10	1.1E-09	3.7E-10	1.4E-09	3.2E-06	6.1E-06
		d-2	5.8E-05	2.8E-04	4.0E-04	1.7E-03	4.3E-04	1.8E-03	5.4E-06	3.7E-05	1.7E-05	1.2E-04	2.7E-04	1.1E-03
		d-3	2.7E-06	1.0E-05	2.8E-05	9.3E-05	3.0E-05	1.0E-04	1.8E-08	1.1E-07	5.3E-08	3.4E-07	1.9E-05	6.5E-05

Table 11: Comparison of difference global performance indices for NNM-RB-SQP algorithm

Problem	Scenario	Case	Fitness		MAE		RMSE		EVAF		ENSE		TIC	
			Mean	STD	Mean	STD	Mean	STD	Mean	STD	Mean	STD	Mean	STD
4.1	1	c-1	3.0E-06	1.4E-05	4.0E-05	2.3E-04	4.8E-05	2.8E-04	2.6E-07	2.5E-06	3.4E-07	3.2E-06	3.5E-05	2.1E-04
		c-2	6.5E-07	1.8E-06	1.3E-05	1.8E-05	1.4E-05	2.1E-05	9.9E-10	4.8E-09	2.4E-09	8.0E-09	1.1E-05	1.6E-05
		c-3	4.7E-05	2.2E-04	6.7E-04	3.5E-03	7.6E-04	3.9E-03	2.1E-05	1.5E-04	6.2E-05	4.4E-04	6.6E-04	3.4E-03
		d-1	9.8E-06	2.3E-05	1.0E-04	2.2E-04	1.1E-04	2.4E-04	1.1E-07	3.8E-07	3.4E-07	1.2E-06	7.0E-05	1.6E-04
		d-2	7.8E-04	7.0E-03	2.9E-03	2.0E-02	3.1E-03	2.2E-02	9.0E-04	8.9E-03	2.7E-03	2.7E-02	2.1E-03	1.5E-02
		d-3	4.7E-03	1.9E-02	2.0E-02	5.7E-02	2.2E-02	6.0E-02	5.7E-03	2.8E-02	2.5E-02	1.2E-01	1.4E-02	4.2E-02
	2	c-2	1.3E-05	7.6E-05	1.1E-04	5.2E-04	1.3E-04	6.9E-04	1.9E-06	1.9E-05	2.0E-06	2.0E-05	9.8E-05	5.0E-04
		c-3	8.6E-05	5.0E-04	7.1E-04	3.5E-03	8.2E-04	3.8E-03	1.8E-05	1.6E-04	6.4E-05	5.9E-04	7.6E-04	3.6E-03
		d-2	3.4E-05	1.1E-04	3.4E-04	1.1E-03	3.7E-04	1.1E-03	2.1E-06	1.8E-05	7.2E-06	6.3E-05	2.3E-04	7.1E-04
		d-3	6.4E-03	2.2E-02	2.7E-02	7.5E-02	2.9E-02	7.9E-02	1.0E-02	4.4E-02	4.4E-02	1.9E-01	2.0E-02	5.9E-02
	3	c-2	5.3E-06	4.4E-06	3.6E-05	2.7E-05	4.3E-05	3.4E-05	9.3E-09	2.0E-08	1.3E-08	2.1E-08	3.1E-05	2.4E-05
		c-3	1.0E-05	1.7E-05	5.6E-05	7.4E-05	6.8E-05	9.3E-05	4.7E-08	2.1E-07	5.9E-08	2.3E-07	4.6E-05	6.4E-05
		d-2	4.0E-05	2.0E-04	3.3E-04	1.4E-03	3.6E-04	1.5E-03	3.6E-06	3.3E-05	1.3E-05	1.1E-04	2.3E-04	9.7E-04
		d-3	8.0E-05	3.1E-04	5.8E-04	1.6E-03	6.4E-04	1.8E-03	9.9E-06	7.6E-05	1.9E-05	1.3E-04	4.0E-04	1.1E-03
	4	c-2	1.3E-06	1.8E-06	1.1E-05	1.7E-05	1.3E-05	2.2E-05	2.4E-09	2.0E-08	2.8E-09	1.8E-08	9.5E-06	1.6E-05
		c-3	3.1E-06	1.5E-05	2.2E-05	8.9E-05	2.6E-05	1.0E-04	2.7E-08	1.5E-07	4.7E-08	2.9E-07	1.8E-05	7.2E-05
		d-2	1.1E-05	3.4E-05	9.2E-05	2.5E-04	9.9E-05	2.7E-04	1.4E-07	8.8E-07	4.1E-07	2.5E-06	6.4E-05	1.8E-04
		d-3	2.9E-06	6.2E-06	2.5E-05	4.8E-05	2.7E-05	5.3E-05	5.8E-09	2.2E-08	1.6E-08	5.8E-08	1.8E-05	3.5E-05
4.2	1	c-1	1.8E-07	1.9E-07	9.0E-06	9.0E-06	1.0E-05	9.7E-06	2.9E-10	6.3E-10	7.9E-10	1.5E-09	7.6E-06	7.4E-06
		c-2	1.4E-04	9.6E-04	9.6E-04	6.2E-03	1.2E-03	7.4E-03	1.3E-04	9.5E-04	2.3E-04	1.7E-03	1.0E-03	6.6E-03
		c-3	4.9E-04	2.4E-03	3.1E-03	1.0E-02	3.7E-03	1.1E-02	2.0E-04	1.3E-03	6.2E-04	4.9E-03	3.7E-03	1.2E-02
		d-1	3.7E-05	1.4E-04	3.3E-04	1.1E-03	3.5E-04	1.2E-03	2.2E-06	1.4E-05	7.4E-06	4.7E-05	2.2E-04	7.5E-04
		d-2	1.4E-03	9.6E-03	7.0E-03	2.9E-02	7.4E-03	3.1E-02	1.6E-03	1.3E-02	6.2E-03	5.1E-02	4.8E-03	2.2E-02
		d-3	3.8E-02	5.5E-02	1.3E-01	1.5E-01	1.4E-01	1.6E-01	5.8E-02	9.6E-02	2.9E-01	4.7E-01	9.4E-02	1.2E-01
	2	c-2	3.6E-06	4.7E-06	8.5E-05	1.0E-04	9.8E-05	1.1E-04	4.0E-08	7.9E-08	8.8E-08	2.1E-07	7.6E-05	8.6E-05
		c-3	1.1E-03	4.0E-03	6.7E-03	1.4E-02	8.1E-03	1.6E-02	5.2E-04	3.1E-03	1.6E-03	1.1E-02	8.6E-03	1.8E-02
		d-2	8.3E-05	2.1E-04	7.1E-04	1.1E-03	7.7E-04	1.2E-03	4.1E-06	1.7E-05	1.1E-05	3.7E-05	4.7E-04	7.3E-04
		d-3	3.7E-02	5.1E-02	1.3E-01	1.5E-01	1.3E-01	1.5E-01	5.7E-02	9.5E-02	2.9E-01	4.9E-01	9.2E-02	1.2E-01
	3	c-2	1.1E-05	1.3E-05	9.8E-05	9.6E-05	1.2E-04	1.1E-04	7.2E-08	1.0E-07	1.1E-07	1.6E-07	8.8E-05	8.3E-05
		c-3	2.0E-05	2.5E-05	1.5E-04	2.0E-04	1.8E-04	2.3E-04	2.3E-07	5.6E-07	3.7E-07	9.0E-07	1.3E-04	1.7E-04
		d-2	1.0E-04	2.9E-04	8.3E-04	1.8E-03	8.9E-04	2.0E-03	7.5E-06	3.9E-05	2.5E-05	1.3E-04	5.5E-04	1.2E-03
		d-3	1.1E-04	1.5E-04	1.1E-03	1.4E-03	1.2E-03	1.5E-03	6.1E-06	1.6E-05	2.1E-05	5.9E-05	7.3E-04	9.5E-04
	4	c-2	1.4E-07	2.7E-07	1.2E-05	1.9E-05	1.3E-05	2.0E-05	7.1E-10	1.8E-09	2.3E-09	5.4E-09	9.8E-06	1.6E-05
		c-3	2.0E-06	9.2E-06	1.8E-05	5.2E-05	2.2E-05	6.0E-05	9.7E-09	5.3E-08	1.7E-08	1.0E-07	1.6E-05	4.4E-05
		d-2	4.6E-05	1.0E-04	5.2E-04	1.1E-03	5.6E-04	1.2E-03	2.5E-06	1.7E-05	9.4E-06	6.8E-05	3.5E-04	7.7E-04
		d-3	1.3E-05	4.4E-05	1.2E-04	3.9E-04	1.3E-04	4.2E-04	3.0E-07	1.8E-06	9.3E-07	5.4E-06	8.2E-05	2.7E-04
4.3	1	c-1	4.6E-07	6.7E-07	1.4E-05	2.3E-05	1.7E-05	2.6E-05	1.9E-09	6.3E-09	3.9E-09	1.3E-08	1.2E-05	2.0E-05
		c-2	7.2E-06	1.1E-05	7.5E-05	1.0E-04	8.9E-05	1.2E-04	4.9E-08	1.8E-07	9.0E-08	2.9E-07	7.7E-05	1.0E-04
		c-3	1.5E-04	3.6E-04	1.4E-03	2.9E-03	1.7E-03	3.4E-03	2.9E-05	1.1E-04	6.3E-05	2.3E-04	1.6E-03	3.3E-03
		d-1	2.1E-05	6.0E-05	2.3E-04	6.4E-04	2.5E-04	6.9E-04	8.0E-07	3.3E-06	2.6E-06	1.1E-05	1.6E-04	4.4E-04
		d-2	6.2E-04	3.9E-03	4.0E-03	1.7E-02	4.3E-03	1.8E-02	4.9E-04	4.4E-03	1.9E-03	1.7E-02	2.7E-03	1.2E-02
		d-3	2.1E-02	4.0E-02	7.9E-02	1.2E-01	8.3E-02	1.3E-01	3.1E-02	7.2E-02	1.5E-01	3.5E-01	5.7E-02	9.4E-02
	2	c-2	3.6E-06	5.9E-06	5.6E-05	6.9E-05	6.4E-05	7.7E-05	1.9E-08	3.5E-08	4.0E-08	8.2E-08	4.9E-05	5.9E-05
		c-3	3.5E-04	5.6E-04	2.8E-03	3.9E-03	3.5E-03	4.8E-03	7.8E-05	2.0E-04	1.7E-04	4.1E-04	3.5E-03	4.9E-03
		d-2	5.9E-05	1.0E-04	6.2E-04	8.0E-04	6.6E-04	8.7E-04	2.1E-06	7.7E-06	6.4E-06	1.9E-05	4.1E-04	5.4E-04
		d-3	2.2E-02	4.1E-02	8.4E-02	1.2E-01	8.9E-02	1.3E-01	3.2E-02	7.1E-02	1.6E-01	3.5E-01	6.0E-02	9.2E-02
	3	c-2	1.1E-05	1.1E-05	1.0E-04	1.3E-04	1.2E-04	1.4E-04	7.8E-08	2.3E-07	1.4E-07	5.3E-07	8.8E-05	1.0E-04
		c-3	4.0E-04	2.7E-03	1.4E-03	8.5E-03	1.6E-03	1.0E-02	3.3E-04	2.3E-03	4.6E-04	3.2E-03	1.2E-03	7.2E-03
		d-2	1.2E-04	4.8E-04	9.5E-04	3.0E-03	1.0E-03	3.2E-03	1.6E-05	1.2E-04	5.9E-05	4.2E-04	6.4E-04	2.0E-03
		d-3	1.1E-04	2.7E-04	9.3E-04	1.7E-03	1.0E-03	1.9E-03	8.8E-06	3.3E-05	2.5E-05	9.3E-05	6.2E-04	1.2E-03
	4	c-2	1.5E-06	2.2E-06	3.2E-05	5.9E-05	3.7E-05	6.5E-05	1.1E-08	4.7E-08	2.3E-08	1.1E-07	2.8E-05	5.0E-05
		c-3	2.2E-05	1.2E-04	1.6E-04	7.9E-04	1.8E-04	8.6E-04	1.1E-06	6.7E-06	3.2E-06	1.8E-05	1.3E-04	6.2E-04
		d-2	4.1E-05	1.3E-04	4.0E-04	1.1E-03	4.3E-04	1.2E-03	2.3E-06	1.6E-05	8.0E-06	5.5E-05	2.7E-04	7.4E-04
		d-3	1.6E-05	7.6E-05	1.3E-04	5.5E-04	1.4E-04	5.9E-04	5.7E-07	4.7E-06	1.8E-06	1.5E-05	9.1E-05	3.8E-04

Table 12: Comparison of difference global performance indices for NNM-TS-SQP algorithm

Problem	Scenario	Case	Fitness		MAE		RMSE		EVAF		ENSE		TIC	
			Mean	STD	Mean	STD	Mean	STD	Mean	STD	Mean	STD	Mean	STD
4.1	1	c-1	1.3E-07	4.3E-07	1.9E-06	3.7E-06	2.1E-06	4.1E-06	3.4E-11	1.2E-10	8.8E-11	3.3E-10	1.5E-06	3.0E-06
		c-2	4.0E-07	1.4E-06	1.2E-05	4.1E-05	1.2E-05	4.3E-05	1.5E-09	9.4E-09	7.9E-09	4.8E-08	9.8E-06	3.4E-05
		c-3	6.9E-07	1.1E-06	1.7E-05	2.8E-05	2.0E-05	3.4E-05	3.7E-09	1.1E-08	6.2E-09	1.8E-08	1.7E-05	2.9E-05
		d-1	4.6E-07	9.3E-07	4.9E-06	9.8E-06	5.3E-06	1.1E-05	2.2E-10	8.2E-10	6.7E-10	2.4E-09	3.5E-06	6.9E-06
		d-2	9.2E-05	2.6E-04	5.8E-04	1.5E-03	6.4E-04	1.6E-03	6.6E-06	2.3E-05	1.6E-05	5.5E-05	3.9E-04	9.9E-04
		d-3	1.1E-04	8.1E-05	1.4E-03	9.3E-04	1.5E-03	1.0E-03	7.2E-06	5.7E-06	2.1E-05	1.7E-05	9.1E-04	6.0E-04
	2	c-2	4.4E-07	9.4E-07	4.6E-06	7.5E-06	5.4E-06	8.9E-06	2.8E-10	9.4E-10	4.5E-10	1.5E-09	4.0E-06	6.5E-06
		c-3	3.7E-06	1.1E-05	4.3E-05	1.2E-04	5.4E-05	1.6E-04	7.6E-08	3.3E-07	1.2E-07	5.2E-07	4.9E-05	1.5E-04
		d-2	2.3E-06	5.7E-06	2.7E-05	6.7E-05	2.9E-05	7.2E-05	9.2E-09	4.7E-08	3.1E-08	1.6E-07	1.8E-05	4.5E-05
		d-3	1.2E-04	2.3E-04	1.5E-03	2.0E-03	1.6E-03	2.1E-03	1.1E-05	5.3E-05	4.3E-05	2.5E-04	9.5E-04	1.2E-03
	3	c-2	5.3E-07	9.8E-07	5.1E-06	8.5E-06	6.0E-06	1.0E-05	3.7E-10	1.1E-09	5.8E-10	1.6E-09	4.2E-06	7.2E-06
		c-3	8.4E-07	1.4E-06	6.7E-06	8.8E-06	7.6E-06	9.9E-06	3.3E-10	8.7E-10	6.9E-10	1.7E-09	5.2E-06	6.7E-06
		d-2	2.1E-06	4.8E-06	2.0E-05	4.6E-05	2.1E-05	4.9E-05	4.3E-09	2.5E-08	1.5E-08	8.7E-08	1.4E-05	3.1E-05
		d-3	5.3E-05	2.3E-04	4.6E-04	1.7E-03	5.0E-04	1.8E-03	6.2E-06	3.1E-05	1.9E-05	9.0E-05	3.1E-04	1.1E-03
	4	c-2	3.5E-07	1.0E-06	2.9E-06	7.4E-06	3.4E-06	8.6E-06	2.2E-10	1.5E-09	3.6E-10	2.5E-09	2.4E-06	6.2E-06
		c-3	1.0E-07	1.3E-07	1.5E-06	2.1E-06	1.7E-06	2.2E-06	9.1E-12	1.9E-11	3.3E-11	1.2E-10	1.2E-06	1.6E-06
		d-2	1.1E-06	6.5E-06	9.5E-06	5.2E-05	1.0E-05	5.6E-05	5.6E-09	5.4E-08	1.6E-08	1.5E-07	6.7E-06	3.6E-05
		d-3	3.5E-08	4.7E-08	5.9E-07	7.4E-07	6.4E-07	8.3E-07	2.3E-12	1.3E-11	5.2E-12	1.4E-11	4.2E-07	5.5E-07
4.2	1	c-1	1.2E-07	2.1E-07	7.9E-06	1.3E-05	8.7E-06	1.4E-05	3.6E-10	1.0E-09	1.1E-09	3.5E-09	6.6E-06	1.1E-05
		c-2	4.0E-06	1.5E-05	5.9E-05	2.8E-04	7.0E-05	3.2E-04	1.8E-07	1.5E-06	4.2E-07	3.7E-06	6.1E-05	2.8E-04
		c-3	6.6E-06	2.1E-05	6.7E-05	1.5E-04	8.5E-05	1.9E-04	1.2E-07	6.0E-07	2.0E-07	1.0E-06	8.3E-05	1.9E-04
		d-1	1.3E-06	2.5E-06	1.5E-05	4.5E-05	1.7E-05	4.9E-05	3.8E-09	2.8E-08	1.3E-08	1.0E-07	1.1E-05	3.1E-05
		d-2	1.3E-04	1.3E-04	1.3E-03	1.3E-03	1.4E-03	1.4E-03	8.7E-06	1.1E-05	2.4E-05	2.9E-05	8.6E-04	8.3E-04
		d-3	6.7E-03	3.3E-02	1.7E-02	7.9E-02	1.8E-02	8.4E-02	1.0E-02	5.0E-02	5.0E-02	2.5E-01	1.3E-02	6.1E-02
	2	c-2	1.6E-06	6.0E-06	5.2E-05	2.0E-04	5.7E-05	2.1E-04	6.2E-08	4.7E-07	2.0E-07	1.6E-06	4.5E-05	1.7E-04
		c-3	3.0E-04	1.3E-03	1.7E-03	6.3E-03	2.2E-03	8.0E-03	1.6E-04	7.9E-04	3.4E-04	1.7E-03	2.3E-03	8.4E-03
		d-2	5.5E-05	2.3E-04	3.9E-04	1.3E-03	4.2E-04	1.4E-03	4.8E-06	2.5E-05	1.2E-05	6.1E-05	2.6E-04	8.9E-04
		d-3	7.4E-03	3.2E-02	2.1E-02	8.3E-02	2.2E-02	8.8E-02	1.2E-02	5.3E-02	5.7E-02	2.6E-01	1.6E-02	6.4E-02
	3	c-2	1.2E-06	3.7E-06	1.7E-05	8.1E-05	1.8E-05	8.4E-05	5.1E-09	3.0E-08	3.0E-08	2.6E-07	1.4E-05	6.2E-05
		c-3	1.0E-06	2.7E-06	7.3E-06	1.7E-05	8.5E-06	2.0E-05	1.1E-09	6.3E-09	2.0E-09	1.3E-08	6.0E-06	1.4E-05
		d-2	7.0E-05	2.8E-04	4.3E-04	1.5E-03	4.7E-04	1.6E-03	5.7E-06	2.8E-05	1.6E-05	7.2E-05	2.9E-04	1.0E-03
		d-3	1.1E-04	2.5E-04	9.2E-04	1.7E-03	1.0E-03	1.9E-03	9.8E-06	2.7E-05	2.6E-05	6.7E-05	6.1E-04	1.2E-03
	4	c-2	1.6E-07	3.1E-07	3.3E-05	5.6E-05	3.5E-05	5.9E-05	3.5E-09	1.2E-08	1.9E-08	6.3E-08	2.7E-05	4.5E-05
		c-3	2.9E-07	1.0E-06	3.6E-06	1.2E-05	4.4E-06	1.6E-05	1.1E-09	1.0E-08	1.2E-09	9.6E-09	3.3E-06	1.2E-05
		d-2	4.0E-05	2.9E-04	2.1E-04	1.0E-03	2.3E-04	1.1E-03	2.9E-06	2.7E-05	7.0E-06	6.2E-05	1.4E-04	7.1E-04
		d-3	1.4E-06	4.8E-06	1.4E-05	4.5E-05	1.5E-05	4.8E-05	3.8E-09	2.6E-08	1.2E-08	8.5E-08	9.7E-06	3.1E-05
4.3	1	c-1	1.3E-07	2.7E-07	4.5E-06	7.8E-06	5.0E-06	8.5E-06	1.5E-10	6.7E-10	4.0E-10	1.4E-09	3.7E-06	6.4E-06
		c-2	1.4E-06	4.6E-06	2.1E-05	5.5E-05	2.5E-05	6.7E-05	1.2E-08	9.0E-08	2.0E-08	1.4E-07	2.1E-05	5.7E-05
		c-3	1.0E-05	6.5E-05	1.4E-04	8.0E-04	1.8E-04	9.9E-04	2.4E-06	2.1E-05	4.3E-06	3.3E-05	1.7E-04	9.4E-04
		d-1	2.0E-06	9.5E-06	1.7E-05	7.5E-05	1.9E-05	8.1E-05	1.1E-08	9.9E-08	3.4E-08	3.0E-07	1.2E-05	5.2E-05
		d-2	1.3E-04	1.7E-04	1.2E-03	1.4E-03	1.3E-03	1.5E-03	9.0E-06	1.3E-05	2.4E-05	3.5E-05	7.8E-04	9.2E-04
		d-3	2.0E-03	1.7E-02	6.0E-03	4.1E-02	6.4E-03	4.3E-02	2.7E-03	2.5E-02	1.3E-02	1.2E-01	4.4E-03	3.1E-02
	2	c-2	1.5E-06	6.8E-06	2.0E-05	6.0E-05	2.3E-05	7.5E-05	2.0E-08	1.6E-07	2.5E-08	1.7E-07	1.8E-05	5.7E-05
		c-3	1.1E-05	4.4E-05	1.3E-04	4.7E-04	1.6E-04	6.1E-04	1.0E-06	7.2E-06	1.9E-06	1.3E-05	1.7E-04	6.2E-04
		d-2	2.7E-05	1.2E-04	2.3E-04	9.4E-04	2.5E-04	1.0E-03	1.6E-06	9.8E-06	5.8E-06	3.5E-05	1.6E-04	6.3E-04
		d-3	1.9E-03	1.7E-02	5.7E-03	4.0E-02	6.2E-03	4.2E-02	2.7E-03	2.5E-02	1.2E-02	1.2E-01	4.2E-03	3.1E-02
	3	c-2	7.7E-07	1.7E-06	7.6E-06	1.9E-05	8.8E-06	2.1E-05	9.8E-10	5.2E-09	2.1E-09	1.3E-08	6.4E-06	1.5E-05
		c-3	2.8E-05	2.7E-04	1.3E-04	1.1E-03	1.5E-04	1.3E-03	4.9E-06	4.9E-05	7.8E-06	7.8E-05	1.0E-04	9.4E-04
		d-2	1.3E-05	6.2E-05	1.0E-04	4.1E-04	1.1E-04	4.5E-04	3.7E-07	2.7E-06	1.1E-06	7.7E-06	6.8E-05	2.8E-04
		d-3	7.7E-05	2.3E-04	6.3E-04	1.6E-03	6.9E-04	1.8E-03	7.4E-06	2.8E-05	2.0E-05	7.4E-05	4.2E-04	1.1E-03
	4	c-2	5.9E-07	1.6E-06	1.7E-05	3.9E-05	1.9E-05	4.5E-05	5.2E-09	3.0E-08	9.7E-09	4.3E-08	1.5E-05	3.4E-05
		c-3	1.7E-07	4.3E-07	2.4E-06	5.4E-06	2.8E-06	6.9E-06	1.9E-10	1.5E-09	2.3E-10	1.4E-09	2.1E-06	5.0E-06
		d-2	2.0E-06	4.2E-06	2.2E-05	4.1E-05	2.3E-05	4.4E-05	3.5E-09	1.1E-08	1.3E-08	4.0E-08	1.5E-05	2.7E-05
		d-3	3.1E-07	5.2E-07	3.9E-06	6.9E-06	4.2E-06	7.6E-06	1.4E-10	6.2E-10	3.6E-10	1.3E-09	2.7E-06	4.9E-06

Table 13: Complexity analysis of the results

Problem	Scenario	Case	NNM-LS-SQP			NNM-RB-SQP			NNM-TS-SQP		
			MT	MGs	MFCs	MT	MGs	MFCs	MT	MGs	MFCs
4.1	1	c-1	22.9	633.3	39059.8	25.6	750.6	46299.9	28.9	724.7	44682.5
		c-2	27.1	752.0	46340.5	29.8	875.2	53891.4	28.5	713.2	43990.2
		c-3	24.3	674.0	41603.4	31.5	930.2	57273.3	28.2	709.4	43823.5
		d-1	26.4	726.9	44832.5	27.2	791.1	48819.8	30.9	770.9	47553.4
		d-2	32.6	883.4	54441.0	29.3	841.8	51953.5	34.0	836.2	51583.1
		d-3	31.7	868.8	53578.4	32.2	936.1	57702.2	30.3	747.8	46249.6
	2	c-2	24.6	659.0	40652.4	28.7	812.7	50096.2	28.9	700.9	43231.0
		c-3	24.6	660.2	40777.2	31.3	893.7	55061.6	29.8	726.6	44854.0
		d-2	29.7	813.7	50231.9	26.6	774.1	47794.2	31.8	793.4	48944.2
		d-3	32.0	858.3	52959.7	33.5	951.5	58719.3	30.6	744.0	45985.9
	3	c-2	26.4	703.5	43364.6	26.3	740.8	45740.4	28.4	685.9	42304.3
		c-3	20.5	568.7	35175.9	16.7	490.4	30416.1	22.0	554.3	34305.2
		d-2	30.0	825.0	50854.6	26.6	778.7	48055.2	31.5	786.7	48549.6
		d-3	31.9	883.5	54428.8	26.9	788.2	48673.4	31.5	791.0	48814.3
	4	c-2	23.1	631.5	38971.5	20.8	603.8	37297.3	28.8	716.2	44165.6
		c-3	28.2	765.0	47126.4	22.0	630.2	38924.6	28.6	703.2	43334.6
		d-2	27.2	746.4	46029.9	27.8	805.9	49726.8	30.1	751.9	46383.1
		d-3	26.4	724.3	44672.7	27.6	801.2	49428.4	26.5	658.5	40638.2
4.2	1	c-1	30.0	800.5	49303.2	32.9	929.2	57174.1	34.0	823.7	50733.7
		c-2	23.9	638.3	39418.4	29.9	846.5	52166.1	26.3	635.1	39269.2
		c-3	29.9	715.9	44213.9	34.8	938.9	57836.2	34.1	803.2	49553.7
		d-1	40.6	742.2	45790.8	40.6	772.2	47678.6	44.5	769.8	47493.5
		d-2	46.0	828.0	51091.9	47.2	916.8	56537.3	45.6	812.3	50153.3
		d-3	47.7	948.9	58455.1	45.8	986.2	60772.7	41.3	792.6	49011.4
	2	c-2	31.7	752.3	46357.4	35.3	940.9	57891.9	35.1	824.6	50797.1
		c-3	34.0	862.8	53166.1	34.0	969.7	59716.0	36.2	900.8	55533.7
		d-2	68.3	887.8	54688.7	61.2	810.3	50039.3	66.3	822.4	50740.0
		d-3	139.0	972.3	59877.1	119.4	986.0	60781.3	119.4	806.8	49889.8
	3	c-2	45.8	690.3	42568.7	56.3	882.2	54339.2	45.4	662.3	40892.2
		c-3	44.1	664.7	41015.8	43.6	681.1	42082.7	45.0	659.3	40705.3
		d-2	56.7	865.6	53344.1	53.5	838.6	51755.1	57.1	835.9	51538.9
		d-3	58.5	892.9	55028.0	57.9	908.0	56195.5	58.2	854.0	52681.4
	4	c-2	44.3	717.9	44246.9	47.6	807.0	49700.3	56.9	895.6	55113.3
		c-3	34.0	652.8	40258.6	39.4	816.6	50333.7	38.8	729.7	44981.7
		d-2	44.6	863.1	53215.6	38.6	797.9	49258.2	44.0	823.1	50772.1
		d-3	38.1	744.4	45910.4	37.1	770.8	47599.6	39.3	741.5	45753.8
4.3	1	c-1	38.2	734.1	45243.7	44.8	930.2	57229.2	41.5	778.3	47983.8
		c-2	28.9	554.6	34292.0	42.3	872.3	53743.0	34.8	650.5	40196.0
		c-3	37.0	714.0	44085.4	43.4	902.3	55597.7	41.4	778.9	48086.5
		d-1	37.4	729.5	45025.8	35.3	733.3	45293.7	40.8	772.8	47663.5
		d-2	37.0	848.4	52339.6	35.1	892.7	55047.1	34.5	769.1	47490.1
		d-3	40.9	952.3	58672.3	38.1	981.8	60489.1	35.2	791.6	48930.7
	2	c-2	35.3	750.6	46258.9	39.3	922.4	56765.8	38.4	792.7	48855.7
		c-3	57.4	774.0	47759.0	66.9	971.0	59800.9	63.8	831.6	51312.5
		d-2	77.6	884.2	54474.0	67.8	803.1	49597.4	75.8	846.0	52177.0
		d-3	52.9	961.6	59240.1	51.2	984.5	60688.5	44.9	789.4	48801.9
	3	c-2	28.3	678.0	41843.8	32.9	881.7	54334.4	27.9	653.3	40333.1
		c-3	28.1	692.8	42710.7	20.1	547.3	33906.2	27.6	663.2	40956.4
		d-2	35.4	872.0	53721.8	29.2	804.5	49670.0	33.9	816.7	50363.4
		d-3	37.4	921.5	56754.2	30.7	843.1	52003.8	35.0	841.8	51945.0
	4	c-2	29.2	722.3	44536.9	33.8	933.2	57406.5	33.8	814.6	50180.3
		c-3	24.9	613.8	37886.8	27.4	752.7	46403.2	27.5	660.9	40768.2
		d-2	38.8	820.9	50600.9	35.1	808.6	49913.1	38.6	796.3	49116.8
		d-3	49.4	767.4	47323.0	44.2	762.7	47087.8	45.7	702.9	43387.4

6. Conclusions

Neurocomputing based computational intelligence algorithms are designed for solving nanofluidics problems based nonlinear Jeffery-Hamel Flow problems involving nanoparticles in the presence of high magnetic fields by exploiting the renewed strength of artificial neural network modelling optimized with efficient local search methodology through SQP. The proposed schemes NNM-LS-SQP, NNM-RB-SQP and NNM-TS-SQP are applied to number of variants of the nonlinear MHD-JHF problems by taking the different values for Reynolds number, angles of channel, Hartmann numbers and concentration levels of nanoparticles and results show that the given velocity profile of the fluids are consistently overlapping the reference results calculated from Adams numerical solver. Comparative studies of the results for proposed three models NNM-LS-SQP, NNM-RB-SQP and NNM-TS-SQP show that the matching up to 3 to 7 decimal of accuracy is achieved for each variant of the problems but relatively better results are obtained with NNM-TS-SQP algorithm from the rest. Comparative study through results of statistical analysis based on 100 independent runs of each model in terms of mean and STD show that these parameters are generally close to zero but the values of statistical measures are relatively better for NNM-LS-SQP and NNM-TS-SQP from NNM-RB-SQP. While comparing the performance of NNM-LS-SQP and NNM-TS-SQP algorithms, the results of NNM-TS-SQP are slightly superior. Additionally, the small STDs further validate the consistency of the all three algorithms for finding the solution all three problems of nonlinear MHD-JHF. Comparative analysis of proposed three schemes NNM-LS-SQP, NNM-RB-SQP and NNM-TS-SQP has been further evaluated based on performance indices of MAE, RMSE, EVAF, TIC and ENSE, as well as, their global updates for all three problems of nonlinear MHD-JHF with base fluid water mixed with nanoparticles and results show that close to optimal values

of these indicators are obtained from all three models but the results of NNM-TS-SQP are relatively better in accuracy and convergent from other two counterparts. Computational complexity of the models has been monitored through mean execution time, generations and function counts consumed during the process of optimization of design variables of the network to solve nonlinear MDH-JHF type nanofluidics problems and it is found that the values of complexity operators are relatively less for the convergent cases than that of divergent flow scenarios for all three models, but least for NNM-LS-SQP model as compared with rest of the algorithms.

The application of the design schemes can also be extended to deal with nonlinear MHD JHF problems by considering heat and energy effects, as well as take different base fluids contaminated with nano-materials [83-86]. Modeling error can be reduced considerably with the introduction of support vector machine as an alternative involving transfer function based on radial, tan-sigmoid, Mexican, and wavelet hat kernels. Role of modern optimization algorithms introduced recently cannot be denied and with the help of these procedures improvements in the accuracy and convergence of results may be achieved. Few good alternatives include genetic programming, fractional variants of particle swarm optimization, chaos optimization algorithm, firefly method, fireworks schemes and gravitational search algorithms etc.

References

[1] Bahiraei, M., Godini, A. and Shahsavar, A., 2018. Thermal and hydraulic characteristics of a minichannel heat exchanger operated with a non-Newtonian hybrid nanofluid. *Journal of the Taiwan Institute of Chemical Engineers*, *84*, pp.149-161.

[2] Esfahani, M.A. and Toghraie, D., 2017. Experimental investigation for developing a new model for the thermal conductivity of silica/water-ethylene glycol (40%–60%) nanofluid at different temperatures and solid volume fractions. *Journal of Molecular Liquids*, *232*, pp.105-112.

[3] Kabeel, A.E., Omara, Z.M. and Essa, F.A., 2017. Numerical investigation of modified solar still using nanofluids and external condenser. *Journal of the Taiwan Institute of Chemical Engineers*, *75*, pp.77-86.

[4] Zarringhalam, M., Karimipour, A. and Toghraie, D., 2016. Experimental study of the effect of solid volume fraction and Reynolds number on heat transfer coefficient and pressure drop of CuO–water nanofluid. Experimental Thermal and Fluid Science, 76, pp.342-351.

[5] Rahimi-Gorji, M., Pourmehran, O., Gorji-Bandpy, M. and Ganji, D.D., 2016. Unsteady squeezing nanofluid simulation and investigation of its effect on important heat transfer parameters in presence of magnetic field. *Journal of the Taiwan Institute of Chemical Engineers*, *67*, pp.467-475.

[6] Karimipour, A., Alipour, H., Akbari, O.A., Semiromi, D.T. and Esfe, M.H., 2015. Studying the effect of indentation on flow parameters and slow heat transfer of water-silver nano-fluid with varying volume fraction in a rectangular two-dimensional micro channel. *Indian Journal of Science and Technology*, *8*(15).

[7] Akbari, O.A., Safaei, M.R., Goodarzi, M., Akbar, N.S., Zarringhalam, M., Shabani, G.A.S. and Dahari, M., 2016. A modified two-phase mixture model of nanofluid flow and heat transfer in a 3-D curved microtube. *Advanced Powder Technology*, *27*(5), pp.2175-2185.

[8] Akbari, O.A., Toghraie, D., Karimipour, A., Marzban, A. and Ahmadi, G.R., 2017. The effect of velocity and dimension of solid nanoparticles on heat transfer in non-Newtonian nanofluid. *Physica E: Low-dimensional Systems and Nanostructures*, *86*, pp.68-75.

[9] Akbari, O.A., Toghraie, D., Karimipour, A., Safaei, M.R., Goodarzi, M., Alipour, H. and Dahari, M., 2016. Investigation of rib's height effect on heat transfer and flow parameters of laminar water–Al2O3 nanofluid in a rib-microchannel. *Applied Mathematics and Computation*, *290*, pp.135-153.

[10] Akbari, O.A., Toghraie, D. and Karimipour, A., 2015. Impact of ribs on flow parameters and laminar heat transfer of water–aluminum oxide nanofluid with different nanoparticle volume fractions in a three-dimensional rectangular microchannel. *Advances in Mechanical Engineering*, *7*(11), p.1687814015618155.

[11] Safaei, M.R., Gooarzi, M., Akbari, O.A., Shadloo, M.S. and Dahari, M., 2016. Performance evaluation of nanofluids in an inclined ribbed microchannel for electronic cooling applications. In *Electronics Cooling*. InTech.

[12] Karimipour, A., Esfe, M.H., Safaei, M.R., Semiromi, D.T., Jafari, S. and Kazi, S.N., 2014. Mixed convection of copper–water nanofluid in a shallow inclined lid driven cavity using the lattice Boltzmann method. *Physica A: Statistical Mechanics and its Applications*, *402*, pp.150-168.

[13] Karimipour, A., Nezhad, A.H., D'Orazio, A., Esfe, M.H., Safaei, M.R. and Shirani, E., 2015. Simulation of copper–water nanofluid in a microchannel in slip flow regime using the lattice Boltzmann method. *European Journal of Mechanics-B/Fluids*, *49*, pp.89-99.

[14] Afrand, M., Rostami, S., Akbari, M., Wongwises, S., Esfe, M.H. and Karimipour, A., 2015. Effect of induced electric field on magneto-natural convection in a vertical cylindrical annulus filled with liquid potassium. *International Journal of Heat and Mass Transfer*, *90*, pp.418-426.

[15] Mahmoodi, M., Esfe, M.H., Akbari, M., Karimipour, A. and Afrand, M., 2015. Magneto-natural convection in square cavities with a source-sink pair on different walls. *International Journal of Applied Electromagnetics and Mechanics*, *47*(1), pp.21-32.

[16] Safaei, M.R., Mahian, O., Garoosi, F., Hooman, K., Karimipour, A., Kazi, S.N. and Gharehkhani, S., 2014. Investigation of micro-and nanosized particle erosion in a 90 pipe bend using a two-phase discrete phase model. *The scientific world journal*, *2014*.

[17] Sajadifar, S.A., Karimipour, A. and Toghraie, D., 2017. Fluid flow and heat transfer of non-Newtonian nanofluid in a microtube considering slip velocity and temperature jump boundary conditions. *European Journal of Mechanics-B/Fluids*, *61*, pp.25-32.

[18] Toghraie, D., Alempour, S.M. and Afrand, M., 2016. Experimental determination of viscosity of water based magnetite nanofluid for application in heating and cooling systems. *Journal of Magnetism and Magnetic Materials*, *417*, pp.243-248.

[19] Alipour, H., Karimipour, A., Safaei, M.R., Semiromi, D.T. and Akbari, O.A., 2017. Influence of T-semi attached rib on turbulent flow and heat transfer parameters of a silver-water nanofluid with different volume fractions in a three-dimensional trapezoidal microchannel. *Physica E: Low-dimensional Systems and Nanostructures*, *88*, pp.60-76.

[20] Afrand, M., Toghraie, D. and Ruhani, B., 2016. Effects of temperature and nanoparticles concentration on rheological behavior of Fe3O4–Ag/EG hybrid nanofluid: an experimental study. *Experimental Thermal and Fluid Science*, *77*, pp.38-44.

[21] Sheikholeslami, M., Mollabasi, H. and Ganji, D.D., 2015. Analytical investigation of MHD Jeffery–Hamel nanofluid flow in non-parallel walls. *International Journal of Nanoscience and Nanotechnology*, *11*(4), pp.241-248.

[22] Dogonchi, A.S. and Ganji, D.D., 2016. Study of nanofluid flow and heat transfer between non-parallel stretching walls considering Brownian motion. *Journal of the Taiwan Institute of Chemical Engineers*, *69*, pp.1-13.

[23] Nagler, J., 2017. Jeffery-Hamel flow of non-Newtonian fluid with nonlinear viscosity and wall friction. *Applied Mathematics and Mechanics*, *38*(6), pp.815-830.

[24] Sheikholeslami, M., 2018. Numerical simulation for solidification in a LHTESS by means of Nano-enhanced PCM. *Journal of the Taiwan Institute of Chemical Engineers* 86:25-41.

[25] Sheikholeslami, M. and Ganji, D.D., 2016. Nanofluid convective heat transfer using semi analytical and numerical approaches: a review. *Journal of the Taiwan Institute of Chemical Engineers*, *65*, pp.43-77.

[26] Nazari, S. and Toghraie, D., 2017. Numerical simulation of heat transfer and fluid flow of Water-CuO Nanofluid in a sinusoidal channel with a porous medium. *Physica E: Low-dimensional Systems and Nanostructures*, *87*, pp.134-140.

[27] Aghanajafi, A., Toghraie, D. and Mehmandoust, B., 2017. Numerical simulation of laminar forced convection of water-CuO nanofluid inside a triangular duct. *Physica E: Low-dimensional Systems and Nanostructures*, *85*, pp.103-108.

[28] Akbari, O.A., Toghraie, D. and Karimipour, A., 2016. Numerical simulation of heat transfer and turbulent flow of water nanofluids copper oxide in rectangular microchannel with semi-attached rib. *Advances in Mechanical Engineering*, *8*(4), p.1687814016641016.

[29] Rezaei, M., Azimian, A.R. and Semiromi, D.T., 2015. The surface charge density effect on the electro-osmotic flow in a nanochannel: a molecular dynamics study. *Heat and Mass Transfer*, *51*(5), pp.661-670.

[30] Rezaei, M., Azimian, A.R. and Toghraie, D., 2015. Molecular dynamics study of an electro-kinetic fluid transport in a charged nanochannel based on the role of the stern layer. *Physica A: Statistical Mechanics and its Applications*, *426*, pp.25-34.

[31] Esfe, M.H., Afrand, M., Yan, W.M., Yarmand, H., Toghraie, D. and Dahari, M., 2016. Effects of temperature and concentration on rheological behavior of MWCNTs/SiO2 (20–80)-SAE40 hybrid nano-lubricant. *International Communications in Heat and Mass Transfer*, *76*, pp.133-138.

[32] Karimipour, A., Esfe, M.H., Safaei, M.R., Semiromi, D.T., Jafari, S. and Kazi, S.N., 2014. Mixed convection of copper–water nanofluid in a shallow inclined lid driven cavity using the lattice Boltzmann method. *Physica A: Statistical Mechanics and its Applications*, *402*, pp.150-168.

[33] Sheikholeslami, M., 2017. Numerical simulation of magnetic nanofluid natural convection in porous media. *Physics Letters A*, *381*(5), pp.494-503.

[34] Ali, H. and Park, C.W., 2017. Numerical heat transfer analysis in a two-phase microorganism malodor removing system with the effect of internal structures. *Journal of the Taiwan Institute of Chemical Engineers*, *75*, pp.119-130.

[35] Raja, M.A.Z., Khan, J.A. and Haroon, T., 2015. Stochastic numerical treatment for thin film flow of third grade fluid using unsupervised neural networks. *Journal of the Taiwan Institute of Chemical Engineers*, *48*, pp.26-39.

[36] Razzaghi, M., Karimi, A., Ansari, Z. and Aghdasinia, H., 2018. Phenol removal by HRP/GOx/ZSM-5 from aqueous solution: Artificial neural network simulation and genetic algorithms optimization. *Journal of the Taiwan Institute of Chemical Engineers*.

[37] Raja, M.A.Z., Shah, F.H., Khan, A.A. and Khan, N.A., 2016. Design of bio-inspired computational intelligence technique for solving steady thin film flow of Johnson–Segalman fluid on vertical cylinder for drainage problems. *Journal of the Taiwan Institute of Chemical Engineers*, *60*, pp.59-75.

[38] Oladipo, A.A., Vaziri, R. and Abureesh, M.A., 2017. Highly robust AgIO 3/MIL-53 (Fe) nanohybrid composites for degradation of organophosphorus pesticides in single and binary systems: Application of artificial neural networks modelling. *Journal of the Taiwan Institute of Chemical Engineers*.

[39] Esfe, M.H., Saedodin, S., Bahiraei, M., Toghraie, D., Mahian, O. and Wongwises, S., 2014. Thermal conductivity modeling of MgO/EG nanofluids using experimental data and artificial neural network. *Journal of Thermal Analysis and Calorimetry*, *118*(1), pp.287-294.

[40] Raja, M.A.Z., Niazi, S.A. and Butt, S.A., 2017. An intelligent computing technique to analyze the vibrational dynamics of rotating electrical machine. *Neurocomputing*, *219*, pp.280-299.

[41] Ahmad, I., et al., 2018. Intelligent computing to solve fifth-order boundary value problem arising in induction motor models. *Neural Computing and Applications*, *29*(7), pp.449-466.

[42] Khan, Junaid Ali, et al. "Nature-inspired computing approach for solving non-linear singular Emden–Fowler problem arising in electromagnetic theory." *Connection Science* 27.4 (2015): 377-396.

[43] Akbar, S., et al., 2017. Design of Bio-inspired Heuristic Techniques Hybridized with Sequential Quadratic Programming for Joint Parameters Estimation of Electromagnetic Plane Waves. *Wireless Personal Communications*, *96*(1), pp.1475-1494.

[44] Raja, M.A.Z., Samar, R., Alaidarous, E.S. and Shivanian, E., 2016. Bio-inspired computing platform for reliable solution of Bratu-type equations arising in the modeling of electrically conducting solids. *Applied Mathematical Modelling*, *40*(11), pp.5964-5977.

[45] Masood, Zaheer, et al. "Design of Mexican Hat Wavelet neural networks for solving Bratu type nonlinear systems." *Neurocomputing* 221 (2017): 1-14.

[46] Raja, M.A.Z., Mehmood, A., Niazi, S.A. and Shah, S.M., Computational intelligence methodology for the analysis of RC circuit modelled with nonlinear differential order system. *Neural Computing and Applications*, pp.1-20.

[47] Raja, M.A.Z., Shah, A.A., Mehmood, A., Chaudhary, N.I. and Aslam, M.S., 2016. Bio-inspired computational heuristics for parameter estimation of nonlinear Hammerstein controlled autoregressive system. *Neural Computing and Applications*, pp.1-20.

[48] Mehmood, A., et al., Chaudhary, N.I. and Aslam, M.S., Nature-inspired heuristic paradigms for parameter estimation of control autoregressive moving average systems. *Neural Computing and Applications*, pp.1-24.

[49] Raja, M.A.Z., Aslam, M.S., Chaudhary, N.I., Nawaz, M. and Shah, S.M., Design of hybrid nature-inspired heuristics with application to active noise control systems. *Neural Computing and Applications*, pp.1-29.

[50] Akbar, S., et al., Novel application of FO-DPSO for 2-D parameter estimation of electromagnetic plane waves. *Neural Computing and Applications*, pp.1-10.

[51] Zameer, Aneela, et al. "Intelligent and robust prediction of short term wind power using genetic programming based ensemble of neural networks." *Energy Conversion and Management* 134 (2017): 361-372.

[52] Chaudhry, Z.R., et al., 2017. Design of reduced search space strategy based on integration of Nelder–Mead method and pattern search algorithm with application to economic load dispatch problem. *Neural Computing and Applications*, pp.1-13.

[53] Raja, M.A.Z., Zameer, A., Khan, A.U. and Wazwaz, A.M., 2016. A new numerical approach to solve Thomas–Fermi model of an atom using bio-inspired heuristics integrated with sequential quadratic programming. *SpringerPlus*, *5*(1), p.1400.

[54] Sabir, Z., et al., 2018. Neuro-heuristics for nonlinear singular Thomas-Fermi systems. *Applied Soft Computing*, *65*, pp.152-169.

[55] Esfe, M.H., Ahangar, M.R.H., Rejvani, M., Toghraie, D. and Hajmohammad, M.H., 2016. Designing an artificial neural network to predict dynamic viscosity of aqueous nanofluid of TiO2 using experimental data. *International Communications in Heat and Mass Transfer*, *75*, pp.192-196.

[56] Esfe, M.H., Yan, W.M., Afrand, M., Sarraf, M., Toghraie, D. and Dahari, M., 2016. Estimation of thermal conductivity of Al2O3/water (40%)–ethylene glycol (60%) by artificial neural network and correlation using experimental data. *International Communications in Heat and Mass Transfer*, *74*, pp.125-128.

[57] Raja, M.A.Z., 2014. Solution of the one-dimensional Bratu equation arising in the fuel ignition model using ANN optimised with PSO and SQP. *Connection Science*, *26*(3), pp.195-214.

[58] Raja, M.A.Z., Ahmed S.I., 2014. Numerical treatment for solving one-dimensional Bratu problem using neural networks. *Neural Computing and Applications*, *24*(3-4), pp.549-561.

[59] Raja, M.A.Z., Ahmed, I., Khan, I., Syam, M.I. and Wazwaz, A.M., 2016. Neuro-heuristic computational intelligence for solving nonlinear pantograph systems. *Front Inf Technol Electron Eng. doi*, *10*, p.1631.

[60] Raja, M.A.Z., 2014. Numerical treatment for boundary value problems of pantograph functional differential equation using computational intelligence algorithms. *Applied Soft Computing*, *24*, pp.806-821.

[61] Raja, M.A.Z., Farooq, U., Chaudhary, N.I. and Wazwaz, A.M., 2016. Stochastic numerical solver for nanofluidic problems containing multi-walled carbon nanotubes. *Applied Soft Computing*, *38*, pp.561-586.

[62] Raja, M.A.Z., Khan, M.A.R., Mahmood, T., Farooq, U. and Chaudhary, N.I., 2016. Design of bio-inspired computing technique for nanofluidics based on nonlinear Jeffery–Hamel flow equations. *Canadian Journal of Physics*, *94*(5), pp.474-489.

[63] Raja, M.A.Z. and Samar, R., 2014. Numerical treatment of nonlinear MHD Jeffery–Hamel problems using stochastic algorithms. *Computers & Fluids*, *91*, pp.28-46.

[64] Raja, M.A.Z. and Samar, R., 2014. Numerical treatment for nonlinear MHD Jeffery–Hamel problem using neural networks optimized with interior point algorithm. *Neurocomputing*, *124*, pp.178-193.

[65] Raja, M.A.Z., Azad, S. and Shah, S.M., 2017. Bio-inspired computational heuristics to study the boundary layer flow of the Falkner-Scan system with mass transfer and wall stretching. *Applied Soft Computing*.

[66] Ahmad, Iftikhar, et al. "Neural network methods to solve the Lane–Emden type equations arising in thermodynamic studies of the spherical gas cloud model." *Neural Computing and Applications* (2016): 1-16.

[67] Raja, M.A.Z., Khan, J.A., Chaudhary, N.I. and Shivanian, E., 2016. Reliable numerical treatment of nonlinear singular Flierl–Petviashivili equations for unbounded domain using ANN, GAs, and SQP. *Applied Soft Computing*, *38*, pp.617-636.

[68] Raja, M.A.Z., 2014. Stochastic numerical treatment for solving Troesch's problem. *Information Sciences*, *279*, pp.860-873.

[69] Majeed, Khalid, et al. "A genetic algorithm optimized Morlet wavelet artificial neural network to study the dynamics of nonlinear Troesch's system." *Applied Soft Computing* 56 (2017): 420-435.

[70] Raja, M.A.Z., Shah, F.H., Alaidarous, E.S. and Syam, M.I., 2017. Design of bio-inspired heuristic technique integrated with interior-point algorithm to analyze the dynamics of heartbeat model. *Applied Soft Computing*, *52*, pp.605-629.

[71] Raja, M.A.Z., Shah, F.H. and Syam, M.I., 2017. Intelligent computing approach to solve the nonlinear Van der Pol system for heartbeat model. *Neural Computing and Applications*, pp.1-25.

[72] Raja, M.A.Z., Khan, J.A. and Qureshi, I.M., 2010. A new stochastic approach for solution of Riccati differential equation of fractional order. *Annals of Mathematics and Artificial Intelligence*, *60*(3), pp.229-250.

[73] Li, H.L., Hu, C., Jiang, Y.L., Zhang, L. and Teng, Z., 2016. Global Mittag–Leffler stability for a coupled system of fractional-order differential equations on network with feedback controls. Neurocomputing, 214, pp.233-241.

[74] Raja, M.A.Z., Manzar, M.A. and Samar, R., 2015. An efficient computational intelligence approach for solving fractional order Riccati equations using ANN and SQP. *Applied Mathematical Modelling*, *39*(10), pp.3075-3093.

[75] Raja, M.A.Z., Samar, R., Manzar, M.A. and Shah, S.M., 2017. Design of unsupervised fractional neural network model optimized with interior point algorithm for solving Bagley–Torvik equation. *Mathematics and Computers in Simulation*, *132*, pp.139-158.

[76] Nocedal, J. and Wright, S.J., 2006. *Sequential quadratic programming* (pp. 529-562). Springer New York.

[77] Fesanghary, M., Mahdavi, M., Minary-Jolandan, M. and Alizadeh, Y., 2008. Hybridizing harmony search algorithm with sequential quadratic programming for engineering optimization problems. *Computer methods in applied mechanics and engineering*, *197*(33-40), pp.3080-3091.

[78] Mehmood, A., Zameer, A. and Raja, M.A.Z., 2018. Intelligent computing to analyze the dynamics of Magnetohydrodynamic flow over stretchable rotating disk model. *Applied Soft Computing*, *67*, pp.8-28.

[79] Long, K., Wang, X. and Gu, X., 2018. Multi-material topology optimization for the transient heat conduction problem using a sequential quadratic programming algorithm. *Engineering Optimization*, pp.1-17.

[80] Lang, A., Song, Z., He, G. and Sang, Y., 2017. Profile error evaluation of free-form surface using sequential quadratic programming algorithm. *Precision Engineering*, *47*, pp.344-352.

[81] Angalaeswari, S. and Jamuna, K., 2017. Optimal Energy Management Using Sequential Quadratic Programming Algorithm for Stand Alone PV System. *International Journal of Applied Engineering Research*, *12*(22), pp.12250-12255.

[82] Kunze, H., La Torre, D. and Lin, J., 2017, January. IFSM fractal image compression with entropy and sparsity constraints: A sequential quadratic programming approach. In *AIP Conference Proceedings* (Vol. 1798, No. 1, p. 020090). AIP Publishing.

[83] Toghraie, D., Alempour, S.M. and Afrand, M., 2016. Experimental determination of viscosity of water based magnetite nanofluid for application in heating and cooling systems. *Journal of Magnetism and Magnetic Materials*, *417*, pp.243-248.

[84] Esfe, M.H., Saedodin, S., Wongwises, S. and Toghraie, D., 2015. An experimental study on the effect of diameter on thermal conductivity and dynamic viscosity of Fe/water nanofluids. *Journal of Thermal Analysis and Calorimetry*, *119*(3), pp.1817-1824.

[85] Esfe, M.H., Afrand, M., Gharehkhani, S., Rostamian, H., Toghraie, D. and Dahari, M., 2016. An experimental study on viscosity of alumina-engine oil: effects of temperature and nanoparticles concentration. *International Communications in Heat and Mass Transfer*, *76*, pp.202-208

[86] Zarringhalam, M., Karimipour, A. and Toghraie, D., 2016. Experimental study of the effect of solid volume fraction and Reynolds number on heat transfer coefficient and pressure drop of CuO–water nanofluid. *Experimental Thermal and Fluid Science*, *76*, pp.342-351.